

WAVE-CURRENT-INDUCED SCOURING PROCESSES  
AROUND COMPLEX OFFSHORE STRUCTURES

Von der Fakultät für Bauingenieurwesen und Geodäsie  
der Gottfried Wilhelm Leibniz Universität Hannover

zur Erlangung des Grades  
DOKTOR-INGENIEUR  
Dr.-Ing.

genehmigte Dissertation

von

Mario Welzel M. Eng.  
geboren am 26. November 1983  
In Berlin

Hannover, 2021

This thesis is an open access thesis and distributed under the terms and conditions of the Creative Commons Attribution (CC BY 3.0 DE) license (<http://creativecommons.org/licenses/by/3.0/de/>).

The original source of third-party figures is cited in the present thesis. These figures are excluded from the open access license.

---

Referent:	Prof. Dr.-Ing. habil. Torsten Schlurmann
Korreferent:	Prof. Dr. Francisco Taveira-Pinto
Korreferent:	Prof. Dr. rer. nat. Corinna Schrum
Tag der Promotion:	07.05.2021

---

## DANKSAGUNG

---

Ich danke Herrn Prof. Dr.-Ing. Stefan Heimann, der Beuth Hochschule Berlin, der mich gefördert und mein Interesse für die Forschung geweckt hat. Die vorliegende Arbeit entstand während meiner Zeit als wissenschaftlicher Mitarbeiter am Ludwig-Franzius-Institut für Wasserbau, Ästuar- und Küsteningenieurwesen der Leibniz Universität Hannover. Die Bearbeitung verschiedener Forschungsprojekte ermöglichte es mir unterschiedliche Forschungsbereiche der Kolkgenese sowie des Kolkschutzes, um verschiedene Offshore-Gründungsstrukturen zu studieren. Die Idee zur Untersuchung von Erosionsprozessen an Gründungsstrukturen für Offshore-Windenergieanlagen entstand frühzeitig im Rahmen des Forschungsvorhabens „HyConCast – Hybride Substruktur aus hochfestem Beton und Sphäroguss für Offshore- Windenergieanlagen“. Besonderer Dank gilt meinem Doktorvater Herrn Prof. Dr.-Ing. habil. Torsten Schlurmann, für das mir entgegengebrachte Vertrauen, für die Förderung, hilfreichen Anregungen und Kritik sowie den überlassenen Freiraum zur inhaltlichen und kreativen Gestaltung dieser Arbeit.

Weiterer Dank gebührt Herrn Prof. Dr. Francisco Taveira-Pinto und Frau Prof. Dr. rer. nat. Corinna Schrum für die Übernahme des Koreferates und das Anfertigen ihrer schriftlichen Gutachten. Die wesentlichen Ergebnisse dieser kumulativen Dissertation wurden in internationalen Fachjournalen veröffentlicht. Dies wäre ohne die Mithilfe der Koautoren Dr.-Ing. Alexander Schendel, Prof. Dr.-Ing. habil Torsten Schlurmann, Prof. Dr.-Ing. Arndt Hildebrandt, Ph.D. Tiago Fazeres Ferradosa, Prof. Dr.-Ing. habil. Nils Goseberg nicht möglich gewesen. Ich bedanke mich daher bei meinen Koautoren für die hilfreichen und anregenden Diskussionen der Ergebnisse sowie den inhaltlichen und redaktionellen Ergänzungen der Publikations-Manuskripte.

Weiterhin möchte ich mich bei meinen Kollegen, HiWis und Studenten am Ludwig-Franzius-Institut, für die herzliche Arbeitsatmosphäre sowie die gute Zusammenarbeit und Unterstützung bedanken, welche mich über die Jahre begleitet haben. Danken möchte ich außerdem den technischen Mitarbeitern für ihre stete Unterstützung im Rahmen der diversen Projekte und Modellversuche.

Mein größter und damit abschließender Dank gilt meiner Familie, insbesondere meinen Kindern und meiner Frau Anna, die mich während der gesamten Zeit meiner Promotion mit ihrer Geduld und ihrem Verständnis unterstützt hat.

Mario Welzel



## ABSTRACT

---

The expansion of the offshore wind energy sector is important for the fulfilment of renewable energy targets. An accelerated growth of the worldwide offshore wind capacity will be required to meet the target of a climate neutral economy. In search of available space and higher load factors in the contested coastal areas, offshore wind parks are more often planned and installed in deeper waters or have to sustain intensified hydrodynamic loads. In consequence, complex offshore foundation structures such as jacket-type foundations are adopted, as they have an increased structural stability. However, the literature review of the present thesis reveals large knowledge gaps regarding the prediction of scouring processes around complex offshore foundations. These knowledge gaps are highlighted by the intensified demand of the expansion of offshore wind energy and show the requirement of an improved prediction and design of scour and scour protection systems. A reliable prediction of scouring processes is an important aspect of sustainable and economically optimised foundation designs. An improved understanding of morphological processes around offshore foundations is also important to evaluate and predict the man-made impact of offshore foundations on the previously unaffected marine environment.

This thesis aims at contributing to the understanding of morphodynamical processes around offshore structures, with a focus on complex offshore foundations. This is accomplished by addressing different research questions related to: (I) the scouring processes induced by a realistic representation of hydrodynamic conditions around monopiles and jacket-type structures; (II) the spatial scour depth changes and deposition patterns around offshore foundation structures; (III) the damage assessment and stability of scour protections. A series of novel hydraulic model tests were carried out to systematically work on different aspects of these topics.

(I) In order to further improve the understanding and prediction of scouring under realistic hydraulic conditions, the influence of the hydrograph shape on tidal current induced scour as well as scouring induced by multidirectional waves and currents is investigated around a monopile. Further investigations are conducted regarding the scour development, scouring rate and final scour depth in combined waves and current conditions at a jacket-type foundation structure.

(II) In the next step, an approach is developed to quantify and assess spatial changes of the seabed around marine structures. The systematic application of this approach allows the derivation of empirical formulations to predict complex erosion or deposition patterns. This is demonstrated by the investigation of global scour patterns in combined waves and current conditions around jacket-type foundations. In a further study, geostatistical methods are developed for the introduced methodology to further improve the spatial prediction and quantification of complex sediment displacement patterns.

(III) In the final step, the characterisation and assessment of damage patterns of scour protection layers is improved by the derivation of a new approach to quantify damage patterns. Large scale experiments under combined wave-current conditions are conducted in this context for uniformly and widely graded scour protection material in a joint group.

## ZUSAMMENFASSUNG

---

Der fortschreitende Ausbau des Offshore-Wind Energiesektors ist für die Erfüllung der Erneuerbaren Energien Ziele wesentlich. Um das Ziel einer klimaneutralen Wirtschaft zu erreichen, ist ein wesentlich beschleunigter Ausbau der weltweiten Offshore-Wind Kapazität notwendig. Auf der Suche nach höheren Auslastungsfaktoren und freien Flächen werden neue Offshore Wind Parks immer häufiger in tieferen Bereichen geplant und gebaut oder müssen erhöhten hydrodynamischen Belastungen standhalten. Folglich werden komplexe Offshore-Gründungsstrukturen wie Jacket Strukturen häufiger genutzt, da sie eine stabilere Gesamtkonstruktion aufweisen. Die Literaturrecherche der vorliegenden Studie weist große Wissenslücken betreffend der Kolkvorhersage um komplexe Offshore-Gründungsstrukturen auf. Im Hintergrund des rasant fortschreitenden Ausbaus des Offshore-Wind Energiesektors, weist dies deutlich auf die Erfordernis zur Verbesserung der Vorhersage von Kolk und Kolkschutzsystemen hin. Eine verlässliche Kolkvorhersage ist ein wesentlicher Bestandteil zur nachhaltigen und wirtschaftlichen Weiterentwicklung von Offshore-Gründungsstrukturen. Ein verbessertes Verständnis der komplexen morphologischen Prozesse um Offshore-Gründungsstrukturen ist außerdem wichtig, um anthropogene Einflüsse des Menschen auf die umgebende marine Umwelt besser zu bewerten und vorherzusagen.

Die vorliegende Dissertation leistet einen Beitrag zur Verbesserung der Vorhersage von komplexen, morphologischen Prozessen um Offshore-Gründungsstrukturen. Dies wird durch die Bearbeitung verschiedener wissenschaftlicher Fragestellungen zu den folgenden Themen erreicht: (I) Kolkprozesse infolge von komplexen, natürlichen hydrodynamischen Bedingungen um Jacket und Monopile-Strukturen; (II) Volumenbasierte Vorhersage von räumlichen Erosions- und Depositionsmustern um Offshore-Gründungsstrukturen; (III) Schadensbewertung und Stabilität von Kolkschutzsystemen. Unterschiedliche physikalische Modellversuche wurden durchgeführt, um an verschiedenen wissenschaftlichen Fragestellungen dieser Themen zu arbeiten.

(I) Um die Vorhersage von Kolkprozessen infolge von natürlichen hydrodynamischen Randbedingungen zu verbessern, wurde der Einfluss der Abflussganglinie von tideströmungsgeneriertem Kolk sowie Kolk unter multidirektionalem Wellen und Strömungsangriff an einer Monopile-Struktur untersucht. Weitere Untersuchungen wurden betreffend der Kolkentstehung, Kolkrate und Kolkentiefe durch kombinierte Wellen-Strömungsbelastung an einer Jacket-Struktur durchgeführt.

(II) Im nächsten Schritt wurde eine Methode zur Quantifizierung und Analyse von räumlichen Änderungen des Meeresbodens um marine Strukturen entwickelt. Die systematische Anwendung dieser Methode ermöglicht die Herleitung von empirischen Ansätzen zur Vorhersage von komplexen Erosions- und Depositionsmustern. Dies wurde mittels der Analyse der Sohltopografie um eine Jacket-Struktur unter kombinierter Wellen-Strömungsbelastung aufgezeigt. In einer weiteren Studie wurden

verschiedene geostatistische Methoden entwickelt, um die Vorhersage und Analyse komplexer Erosions- und Depositionsmuster weiter zu verbessern.

(III) Im letzten Schritt wurde das zuvor gewonnene Wissen über die Analyse von Sohltopografien auf die Analyse von Schadensmustern an Kolkenschutzsystemen für Versuche um eine Monopile-Struktur angewandt. In diesem Zusammenhang wurden großmaßstäbliche Modellversuche unter kombinierter Wellen-Strömungsbelastung an enggestuftem und weitgestuftem Steinmaterial durchgeführt.

**Keywords:**

Scour, Jacket, Scour Protection, Offshore Wind Energy, Wave-current interaction, erosion patterns, Laboratory Experiments

**Schlüsselwörter:**

Kolk, Jacket, Kolk, Kolkenschutz, Offshore-Windenergie, Wellen Strömungs Interaktion, Erosionsmuster, Physikalische Modellversuche





# CONTENTS

---

1 INTRODUCTION	1
1.1 Motivations	2
1.2 Methodology & Objectives	3
1.3 Outline	6
2 STATE-OF-THE-ART & BACKGROUND	7
2.1 Flow resistance and initiation of motion	7
2.1.1 Velocity distribution	7
2.1.2 Bed shear stress	9
2.1.3 Initiation of motion	10
2.2 Offshore wind foundation types	12
2.3 Scouring around monopiles	13
2.3.1 Hydrodynamics around a circular pile	13
2.3.2 Scour around a pile in steady current	16
2.3.3 Scour around a pile in waves	19
2.3.4 Scour around a pile in combined waves and current	20
2.4 Scouring around complex foundation structures	22
2.4.1 Scour around pile groups	22
2.4.2 Scouring mechanisms and interference effects at two piles	24
2.4.3 Scour around jacket and tripod foundations	28
2.5 Scour protection design of granular scour protections	32
2.5.1 Principles and failure mechanisms	32
2.5.2 Damage analysis of dynamic scour protections	33
2.6 Spatial analysis of sediment displacement processes	35
2.6.1 Spatial measurement techniques	35
2.6.2 Spatial analysing methods of bed topographies	36
2.7 Conclusions and Knowledge gaps	38
3 WAVE-CURRENT-INDUCED SCOURING PROCESSES	41
3.1 Wave-current-induced scouring around monopiles	41
3.2 Wave-current-induced scouring at Jacket Structures	42
3.3 Influence of structural elements on scour at Jacket structures	43
4 SPATIAL ANALYSIS OF SCOUR DEPTH CHANGES AROUND OWF FOUNDATIONS	45
4.1 Analysis and prediction of spatial scour depth changes	45
4.2 Effects of structural elements on spatial displacement patterns	46
4.3 Statistical analysis of spatial scour depth changes	47
4.3.1 Experimental setup & test conditions	47
4.3.2 Calculation of spatial parameters	48
4.3.3 Results	49
4.3.4 Conclusions	53

5 DAMAGE CHARACTERISATION AND SCOUR PROTECTION DESIGN	55
5.1 Large-scale experiments to improve scour protection design	55
5.2 Characterisation of damage patterns in scour protections	56
6 SUMMARY & OUTLOOK	59
6.1 Wave-current induced scouring . . . . .	59
6.2 Spatial analysis of sediment redistribution patterns . . . . .	61
6.3 Damage characterisation and scour protection design . . . . .	62
6.4 Future Work . . . . .	63
BIBLIOGRAPHY	65
APPENDIX	
A.1 Curriculum Vitae . . . . .	79
A.2 Paper 1:	
Schendel, A., Welzel, M., Hildebrandt, A., Schlurmann, T., Hsu, T.-W. (2019). Role and Impact of Hydrograph Shape on Tidal Current-Induced Scour in Physical-Modelling Environments. <i>Water</i> 2019, 11, 2636. DOI: <a href="https://doi.org/10.3390/w11122636">10.3390/w11122636</a> .	
A.3 Paper 2:	
Schendel, A., Welzel, M., Hildebrandt, A., Schlurmann, T., Hsu, T.-W. (2020). Scour around a monopile induced by short-crested waves combined with oblique currents. <i>Coastal Engineering</i> , Vol. 161, 2020 103751. DOI: <a href="https://doi.org/10.1016/j.coastaleng.2020.103751">10.1016/j.coastaleng.2020.103751</a> .	
A.4 Paper 3:	
Welzel, M., Schendel, A., Hildebrandt, A., Schlurmann, T. (2019a). Scour development around a jacket structure in combined waves and current conditions compared to monopile foundations. <i>Coastal Engineering</i> , Vol. 152, 103515. DOI: <a href="https://doi.org/10.1016/j.coastaleng.2019.103515">10.1016/j.coastaleng.2019.103515</a> .	
A.5 Paper 4:	
Welzel, M., Schendel, A., Goseberg, N., Hildebrandt, A., Schlurmann, T. (2020). Influence of structural elements on the spatial sediment displacement around a jacket-type offshore foundation. <i>Water</i> 2020, 12, 1651. DOI: <a href="https://doi.org/10.3390/w12061651">10.3390/w12061651</a> .	
A.6 Paper 5:	
Welzel, M., Schendel, A., Schlurmann, T., Hildebrandt, A. (2019b). Volume-based assessment of erosion patterns around a hydrodynamic transparent offshore structure. <i>Energies</i> 2019, 12, 3089. DOI: <a href="https://doi.org/10.3390/en12163089">10.3390/en12163089</a> .	
A.7 Paper 6:	
Chavez, C.E.A., Stratigaki, V., Wu, M., Troch, P., Schendel, A., Welzel, M., Villanueva, R., Schlurmann, T., De Vos, L., Kisacik, D., Pinto, F.T., Fazerer-Ferradosa, T., Santos, P.R., Baelus, L., Szengel, V., Bolle, A., Whitehouse, R., Todd, D., 2019. Large-scale experiments to improve monopile scour protection design adapted to climate change—the PROTEUS project. <i>Energies</i> 12 (9), 1709. DOI: <a href="https://doi.org/10.3390/en12091709">10.3390/en12091709</a> .	
A.8 Paper 7:	
Fazerer-Ferradosa, T.; Welzel, M.; Schendel, A.; Baelus, L.; Santos, P.R.; Pinto, F.T. Extended characterization of damage in rubble mound scour protections. <i>Coastal Engineering</i> , Vol. 158, 2020, 103671. DOI: <a href="https://doi.org/10.1016/j.coastaleng.2020.103671">10.1016/j.coastaleng.2020.103671</a> .	

## LIST OF SYMBOLS

---

$A$	reference distance times the structure footprint length; $A = x$ or $y$ distance / structure footprint distance, e.g. $0.5A = 0.25\text{m} / 0.55\text{m}$ for present model tests presented in chapter 4.3
$A_{sub}$	predefined sub-area to calculate the damage number $S_{3D}$
$A_w$	amplitude of wave orbital motion at the bed
$C_D$	drag coefficient
$D$	pile Diameter
$D_{A,i}$	cumulative volume depth; relative volume change per surface area of an individual volume $V_i$ of an area $a_i$ in reference to the pile diameter $D$
$D_{I,i}$	incremental volume depth; relative volume change per surface area of an individual volume $V_i - V_{i-1}$ within adjacent areas $a_i - a_{i-1}$ in reference to the pile diameter $D$
$D_{post}$	post pile / skirt pile Diameter of a jacket structure
$D_*$	dimensionless grain diameter
$G$	gap between two piles
$H$	wave height
$H_s$	significant wave height
$I$	bed slope
$KC$	Keulegan-Carpenter number
$L$	wave length
$Re_*$	grain Reynolds number
$Re_D$	pile Reynolds number
$S$	scour depth
$S_i$	scour depth at the front or rear pile of two piles in a tandem arrangement
$S_c$	current induced scour depth
$S_u(f)$	velocity frequency spectrum
$S_{3D}$	maximum damage number of all sub-areas
$S_{3D,sub}$	damage number of a predefined sub-area
$T$	wave period
$T_p$	peak wave period
$T_s$	time scale of the scouring process
$T^*$	dimensionless time scale of the scouring process
$U$	depth averaged current velocity
$U_c$	undisturbed current velocity
$U_{cr}$	critical flow velocity of $U$

$U_{cw}$	wave-current velocity ratio
$\bar{U}$	time and depth-averaged current velocity
$U_m$	maximum value of the undisturbed orbital velocity
$U_{rms}$	root-mean-square value of the orbital flow velocity
$V_{A,i}$	dimensionless cumulative volume; $V_{D,i}$ in relation to each normalised area
$V_{D,i}$	dimensionless volume; $V_i$ of an interrogation area $a_i$ in relation to the structural reference volume
$V_{I,i}$	dimensionless incremental volume; the net gradient volume $V_{D,i} - V_{D,i-1}$ in relation to each corresponding area $a_i - a_{i-1}$
$V_e$	eroded volume
$V_i$	displaced sediment volume in reference to a pre-scan in $m^3$ of the interrogation area $a_i$
$a_i$	interrogation area $a_i$ in dependence to $i$
$d$	grain diameter
$d_{n,50}$	nominal grain diameter
$d_{50}$	grain size within the grading curve for which 50% of the material is finer
$f_w$	wave friction factor
$g$	gravitational acceleration
$h$	water depth
$k_s$	equivalent sand grain roughness
$t_e$	characteristic time needed at which the increase of the scour depth is not exceeded by 5%
$u(z)$	flow velocity at the distance $z$ above the bed
$u_*$	shear velocity
$w_s$	fall velocity of isolated sediment grains
$z$	vertical distance from the bed
$z_0$	bed roughness length
$\alpha_{amp}$	amplification factor of the bed shear stress
$\theta$	Shields parameter
$\theta_{cr}$	critical Shields parameter
$\delta$	boundary layer thickness
$\kappa$	Kármán constant
$\mu$	dynamic viscosity of the fluid
$\nu$	kinematic viscosity of the fluid
$\rho$	fluid density
$\rho_s$	density of sediment grains
$\tau$	shear stress
$\tau_b$	bed shear stress
$\tau_{b,cr}$	critical bed shear stress

$\tau_c$	current induced bed shear stress
$\tau_m$	cycle-mean shear stress under combined wave-current load
$\tau_{max}$	maximum shear stress value under combined wave-current load
$\tau_w$	wave induced bed shear stress
$\tau_\infty$	bed shear stress due to undisturbed flow conditions
$\phi$	angle of repose of sediment

## ACRONYMS

---

ADV	Acoustic Doppler Velocimeter
CFD	Computational Fluid Dynamics
DEM	Digital Elevation Model
ECDF	Empirical Cumulative Distribution Function
GWEC	Global Wind Energy Council
GWK	Large Wave Flume in Hannover
HSV	Horseshoe Vortex
IPCC	Intergovernmental Panel on Climate Change
IRENA	International Renewable Energy Agency
JONSWAP	Joint North Sea Wave Project
LDS	Laser Distance Sensor
OpenFOAM	Open Source Field Operation and Manipulation
OWF	Offshore Wind Farm
PIV	Particle Image Velocimetry
RANS	Reynolds-averaged Navier-Stokes (equations)
RAVE	Research at Alpha Ventus

## INTRODUCTION

---

In recent decades, human activities have led to an anthropogenic caused global climate change, affecting the natural marine and terrestrial environment (IPCC 2014). Within the framework of the Paris Agreement, the goal of a climate neutral economy by 2050 was defined to globally reduce greenhouse gases and to limit the rise of global temperatures to 2°C or less. The European Union defined strategies to reach this goal, including an increase of the share of energy consumption from renewable energy sources to at least 20% by 2020 and 32% by 2030, Amanatidis (2019) (Directive: 2018/2001/EU). An important contribution to the fulfilment of the overall goal of a climate neutral economy might come from the offshore wind energy sector. Over the last few decades, the worldwide capacity of offshore wind energy has increased from 1.4 GW in 2008 to 29.1 GW in 2019 (IRENA, 2018; Lee and Zhao, 2019). To meet the target of a climate neutral economy by 2050 requires tremendous efforts including an accelerated growth of offshore wind capacity over the next decades. The Global Wind Energy Council (Lee and Zhao, 2019) estimates a global growth of newly installed offshore wind capacity from 6 GW in 2019 to 15 GW in 2024. By 2030, the worldwide offshore wind capacity is projected to grow to a cumulative capacity beyond 200 GW (IRENA, 2019). These statistics and projections highlight the requirement of a sustainable and economically optimised design of foundation structures and scour protection of offshore wind turbines combined with the need of a more detailed evaluation of environmental impacts (Elliott, 2002; Shields et al., 2011; Carpenter et al., 2016) on the formerly unaffected marine environment.

Offshore wind foundations are continuously exposed to hydrodynamic loads, such as tidal currents and waves. The placed foundation structure obstructs the flow, which causes complex hydrodynamic effects such as vortices and turbulent mixing in the near- and far-field (Vanhellemont and Ruddick, 2014; Grashorn and Stanev, 2016). In consequence, bed shear stresses are amplified, leading to an increased sediment mobility around the structure. The developing scour hole can then affect the structural stability of the structure itself and thus has to be considered in the design process of an offshore structure.

Although offshore wind farms (OWF) contribute to a reduction of greenhouse gas emissions, they also have an impact on the environment, either leading to habitat loss but also to habitat gain (Wilson and Elliott, 2009; Miller et al., 2013). While different ecological aspects have already been studied, the understanding of ecological consequences over the operational life of OWFs on the benthic environment is still limited (Miller et al., 2013; Heery et al., 2017).

Thus, a reliable prediction of evolving scour depths and the associated influence on the spatial sediment displacement in the near- and far-field of OWFs might be essential to secure a sustainable expansion of offshore wind energy and to quantify the impact of OWF induced sediment displacement on the benthic flora and fauna.

## 1.1 Motivation

In search of available space and higher wind energy load factors, offshore wind farms are moving further away from the shore into deeper waters. The average distance to the shore of OWFs in Europe increased from 35 km in 2018 to 59 km in 2019 WindEurope (2019). While monopiles remained the most common substructure type in 2019 with 70% of all new installations, jacket structures were the second most installed foundation type with 29% WindEurope (2019). As the water depth or hydrodynamic loads increase, different foundation types are adopted that are more complex, which often exhibit larger footprints. In consequence, complex offshore foundation structures such as jacket-type foundations are planned and installed more frequently. However, the literature research of the present thesis reveals large knowledge gaps regarding the prediction of scouring processes around complex offshore foundations. This knowledge gap is underlined by the intensified demand of the expansion of offshore wind energy and highlights the requirement of an improved prediction and design of scour and scour protection systems.

While the literature review (chapter 2) reveals that scour around monopile foundation has been investigated and published quite extensively, it also shows that available approaches often rely on simplified hydraulic conditions, neglecting the influence of directional flow or more realistic offshore sea states. The literature study also shows a lack of knowledge regarding scouring processes around more complex foundation structures. The scour prediction and protection of those structures are often designed following a conservative, and thus more inefficient and uneconomical approach, as they are based on studies related to monopiles.

While the literature also reveals that spatial measurement techniques such as photogrammetry, laser probe bottom profiler or laser scanner are more commonly used to investigate scouring processes around offshore foundations, few articles concentrate on a systematic volume-based analysis. In addition, there is a lack of knowledge regarding the description and quantification of such spatial erosion or deposition patterns and only a few approaches exist that strive to predict and to quantify these displacement patterns.

A reliable quantification and assessment of volume-based scour depth changes around offshore foundations allows the derivation of formulations to predict even complex erosion or deposition patterns. This information can be crucial for an improved design process of offshore foundations, also as a basis to determine whether additional scour protection is required or not and if so, which areas are exposed, and which volumes of scour protection material are required. An emerging scour hole can significantly affect the dynamic characteristics and thus the structural stability of a wind turbine support structure. This can result in an increased bending moment and an accelerated fatigue damage due to a change in the natural frequency and cyclic loading of the rotor (Achmus et al., 2010; Mayall et al., 2020). Furthermore, an estimate of spatial sediment displacement patterns can help to better understand OWF induced influences on the natural sediment mobility. Thus, a reliable calculation and prediction of volume changes of eroded and deposited material could serve as an indication to better assess and quantify the impact on benthic flora and fauna.



In general, a scour protection system is chosen as the most economical solution to reduce the risk of structural instability. This can be the case, if the scouring process is unpredictable or exceeds a certain foundation or site-specific scour depth threshold which might lead to structural adjustments or large maintenance costs over the lifetime.

Typically, a statically stable design approach is used to build scour protection systems for offshore wind turbines, which prevents movement of armour layer stones under design conditions, leading to conservative (increased) stone sizes (Soulsby 1997; Whitehouse 1998; Den Boon et al., 2004; De Vos et al., 2011). De Vos et al. (2012) derived a dynamically stable design approach which allows a limited movement, leading to reduced stone sizes and thus to a more economically scour protection design. However, large scale experiments under combined wave-current conditions for uniformly and widely graded scour protection materials are still missing. The prediction and assessment of the stability of the scour protection system is an important topic in this context. However only few studies have been conducted in the past decade, which strive to further enhance and develop such damage characterisation methodologies, to improve prediction methods and design guidelines for scour protections.

## 1.2 Methodology & Objectives

This thesis aims at contributing to the understanding of morpho-dynamical processes around offshore structures. The main topic of this thesis is the investigation of wave-current-induced scouring processes around complex offshore foundations, with the focus on jacket-type structures. This is achieved by addressing different aspects of three major topics (I) the local maximum scour depth, (II) spatial scour depth changes and (III) scour protection design.

(I) First, in order to improve the prediction of scouring mechanisms, scour under realistic hydraulic conditions is studied for monopile and jacket-type foundation structures (chapter 3).

(II) In the next step, novel methods are derived which enable the analysis and prediction of spatial scour depth changes and sediment deposition changes of the seabed topography. On the one hand, this allows to gain knowledge and to improve prediction methods for a sustainable and economically optimised design of foundation structures. On the other hand, the spatial quantification and prediction of sediment displacement patterns allows an improved assessment of environmental impacts on the marine environment of offshore foundation structures (chapter 4).

(III) In the final step, the previously derived knowledge on the spatial analysis of scour depth changes and deposition patterns is applied on damage patterns of scour protection layers, to improve the characterisation and assessment of the stability of scour protection systems. Large scale experiments under combined wave-current conditions are conducted in this context for uniformly and widely graded scour protection material (chapter 5). These three topics can be further divided into the following specific objectives:

- (I) Improvement of scour prediction** for monopile and jacket-type foundations by realistic hydraulic conditions:
- a) Advancing the knowledge of scouring processes by describing the influence of the hydrograph shape on tidal current induced scour around monopile offshore foundations. Comparison of different generalizations of the hydrograph's shape on the scour development in comparison to a reference test with continuously changing flow velocities and bidirectional altering flow directions. Improving the prediction of the final scour depth in tidal current dominated waters, which is often based on unidirectional currents with time and depth-averaged velocity assumptions. This is investigated in Schendel et al. (2019) and summarised in chapter 3.1.
  - b) Investigation of scouring mechanisms induced by multidirectional (short-crested) waves as well as multidirectional waves combined with currents. Systematic analysis and comparison of the impact of wave directionality on the scour depth and scouring rate. Improving the prediction of the maximum scour depth distinguished by either multi- or unidirectional waves combined with a current. This is addressed in Schendel et al. (2020), which is summarised in chapter 3.1.
  - c) Systematic investigation of the scour development, scouring rate and final scour depth in combined waves and current conditions at a jacket-type foundation structure. Description of the morpho-dynamical processes around a jacket structure, including differences at the upstream and downstream side of the structure as well as local and global scouring processes. Proposing a scour prediction approach for jacket structures in marine flow conditions. These objectives are addressed in Welzel et al. (2019a) and summarised in chapter 3.2.
  - d) Advancing the understanding of jacket-type foundation induced scour by investigating the influence of the lowest node and diagonal braces to the seabed on the scouring process. Improving the scour prediction for jacket structures, by additionally considering the distance of the lowest node to the seabed. This objective is addressed in Welzel et al. (2020) and summarised in chapter 3.3.
- (II) Improving the spatial analysis and prediction of complex sediment displacement patterns:**
- e) Development of an approach to quantify and assess spatial changes of the seabed around marine structures. Investigation of global scour patterns in combined waves and current conditions around a jacket structure. Proposing an approach to predict spatial scour patterns around jacket structures. Comparison with in-situ field data. These objectives are addressed in Welzel et al. (2019b) and summarised in chapter 4.1.

- f) Investigation of the effect of the lowest nodes and braces of jacket-type foundations on the spatial sediment displacement due to combined wave and current load. Further development of methodologies to describe and easily compare the relative volume change of sediment per surface area for erosion and deposition processes due to structure-seabed interaction. Quantifying the effect on amplified sediment mobility and thus on the impact on benthic flora and fauna. These objectives are addressed in Welzel et al. (2020) and summarised in chapter 4.2.
- g) Development of geostatistical methods to analyse erosion and deposition patterns around offshore wind foundations. To further improve the spatial prediction and quantification of complex sediment displacement patterns. To adopt statistical methods as the standard deviation, the cumulative distribution function or confidence bands on morphometric analyses of the seabed topography. These objectives are addressed in chapter 4.3.

**(III) Advancing the knowledge for scour protection design methodologies:**

- h) Investigation and comparison of scale effects for scour protection design under combined wave and current load. Comparison of the performance of single-layer wide-graded material against classical multi-layer design practices. To provide a benchmark dataset for scour protection design experiments. These objectives are addressed in Chavez et al. (2019) and summarised in chapter 5.1.
- i) Development of a methodology to characterise damage at scour protection layers with the statistical distribution of damage rather than using the maximum damage number. The investigation of the influence of the ratio between stone and sub-area size on the damage number. These objectives are addressed in Fazeres-Ferradosa et al. (2020) and summarised in chapter 5.2.

### 1.3 Outline

The main results of this thesis are published in peer reviewed international journal papers. These articles are complemented by paragraphs, which provide additional information and analysis as a contribution to the described objectives. In the following chapter 2, a literature review is given to provide background information on the scouring processes around cylindrical and complex offshore foundations, to summarise studies on the spatial assessment of erosion processes and to provide an overview on the damage analysis of scour protections. Chapter 3 summarises findings of four published studies regarding the improvement of scour prediction for monopile and jacket-type foundations for realistic hydraulic sea states. Chapter 4 presents findings of three studies, with two of them published in peer reviewed journals, on a new approach to assess and predict spatial seabed changes around marine structures. The spatial analysing methodologies are applied on the scour development around a jacket-type foundation structure, revealing global and local scour depth changes and sediment displacement patterns. Chapter 5 summarises findings of two published articles on the improvement of the design of rubble mound scour protections around offshore foundations. Finally, a summary, conclusions and an outlook on future investigations and remaining research questions is given in chapter 6.

The following chapter 2 provides fundamental knowledge and recent research about scouring processes around offshore wind foundations as well as state of the art concepts for failure and stability assessment of scour protection systems. These topics are given as an introduction to subsequent chapters. Within chapter 2, the focus lies on fully turbulent, hydraulic rough flow conditions. These flow conditions are typically dominant in the marine environment as well as in the introduced laboratory experiments. Although chapter 2 also introduces and discusses complex offshore wind foundation types, priority is given on structures with slender piles, with a focus on jacket-type offshore foundations. Suction bucket or gravity-based foundation structures are not considered. Effects of diffraction, which primarily apply to large pile diameters, as well as layered and cohesive sediments or sediment gradation are not addressed in this chapter.

Although spatial measurement techniques are more commonly applied in the past decade, few studies focus on the volumetric assessment of seabed changes around offshore wind foundations. Therefore, an overview on spatial measurement techniques for the laboratory and topographic analysing methods is given additionally, also partly containing studies acquired in the field of oceanography and river engineering. Finally, chapter 2 is closed with conclusions on knowledge gaps on the introduced topics.

## 2.1 Flow resistance and initiation of motion

### 2.1.1 *Velocity distribution*

**Uniform current close to a wall** A fluid close to a horizontal bottom is affected by the boundary itself and vice versa. Due to the no-slip condition, the velocity at the surface of the wall is zero. Fluid molecules close to the wall (within the boundary layer) are affected by this no-slip condition, which results in an influenced velocity distribution. The boundary layer  $\delta$  starts at the surface of the wall and reaches to the point where about  $\sim 99\%$  of the undisturbed fluid velocity is reached (Zanke, 1982). The thickness of the boundary layer is affected by the surface roughness, the Reynolds number as well as the turbulence intensity of the fluid. The boundary layer can be subdivided into three layers: the near-bed viscous (laminar) sublayer, in which the velocity distribution is linear, the logarithmic layer with a logarithmic velocity distribution as well as the buffer layer, which is located in between the viscous and logarithmic sublayer with a transition between a linear and logarithmic velocity distribution.

Analytical approximations for the viscous sublayer and the logarithmic layer enable the calculation of velocities in relation to the roughness and distance to the wall. Van Driest (1956) introduced an expression which enables the calculation of the continuous velocity distribution for turbulent flow conditions near a smooth wall, including the buffer layer. This

formulation was further developed by Cebeci and Chang (1978) to account for the surface roughness by coordinate shift. For the presented laboratory experiments and typical engineering tasks, the flow conditions are assumed to be turbulent rough, thus the viscous sublayer thickness is reduced significantly and the vertical velocity distribution above this thin sublayer can be described via the log law (Zanke, 1982; van Rijn, 1993; Schlichting and Gersten, 2006) as:

$$\frac{u(z)}{u_*} = \frac{1}{\kappa} \ln \left( \frac{z}{z_0} \right) \quad (2.1.1)$$

with  $u_*$  as the shear velocity, which is defined as  $u_* = \sqrt{\tau_0/\rho}$ ,  $\kappa$  as the von Kármán constant ( $\kappa = 0.4$ ) and  $z_0$  the bed roughness length, with  $z_0 = k_s/30$  for hydraulic rough flow conditions and  $k_s$  the equivalent sand grain roughness (Nikuradse, 1933). A turbulent flow is considered to be hydraulically smooth, if the roughness height is smaller than the thickness of the viscous sublayer. If the roughness height is larger than the viscous sublayer thickness, the flow is known as hydraulically rough.

**Flow under wave conditions** Analytical expressions exist in the form of different wave theories (e.g. Airy, Stokes, stream function or cnoidal theory), which enable to approximate the surface elevation and velocity distribution under waves. Wave theories are based on different idealised boundary conditions and may provide an approximation. Nevertheless, these theories provide good results, in particular for two dimensional undisturbed (wave only) cases. Monochromatic wave parameters are commonly used for practical engineering questions regarding sediment transport processes. According to the linear wave theory, the maximum amplitude of the orbital flow velocity close to the bed  $U_m$  can be determined for regular, small amplitude waves with:

$$U_m = \frac{\pi H}{T \sinh \left( \frac{2\pi h}{L} \right)} \quad (2.1.2)$$

with  $H$  as the wave height,  $T$  the wave period,  $h$  the water depth and  $L$  the wave length. The wave length has to be calculated in reference to the water depth iteratively or for the transition between shallow and deep water following the method introduced by Fenton and McKee (1990).

However, natural sea state conditions are characterised by irregular waves, consisting of large spectra with different irregular wave heights, wave lengths and variable directions. The superposition of different waves can be described with the specific energy distribution over the frequency. The most used formulations, which are still a simplification of natural sea states, are the JONSWAP and Pierson-Moskowitz spectra, while studies presented in this thesis have focused on the JONSWAP spectrum, which was derived from data of the North Sea. For the orbital velocity of a wave spectra, the root-mean-square value of a time series is commonly used to describe the maximum near-bed velocity (Soulsby, 2006; Schendel, 2018). The root-mean-square (RMS) value  $U_{rms}$  of the orbital velocity can be calculated by integration of the velocity frequency spectrum  $S_u(f)$  over all frequencies:

$$U_{rms}^2 = \int_0^\infty S_u(f)df \quad (2.1.3)$$

The maximum value of the orbital velocity  $U_m$  is then given by (Sumer and Fredsøe, 2001):

$$U_m = \sqrt{2}U_{rms} \quad (2.1.4)$$

$U_m$  becomes identical with the maximum orbital flow velocity in case of monochromatic (regular) waves with a small amplitude (Sumer and Fredsøe, 2001).

**Combined wave-current conditions** In the natural marine environment, typically a combined flow of waves and current is predominant. Combined wave-current conditions can also be affected by tidal flow, which is mainly characterised by continuously changing time series and varying flow directions or wind driven type of sheared currents with a maximum current velocity at the free surface. A linear superposition of the wave and current component is not possible. The combination and interaction of waves and current can lead to changed wave lengths resulting in refraction effects, a change in wave heights or an increased bed shear stress due to non-linear interactions within the boundary layer (Soulsby, 1997).

### 2.1.2 Bed shear stress

**Definition** A fluid, which is interacting with boundaries, exerts stress on the surface. The shear stress  $\tau$  is generally defined as the component of stress, exerted on a surface, which is aligned parallel to the material cross section. The bed shear stress is calculated from the near-wall velocity gradient due to the no-slip condition at the wall in the viscous sublayer, with  $\mu$  as the dynamic viscosity of the fluid,  $u$  as the flow velocity along the boundary and  $z$  as the vertical height above the boundary.

$$\tau_b = \mu \frac{\partial u}{\partial z} \quad (2.1.5)$$

**Shear stress in currents** In fluids with a free surface, shear stresses are distributed linearly between the surface of the bed and the surface of the water. The shear stress over the water column in steady current conditions is given with:

$$\tau(z) = \rho g(h - z)I \quad (2.1.6)$$

with  $\rho$  as the fluid density,  $g$  the gravitational acceleration,  $h$  the water depth,  $z$  the vertical distance from the bed and  $I$  the bed slope. Beside applying equation 2.1.5 and 2.1.6, the bed shear stress for turbulent flow, can also be determined according to Soulsby (1997) with the depth-averaged current velocity  $\bar{U}$  in relation to the drag coefficient  $C_D$ , which is dependent on the grain size characteristics (see Stahlmann, 2013; Schendel, 2018).

$$\tau_c = \rho C_D \bar{U}^2 \quad (2.1.7)$$

**Shear stress under waves** The bed shear stress under waves is typically determined with an additional friction factor  $f_w$  in relation to the maximum orbital velocity of the waves  $U_m$  at the bed (Soulsby, 1997):

$$\tau_w = \frac{\rho}{2} f_w U_m^2 \quad (2.1.8)$$

The friction factor  $f_w$  which depends on the hydraulic roughness given by the wave conditions has a significant impact on the bed shear stress. De Vos (2008) compared and discussed the influence of different wave friction formulations on the bed shear stress. Soulsby (1997) suggested the following equation, which can be determined by:

$$f_w = 1.39 \left( \frac{A_w}{z_0} \right)^{-0.52} \quad (2.1.9)$$

for turbulent rough flow, with  $A_w = U_m T / 2\pi$  as the wave amplitude and the coefficient  $z_0$  given by  $z_0 = d_{50} / 12$ . The wave friction factor  $f_w$  has a significant impact on the determination of the bed shear stress under wave conditions. Under wave conditions the boundary layer is significantly thinner as for steady flow conditions. Therefore, larger bed shear stresses are generated and transferred on the seabed.

**Shear stress under combined waves and current** A number of different approaches to determine the shear stress under combined wave–current load have been developed in the past. Soulsby et al. (1993) conducted a comprehensive comparison of existing expressions. Based on a large amount of existing experimental and field data, Soulsby (1995) developed an empirical equation to describe the cycle–mean shear stress  $\tau_m$  due to a combined wave–current load.

$$\tau_m = \tau_c \left[ 1 + 1.2 \left( \frac{\tau_w}{\tau_c + \tau_w} \right)^{3.2} \right] \quad (2.1.10)$$

where  $\tau_w$  is the bed shear stress due to “waves only” and  $\tau_c$  the bed shear stress for “current only” conditions. The maximum shear stress value under combined load can be approximated with:

$$\tau_{max} = [(\tau_m + \tau_w \cos \alpha)^2 + (\tau_w \sin \alpha)^2]^{0.5} \quad (2.1.11)$$

with  $\alpha$  as the angle between wave and current direction. For waves following the current direction  $\alpha = 0^\circ$  and for waves perpendicular to the current direction  $\alpha = 90^\circ$ .

### 2.1.3 Initiation of motion

Due to the formerly described hydrodynamic processes of wave, current or the combined load, shear stresses are exerted on the sediment bed. The sediment transport is initiated if a critical threshold of a flow velocity or bed shear stress is exceeded. The stabilising forces of a single grain are too small to withstand the driving forces. However, the shear stress or flow velocity is strongly affected by near-bed vortices or turbulence. Thus, the initiation of motion and transition into suspended or bed load transport is a probabilistic process and characterised by sliding, rolling or jumping



particles at the bed, while lighter particles loose ground contact and are transitioned in to suspended transport. Shields (1936) introduced a calculation method to describe the threshold of motion based on the bed shear stress. Other approaches also use the shear velocity, the critical flow velocity or the depth-averaged and near-bed flow velocity. A wide range of existing studies relate the threshold value to the critical bed shear stress  $\tau_{b,cr}$  as it directly affects the near bed motion of particles and includes effects of near-bed turbulence and bed roughness in contrast for example to a critical depth-averaged approach (Zanke, 1982). The non-dimensional Shields number  $\theta$  is defined as:

$$\theta = \frac{\tau_b}{(\rho_s - \rho)gd} \quad (2.1.12)$$

with  $\rho$  as the fluid density,  $g$  the gravitational acceleration,  $d$  the characteristic diameter of the sediment grain and  $\rho_s$  as the density of the sediment. The critical Shields number  $\theta_{cr}$  (see Eq. 2.1.14) is related to the critical value of  $\theta$ , corresponding to the initiation of motion. Furthermore, the Shields diagram, shown in Fig. 2.1.1 is presented in a modified form, in which the critical Shields number  $\theta_{cr}$  is related to the grain Reynolds number  $Re_*$ .

$$Re_* = \frac{du_*}{\nu} \quad (2.1.13)$$

with  $u_*$  as the shear velocity and  $\nu$  the kinematic viscosity.

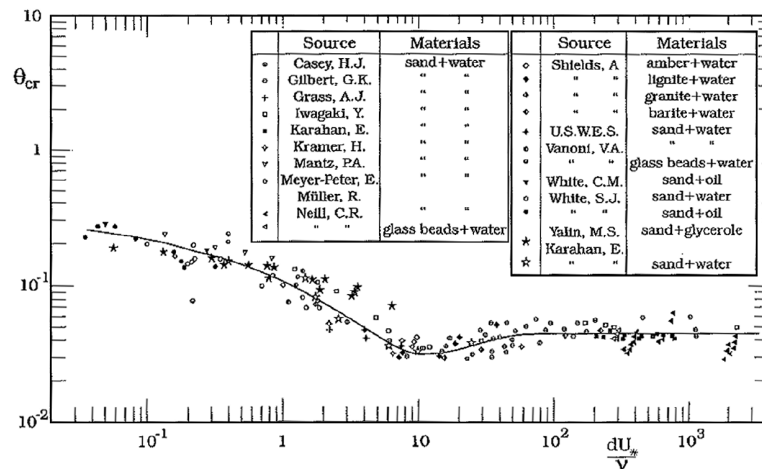


Figure 2.1.1. Modified Shields diagram for the initiation of motion including compiled data by Yalin and Krahan (1979), reproduced figure from Sumer and Fredsøe (2002) with permission, Copyright © 2002 by World Scientific.

Based on Albert Shields findings various studies were conducted in the past century, which confirmed and extended the Shields diagram, e.g. Yalin and Karahan (1979) or Raudkivi (1990). Various studies were also based on the idea of a modification of the Shields approach due to the probabilistic nature of particle entrainment (e.g. Grass, 1970; Paintal, 1971; Zanke, 1990). More recent approaches enable a more precise determination of the Shields parameter due to parametrisation of the Shields curve and modification by use of the non-dimensional grain

diameter  $D_*$ . Soulsby and Whitehouse (1997) introduced an expression for the critical Shields parameter, which was slightly modified by using an improved fitting for fine grain sizes, and additionally validated the approach for a wide set of wave and combined wave and current tests:

$$\theta_{cr} = \frac{0.3}{1 + 1.2D_*} + 0.055[1 - \exp(-0.02D_*)] \quad (2.1.14)$$

with  $D_*$  as the non-dimensional grain diameter:

$$D_* = d \left[ \frac{(\frac{\rho_s}{\rho} - 1)g}{\nu^2} \right]^{\frac{1}{3}} \quad (2.1.15)$$

## 2.2 Offshore wind foundation types

The type of offshore wind foundation (OWF) structure is mainly chosen based on the water depth, site-specific metocean and morphodynamic conditions (Chen et al., 2016). But also, the fabrication of the foundation structure, the transport and the offshore installation process are important aspects affecting the total costs or time windows of the installation of foundation structures and thus the choice of the structure type (see e.g. Welzel et al., 2016; Stümpel et al., 2017). Monopile and gravity-based foundation structures are often found to be most suitable for water depths smaller than 30 m. However, in recent years, monopile foundations have also been installed in water depths greater than 30 m (Golightly, 2014; Sánchez et al., 2019). Monopile structures are generally the most used foundation type in general, and in particular for water depths smaller than 30 m. Tripod and Jacket-type foundation structures are commonly used in intermediate water depths larger than 20 m (Sánchez et al., 2019). As the average distance of OWFs to the shore is increasing with a growing expansion of offshore wind farms, complex substructures are being used more often – such as jacket structures (WindEurope, 2019; Sánchez et al., 2019). Figure 2.2.1 shows common offshore wind foundation types in an overview, including floating substructures.

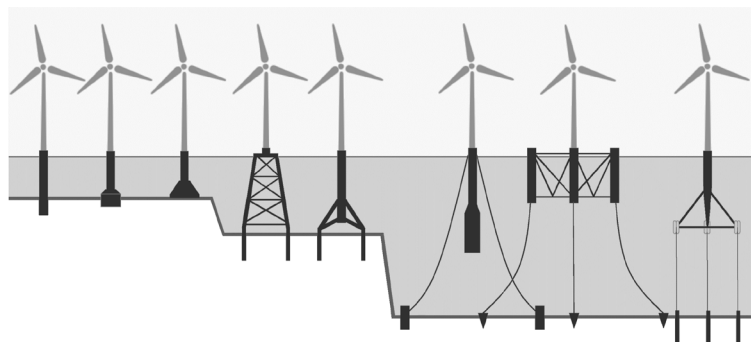


Figure 2.2.1. Common offshore wind foundation types used in Europe. From left to right: monopile, suction bucket, jacket, tripod, spar, semi-submersible and tension-leg platform. Adapted figure from Dornhelm et al. (2019).

Jacket-type foundations are adaptable and have an excellent structural behaviour for intermediate water depths – in particular in conditions in

which monopiles are increasingly unstable (Sánchez et al., 2019; Abhinav and Saha, 2018). Furthermore, jacket-type foundations have several advantages compared to tripod structures and thus are more often used (WindEurope, 2019). Despite of generally larger structural elements, which induce an increased erosion of sediments at the legs and piles, the section under the main column of the tripod generally induces the highest shear stresses and thus significantly larger scour depths as jacket structures with one pile per leg.

In addition to these foundation types (see Fig. 2.2.1), OWF types such as the pile cap foundation (mainly consisting of a group of multiple piles and one single pile cap) are used in Asia, mainly for reasons of the total costs and structural stability (Sánchez et al., 2019). Several prototypes of floating offshore wind foundations have been developed and tested in field conditions in the past decade. Floating offshore wind foundation structures have a huge potential, in particular to explore areas which remain unavailable nowadays. Common floating offshore wind foundations are for example spar, semi-submersible and tension-leg platforms (see Figure 2.2.1). Andersen (2016) and Uzunoglu et al. (2016) give a good overview on floating foundation types and their different stabilizing design concepts, mainly classified by buoyancy, ballast and mooring line stabilization.

## 2.3 Scouring around monopiles

### 2.3.1 Hydrodynamics around a circular pile

A pile which is placed in the marine environment, induces a blockage of the surrounding flow, and thus causes complex hydrodynamic effects leading to an amplification of bed shear stress and increased sediment transport. A complex vortex system is generated by the blockage of the pile, which can be subdivided according to Sumer and Fredsøe (2002) into the following main components (see Fig. 2.3.1): (1) a downflow on the upstream side of the pile, (2) a horseshoe vortex, (3) lee-wake vortices on the back side and (4) streamline contraction on the side edges. An adverse pressure gradient in front of the pile is initiated by the approaching flow and the interaction with the water surface and the pile. In consequence, the approaching boundary layer undergoes a three-dimensional separation (see the dashed separation line, Fig. 2.3.1), rotates and forms the spiral-shaped horseshoe vortex which trails downstream through the side edges of the pile (Fig. 2.3.1).

**Steady current conditions** As a result, the bed shear stress can reach amplification factors for a steady current in the order of  $O(10)$  (Hjorth, 1975; Baker, 1979; Roulund et al., 2005), highlighting the major influence of the horseshoe vortex on the scouring process. The amplification of the bed shear stress is defined as  $\alpha_{amp} = |\tau|/\tau_{\infty}$ , with  $\tau$  as the amplified bed shear stress at the pile and  $\tau_{\infty}$  the undisturbed bed shear stress. According to Hjorth (1975) and Roulund et al. (2005), the amplification factor is largest in a position of about 45–70°, measured in an angle from the main current direction on the upstream side. The horseshoe vortex in steady flow conditions is affected by the strength of the adverse pressure gradient,

the ratio of the boundary layer thickness to the pile diameter  $\delta/D$ , the pile Reynolds number  $Re_D = UD/\nu$  and the bed roughness (Sumer and Fredsøe, 2002; Roulund et al., 2005). As the ratio of the boundary layer to the diameter  $\delta/D$  increases, the size of the horseshoe vortex increases as well and vice versa (Baker, 1985). According to Sumer and Fredsøe (2002), in a turbulent boundary layer, the size of a horseshoe vortex may be decreased with an increasing Reynolds number. The horseshoe vortex is also affected by the emerging scour hole itself. With an increasing scour hole, the core of the horseshoe vortex increases, slows down and initiates decreased bed shear stresses.

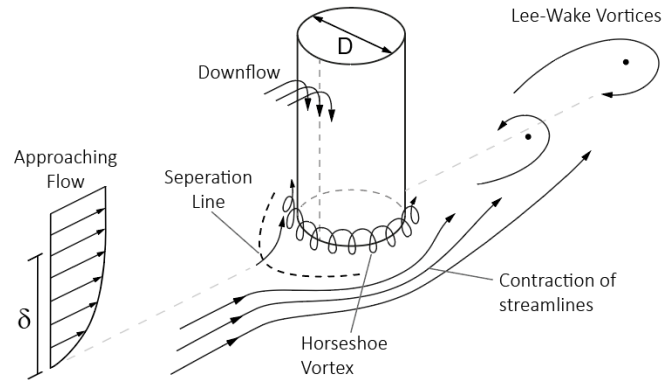


Figure 2.3.1. Sketch of the flow around a circular cylinder, with  $\delta$  representing the boundary layer thickness.

Lee-wake vortices are generated due to the rotating flow of the boundary layer over the surface of the pile and the following separation from the pile. A separated shear layer rolls up and forms vortices in the lee wake side of the pile (Sumer and Fredsøe, 2002). The lee-wake vortex under steady current conditions is mainly influenced by the pile Reynolds number  $Re_D$ , the pile geometry and the surface roughness of the pile in reference to the pile diameter  $k_s/D$ . The flow around and on the lee side of the pile experiences significant changes with an increasing Reynolds number. For smooth, circular cylinders with a Reynolds number ranging from  $Re_D = 40$  to 200, the formerly stable vortices are becoming unstable and laminar vortex shedding can be observed, characterised by a two-dimensional formation without variation in the spanwise direction (Williamson, 1989). For Reynolds numbers between 200 and 300 a transition to turbulent vortices takes place and for  $Re_D$  greater than 300 completely turbulent lee-wake vortices can be observed. For a more detailed description and overview of flow regimes and vortex shedding due to steady currents, the author refers to Sumer and Fredsøe (1997).

**Wave conditions** For wave conditions, the Keulegan-Carpenter number,  $KC$  is introduced (Keulegan and Carpenter, 1958), a non-dimensional parameter, which describes the fluid flow regime for oscillating flow and wave conditions in reference to a characteristic length of an object:

$$KC = \frac{U_m T}{D} \quad (2.3.1)$$

with  $U_m$  as the maximum value of the undisturbed orbital velocity at the bed, for monochromatic (regular) waves defined by Eq. (2.1.2), for wave spectra calculated by Eq. (2.1.4), the wave period  $T$  and the pile diameter  $D$ . In this respect, small  $KC$  numbers indicate a comparably low orbital wave motion relative to the pile diameter, while very large  $KC$  numbers indicate a wave motion in reference to the pile diameter, which is so large that the stroke of each half period is similar to that in a steady current. According to Sumer et al. (1997), horseshoe vortices around cylindrical piles are generated for  $KC > 6$ , as the stroke of the wave motion and thus the approaching boundary layer is not large enough for conditions with  $KC < 6$  to separate and develop a stable horseshoe vortex. Wave conditions with small  $KC$  numbers are consequently leading to a comparably thin wave boundary layer and smaller horseshoe vortices. As the  $KC$  number increases, the orbital velocity increases and the horseshoe vortex is preserved over a larger lifespan and disappears with the flow reversal of the wave motion. According to Sumer and Fredsøe (2001), vortex Shedding is the dominant mechanism of scouring for wave induced scour, in particular for small  $KC$  numbers. Each separated vortex, in each half period transports sediment into the core region of the vortex, which carries the eroded sediment downstream from the pile, causing a deepening of the scour hole (see Fig. 2.3.2).

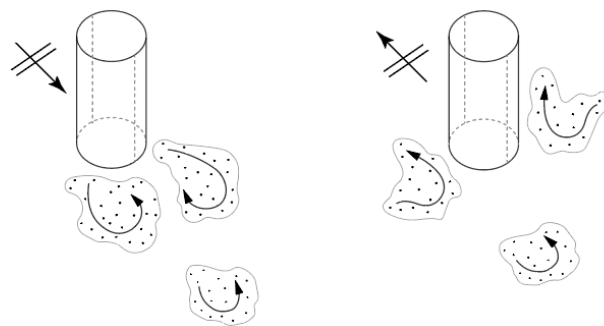


Figure 2.3.2. Sketch of vortex shedding as the dominant scouring mechanism under wave conditions. The left and right sketch depict each half cycle of the wave.

Sumer et al. (1997) also found that the maximum bed shear stress amplification factor in waves increased by  $O(4)$ , due to the combined effects of the horseshoe vortex and streamline contraction, which is considerably smaller than the maximum value under steady currents  $O(10)$ , which might be related to the pronounced presence of the horseshoe vortex (Sumer and Fredsøe, 2002). The lee-wake vortex under oscillating flow and wave conditions is additionally characterised by the Keulegan Carpenter number  $KC$ . Following Sumer et al. (1997), a separated pair of symmetric vortices can be observed for  $2.8 \leq KC < 4$ , while the symmetry is disbanded for  $4 < KC < 6$ , with the vortices still attached to the pile. For Keulegan Carpenter numbers reaching 6, vortex shedding starts to develop and can be observed. In the range of  $6 < KC < 17$ , one vortex is detached in each half period of the wave, while for the regime of  $17 < KC < 23$  two vortices are detached from the pile in each half cycle of the wave, likely also leading to an increased length of the lee-wake vortex behind the pile (Sumer and Fredsøe, 2002).

**Combined wave-current conditions** Furthermore, Sumer et al. (1997) conducted experiments to study the horseshoe vortex and vortex shedding for combined wave-current conditions and found that the size and lifespan of the horseshoe vortex is increased under the influence of a current superimposed on waves. This influence is enhanced for an increasing ratio of  $U_c/U_m$ . Furthermore, the horseshoe vortex also exists for smaller  $KC$  numbers with an increasing ratio of  $U_c/U_m$ , with  $U_c$  as the undisturbed current velocity at the bed (Sumer et al., 1997) and  $U_m$  the maximum value of the undisturbed orbital velocity at the bed (see Eq. 2.1.2).

### 2.3.2 Scour around a circular pile in steady current

The topic of scouring around piles in steady currents has been addressed and investigated thoroughly. In particular in the context of bridge pier failure and river engineering an extensive amount of studies, has been carried out (e.g. Hjorth, 1975; Breusers et al., 1977; Raudkivi and Ettema, 1983; Chiew, 1984; Melville and Coleman, 2000; Sheppard et al., 2004; Pizarro et al. 2020). The scour hole around the pile develops in a conical shape, similar to a frustum of an inverted cone. While the slope angle  $\phi$  on the upstream side of the scour hole can be larger as the critical angle of repose (1.1-1.2  $\phi$ ), the slope on the downstream side of the scour hole has a less steep inclination (see Fig. 2.3.3). Under the influence of steady currents, the driving mechanism of the scouring process is the downflow and horseshoe vortex in front of the pile in combination with streamline contraction at the side edges (see chapter 2.3.1). Hence, increased shear stresses are exerted on the sediment which exceed the critical threshold of the sediment particles and sediment transport is initiated. Displaced sediment particles are transported downstream by the horseshoe vortex and lee-wake vortices, which are then deposited downstream outside the hole in the near field of the pile or entrained by the flow over longer distances. The horseshoe vortex in a scour hole (see Fig. 2.3.3) is increasing with time, evolving into a main vortex and 1-2 smaller vortices (Guan et al., 2019), while velocities and bed shear stresses are decreasing over time, leading to equilibrium conditions.

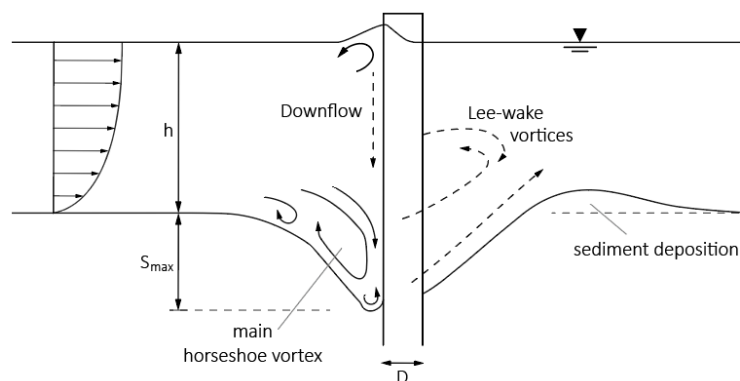


Figure 2.3.3. Sketch of the maximum scour depth, scour shape and main mechanisms, including the horseshoe vortex in a scour hole under equilibrium conditions.

**Scour depth affecting parameters** Various parameters are affecting the scour development around piles in steady currents. The effect of the foundation shape or foundation alignment has been investigated e.g. by Melville and Sutherland (1988) or Melville and Coleman (2000). Despite the foundation shape and alignment, the local scour depth under steady current conditions mainly depends on the following dimensionless parameters, which are namely, (a) the flow intensity, (b) the flow depth to pile size ratio, (c) the coarseness of the sediment (d) the sediment nonuniformity (Raudkivi, 1986; Melville and Coleman, 2000; Pizarro et al., 2020).

The flow intensity (a) is described by the ratio  $U/U_{cr}$  or  $\theta/\theta_{cr}$ , with the mean flow velocity  $U$  and the critical mean flow velocity  $U_{cr}$  corresponding to the initiation of motion at the bed for the undisturbed case. Alternatively, this ratio is described by the relation of the Shields parameter  $\theta$  to the critical Shields parameter  $\theta_{cr}$ . The sediment mobility can be classified in relation to the flow intensity for clear-water or live-bed conditions. In clear-water conditions the mean flow velocity is below the critical value for the initiation of motion ( $U/U_{cr} < 1$  or  $\theta/\theta_{cr} < 1$ ). In this condition, the local scour depth increases nearly linearly with the velocity up to a maximum, the threshold peak (Melville and Coleman, 2000). As the threshold for the initiation of motion is exceeded, the sediment mobility is categorised in to live-bed conditions ( $U/U_{cr} > 1$  or  $\theta/\theta_{cr} > 1$  for uniform sediments) and sediment transport, leading to natural ripple migration prevailing over the entire bed. In consequence, upstream eroded sediment is transported in to the scour hole leading to slightly lower scour depths. As the flow intensity is further increased, the scour depth increases again until it reaches the live-bed peak at the transition to sheet flow conditions (Sumer and Fredsøe, 2002).

The relative flow depth (b) is influencing the boundary layer thickness and consequently the approaching flow conditions and horseshoe vortex generation. Thus, the size of the horseshoe vortex and scour depth is increased with rising relative flow depth  $h/D$  up to a threshold value of about  $h/D > 4$ , beyond which the scour depth and scouring process is not affected any more (Whitehouse, 1998). The relative flow depth is of particular interest for the assessment of scouring processes at bridge piers with lower water depths. According to Breusers et al. (1977) ( $h/D > 3$ ) and Melville and Sutherland (1988) ( $h/D > 2.6$ ), the influence of the relative water depth can be neglected even for a lower ratio as recommended in Whitehouse (1998), if the water depth increases.

The coarseness of the sediment (c) expressed by the pile size to sediment size ratio  $D/d_{50}$  in particular affects nonuniform sediments as well as relatively large sediment grains (Melville and Coleman, 2000). Laboratory data of Ettema (1980) and Chiew (1984), compiled by Melville and Sutherland (1988), show that the local scour depth is influenced by the sediment grain size if  $D/d_{50} < 50$ . With a continuously increasing sediment grain size, reaching  $D/d_{50} < 8$ , the scour depth is further decreased, while the scour hole is focused on the side edges (Melville and Coleman, 2000).

As the sediment nonuniformity (d) rises, the standard deviation  $\sigma_g$  increases and the scour depth can be reduced significantly. Ettema (1976) conducted laboratory tests under clear-water conditions, experiencing a significant reduction of the scour depth with an increasing standard



deviation. Armouring takes place around the threshold condition for initiation of motion  $U/U_{cr} \approx 1$ . A protective armour layer in the erosion zone of the scour hole reduces the scour depth significantly (Melville and Coleman, 2000). With an increasing flow intensity, the sediment mobility is categorised in to live-bed conditions and the flow is entraining a larger share of the sediment bed, thus the armour layer is destructed and the nonuniformity has only a reduced effect on the scour depth (Baker, 1986).

**Equilibrium scour depth and time scale** Scouring around a foundation structure is a time-dependent morphological process. The scour depth under clear-water conditions increases asymptotically (see Fig. 2.3.4) towards an equilibrium stage through a transitional period. As the threshold for the initiation of motion is exceeded under live-bed conditions, the flow intensity increases, and sediment transport prevails over the entire bed. In consequence the equilibrium stage is reached more rapidly, bedforms propagate over the scour hole and the scour depth oscillates around the equilibrium depth (Melville and Coleman, 2000). The scour depth which is corresponding to the equilibrium state is defined as the “equilibrium scour depth”. The equilibrium scour depth is typically used for stability design purposes, as it represents the maximum expected scour depth for a specific hydrodynamic condition. While Sheppard et al. (2014) and Pizarro et al. (2020) both give a good overview of existing equations to calculate the equilibrium scour depth under steady currents, Sheppard et al. (2014) assembled 441 laboratory and 791 field data, which were used to assess the quality of 17 different scour depth equations. A commonly used approach to predict the time  $t_e$  (see Fig. 2.3.4), which is required to achieve the equilibrium scour depth, is given by Melville and Chiew (1999). The parameter  $t_e$  characterises the time at which the increase of the scour depth is not exceeded by 5% of the pile diameter in a time of one day.

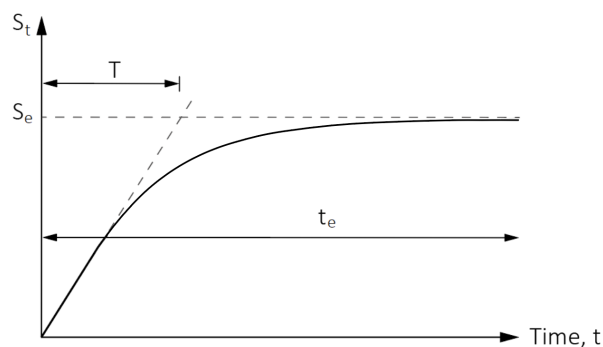


Figure 2.3.4. Sketch of the temporal development of the scour depth under clear-water conditions, including the time scale  $T$  and the time  $t_e$  to reach the equilibrium scour depth  $S_e$  at which the increase of the scour depth is not exceeded by a value of 5% of the pile diameter length in one day.

Beside the method of Melville and Chiew (1999) a commonly used approach to estimate the time  $t_e$  or the equilibrium scour depth  $S_e$  is given by Sheppard et al. (2004), which introduced two mathematical functions (see Eq. 2.3.2 and 2.3.3) to fit the local scour development for clear-water conditions.



$$S_t = a \left( 1 - \frac{1}{(1 + abt)} \right) + c \left( 1 - \frac{1}{1 + cdt} \right) \quad (2.3.2)$$

$$S_t = a(1 - \exp(-bt)) + c(1 - \exp(-dt)) \quad (2.3.3)$$

Once the coefficients  $a, b, c$  and  $d$  were determined for each test by least square fitting, time was increased equal to infinity ( $t \rightarrow \infty$ ) to obtain the equilibrium scour depth. In this way the equilibrium scour depth and time which is required to reach the scour depth could be determined.

The time scale is a reference value, which enables the calculation of the time dependent scouring rate. According to Sumer et al. (1992a), the time scale  $T_s$  is defined as the time which is required to reach 63% of the equilibrium scour depth, utilising a tangent to the scour development curve, starting at  $t = 0$  (see Fig. 2.3.4). The time scale might be calculated via the previously introduced tangent method or by integrating the scour development over a time period (Fredsoe et al., 1992; Fuhrman et al., 2014; Schendel, 2018). For a steady current, the non-dimensional time scale  $T^*$  is given as a function of the Shields parameter  $\theta$ , the boundary layer thickness  $\delta$  and the pile diameter  $D$  (Sumer et al., 1992a):

$$T^* = \frac{1}{2000} \frac{\delta}{D} \theta^{-2.2} \quad (2.3.4)$$

with the translation of  $T^*$  in to the dimensional time scale  $T_s$ , which is given by:

$$T_s = \frac{D^2 T^*}{\left( g \left( \frac{\rho_s}{\rho} - 1 \right) d_{50}^3 \right)^{0.5}} \quad (2.3.5)$$

Numerical simulations of scouring around a cylindrical pile were conducted by Roulund et al. (2005), Stahlmann (2013) and Baykal et al. (2017), just mentioning a few examples. They used different three-dimensional CFD codes, solving the Reynolds-averaged Navier-Stokes equations (RANS equations), combined with a morphological model, based on empirical sediment transport formulas. Recent studies as Nagel et al. (2020) simulate the scouring process with a multiphase model, including a phase simulating the sediment behaviour to circumvent the usage of empirical approaches as done in the former mentioned studies. This incorporates several advantages but also disadvantages as more complex and computational expensive computations.

### 2.3.3 Scour around a pile in waves

For the case of scour around piles due to waves, the Keulegan Carpenter number  $KC$  (see Eq. (2.3.1)) was found to be the main parameter, describing the scouring process in wave conditions (Sumer et al., 1992b; Kobayashi and Oda, 1994). According to Sumer et al. (1992b), the onset of scour corresponds with the development of vortex shedding. For circular piles this appears when  $KC$  reaches 6. The approaching flow rolls up and forms the horseshoe vortex, combined with streamline contraction at the sides, which erodes and transports sediment particles in downstream direction into the core of the lee-wake vortex (see Fig. 2.3.2), which carries the sediment away from the pile (Sumer and Fredsoe, 2002). For

smaller values of  $KC$  ( $KC < 6$ ) the thickness of the wave boundary layer is too thin and the wave period is too short to generate pronounced vortices on the front (horseshoe vortex) and back side (lee-wake vortex) of the structure, leading to comparable small scour depths, induced by flow disturbance and streamline contraction at the sides (Schendel, 2018).

With an increasing  $KC$  number, the flow conditions and vortices are influenced, so that the size and lifespan of the horseshoe vortex as well as the length of the lee-wake vortex increase. As  $KC$  increases ( $KC \rightarrow \infty$ ), the scour depth rises and approaches constant values close to the equilibrium scour depth for current conditions. For  $KC > 100$ , the scouring process is dominated and driven by the horseshoe vortex, while for  $KC < O(10)$  the main factors are the lee-wake vortices, causing a net erosion for each half cycle (Sumer and Fredsøe, 2002). For the case of irregular waves, Sumer and Fredsøe (2001) found a good representation of  $KC$  by the maximum value of the undisturbed orbital velocity  $U_m$  (defined in Eq. 2.1.4) and  $T_p$  the peak period. A commonly used approach to calculate the equilibrium scour depth for  $KC \geq 6$  due to waves is given by Sumer et al. (1992b):

$$S/D = 1.3\{1 - \exp[-0.03(KC - 6)]\} \quad (2.3.6)$$

Note that the effect of various factors previously described, such as the relative flow depth, the coarseness of the sediment, the sediment nonuniformity or the Reynolds number are not included in Eq. (2.3.6). For design purposes Sumer and Fredsøe (2002) recommend the following expression:

$$S/S_c = 1 - \exp[-0.03(KC - 6)]; \quad KC \geq 6 \quad (2.3.7)$$

which allows to take the aforementioned factors into account with the calculation of the current-alone scour depth  $S_c$ .

### 2.3.4 Scour around a pile in combined waves and currents

The scour depth due to combined waves and currents is found to be a function of the wave current velocity ratio. The parameter  $U_{cw}$  represents the ratio of the maximum value of the undisturbed orbital velocity at the bed  $U_m$  to undisturbed current flow at the bed  $U_c$  and is given by Sumer and Fredsøe (2001) as:

$$U_{cw} = \frac{U_c}{U_c + U_m} \quad \begin{array}{l} U_{cw} > 0.5 \text{ current - dominated} \\ U_{cw} < 0.5 \text{ wave - dominated} \end{array} \quad (2.3.8)$$

The scour development around piles due to combined waves and currents has been investigated, for example by: Wang and Herbich (1983), Eadie and Herbich (1986), Sumer and Fredsøe (2001), Rudolph and Bos (2006), Petersen et al. (2012) or Qi and Gao (2014).

Sumer and Fredsøe (2001) conducted a systematic laboratory study and compared scour depths at piles with different diameters subjected to combined irregular waves and currents. The results of Sumer and Fredsøe (2001) showed a general agreement with those of Eadie and Herbich (1986) and Wang and Herbich (1983), even though scour depths appeared

to be slightly larger, which led to the conclusion of Eadie and Herbich (1986) that the equilibrium scour depth for combined waves and currents is larger than in the current alone case. Scour depths with a wave current velocity ratio of  $U_{cw} > 0.5$  become current dominated and approach values, which are obtained in current only conditions for larger ratios of  $U_{cw} \geq 0.7$ . This can be explained due to the permanent presence of the lee-wake vortex on the downstream and its disappearance on the upstream side for current dominated conditions with  $U_{cw} \geq 0.7$ . In a wave dominated regime for  $U_{cw} < 0.5$  with values approaching zero, scour depths close to wave only conditions are obtained. Furthermore, Sumer and Fredsøe (2001) concluded that in case of small  $KC$  numbers, a low superimposed current velocity increases the scour depth significantly, which they explained due to the presence of a more pronounced horseshoe vortex. Whereas for larger  $KC$  numbers, the influence of a current superimposed on waves is insignificant. Rudolph and Bos (2006) studied the scour depth around piles due to combined waves and current for lower  $KC$  numbers of  $1 \leq KC \leq 10$  and thus complemented the data of Sumer and Fredsøe (2001). They additionally proposed an improved empirical expression to predict the equilibrium scour depths due to combined waves and currents. Petersen et al. (2012) studied the time scale of the scour development for combined waves and current and found a significant increase of the time scale for waves superimposed on a current. Qi and Gao (2014) conducted systematic tests regarding the scour development and pore-pressure around cylindrical piles with a large diameter, for a  $KC$  regime of  $0.44 \leq KC \leq 3.65$ . In general, the test results revealed larger scour depths for combined waves and current conditions than under the individual load of wave only or current only conditions. Qi and Gao (2014) also concluded that the maximum flow velocity was much larger for a following current than for an opposing current, which affects the time dependent scour development and equilibrium scour depth.

## 2.4 Scouring around complex foundation structures

Groups of slender piles are widely used in the field of offshore engineering or marine structures. The understanding of related scouring processes and scour depths around vertical pile groups is important as a basis for a better understanding of scouring mechanisms of more complex structures as jackets and tripods and in particular for tripile and pile cap foundations which consist of a group of vertical piles. Bearing this in mind, the following chapter 2.4.1, first gives an overview on studies related to scouring processes around pile groups in general. Chapter 2.4.2 then focuses on scouring mechanisms and interference effects around two piles, which are found to be fundamental for a better understanding of more complex foundation structures such as jacket-type foundations. Finally, chapter 2.4.3 gives an overview on existing studies related to scouring around jacket and tripod foundations.

### 2.4.1 *Scour around pile groups*

**Wave induced scour around pile groups** Scouring around pile groups due to regular waves have been studied by Sumer and Fredsøe (1998). Apart from the Keulegan-Carpenter number and the pile diameter, they found the scour hole mainly dependent on the pile spacing  $G/D$  ( $G$ : gap;  $D$ : diameter) and the pile group orientation. Within the framework of the investigation, a variation of the Keulegan-Carpenter number, the pile spacing and pile group arrangement were investigated. As the pile spacing decreases, the interference between the piles is increasing and the flow and scouring effect around the pile group behaves as the flow near a single body. Sumer and Fredsøe (1998) concluded in their study, that this interference under waves is disappearing for pile spacings of  $G/D > 1-3$  (depending on the pile group arrangement), which was confirmed by Liang et al. (2013) for a group of two piles with a ratio  $G/D > 3$ . Furthermore, Sumer and Fredsøe (1998) found that the scour depths can be increased by a factor of 3 (for  $KC \approx 10$ ) in combination with small pile spacings, which can increase on a factor of 10 for small  $KC$  numbers. Similar to scour depths around a single pile, scour depths around a pile group increase with a rising  $KC$  number for a given pile spacing and pile group orientation.

A field study of Bayram and Larson (2000) verified this by surveying a pier at the Pacific coast of Japan. The results generally agreed with the laboratory study of Sumer and Fredsøe (1998). Bayram and Larson (2000) confirmed the major influence of the  $KC$  number on the scour depth, similar as described by Sumer and Fredsøe (1998). Building on these findings, Myrhaug and Rue (2005) proposed an approach deriving the related scour depth by investigating wave induced scouring around groups of slender piles due to random waves. Liang et al. (2013) studied scouring around pile groups in oscillatory flow of two piles in different arrangements and pile heights and derived an empirical expression to describe the reduction of the scour depth with the pile height.

**Scour around pile groups in steady currents** Scouring around pile groups in steady currents have been mainly investigated in the context of river and bridge engineering. Existing approaches to predict the scour depth around

pile groups mainly adapt empirical approaches for single piles (see chapter 2.3.2). Salim and Jones (1996) conducted laboratory experiments on the scour depth around pile groups due to steady currents, investigating different parameters, such as the pile spacing and the skew angle for submerged and un-submerged pile groups. The authors also presented a method to predict the scour depth around pile groups using the HEC-18 equation for single piles. Sheppard and Renna (2005) recommended a method to predict the scour depth around pile groups utilising the approach for single piles of Sheppard et al. (2004), with an effective width correction factor for pile groups.

Sumer et al. (2005) investigated different pile group arrangements under steady current conditions and introduced a differentiation between the local and global scour mechanism at pile groups. The authors concluded that the local scour around each pile is mainly initiated by the horseshoe vortex combined with stream line contraction at the side edges. Whereas the global scour is eroding sediment on the entire area of the pile group, which is primary caused by an increased flow velocity in the gaps between the piles combined with increased turbulence generated by the individual piles. Figure 2.4.1 (b), reproduced from Sumer et al. (2001), shows the ratio between the total scour depth around an  $N \times N$  pile group and the uninfluenced scour depth around a single pile. Figure 2.4.1 (a) additionally presents the global scour depth to pile diameter ratio in reference to different pile group arrangements.

Amini et al. (2012) conducted additional laboratory experiments for ten different pile group arrangements. They investigated a uniform and nonuniform pile spacing as well as the influence of the submergence ratio of the piles on the scour development. Additionally, Amini et al. (2012) further modified the correction factor introduced by Ataie-Ashtiani and Beheshti (2006) for the HEC-18 equation by distinguishing between submerged and unsubmerged piles.

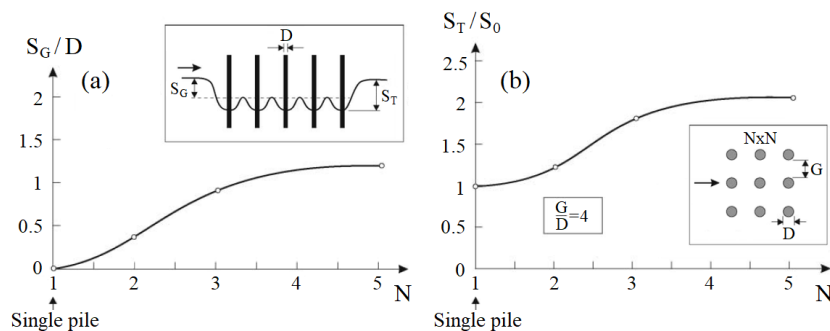


Figure 2.4.1. Global and total scour depth for an  $N \times N$  pile group in a steady current for live bed conditions, (a) maximum global equilibrium scour depth to pile diameter ratio ( $S_G$  as the global scour depth and  $S_T$  the total scour depth); (b) the maximum of the total equilibrium scour depth to single pile  $S_0$  scour depth ratio (pile spacing  $G/D=4$ ), reproduced figure from Sumer et al. (2001) with permission, Copyright © 2001 Elsevier.

Reviews on the subject of scouring around pile groups due to steady currents have been carried out by Hosseini and Amini (2015) and Baghbadorani et al. (2017) which give a good overview on existing studies.

## 2.4.2 Scouring mechanisms and interference effects at two piles

The following subchapter describes flow and scouring mechanisms around a group of two cylinders. These interference effects are fundamental to better understand scouring around more complex foundation structures, e.g. as jacket-type foundations. Similar to a tandem arrangement of two piles, the downstream located piles of a jacket structure are biased by the upstream positioned piles and structural elements, which will be discussed in more detail in chapter 3. Furthermore, it is interesting to compare the variation of scour depth with an increasing pile spacing for a side-by-side arrangement of two piles with local and global scour depths of a jacket structure.

In the present chapter, scouring mechanisms and interference effects around tandem and side-by-side arrangements of two piles are discussed (see Fig. 2.4.2). The influence of a staggered pile arrangement on flow patterns and scouring mechanisms can be found in the relevant literature presented in the following chapter. In the interests of consistency and simplification, the spacing between the cylinders is defined as the gap width,  $G$  for both cases.

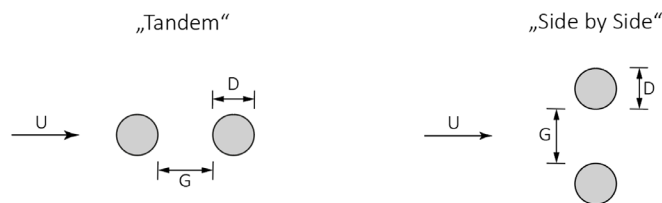


Figure 2.4.2. Definition sketch. Two circular cylinders with an equal pile diameter in a tandem and side-by-side arrangement.

### Scouring mechanisms and interference effects in tandem arrangement

Sumner (2010) distinguishes the flow around two piles in a tandem arrangement into three regimes: the “extended-body” regime, the “reattachment” regime and the “co-shedding” regime (see Fig. 2.4.3). For small pile spacings between the upstream and downstream located pile of  $G/D < 2$ , the two cylinders behave as a single or “extended-body”. The shear layers which are separated from the upstream cylinder are forced to wrap around the downstream positioned cylinder, but do not reattach onto the surface until they are rolling up or transforming into Kármán vortices (Sumner, 2010). For intermediate pile spacing ratios of about  $2 < G/D < 5$  (reattachment regime), shear layers formed by the upstream cylinder are no longer able to enclose the downstream located cylinder, vortices are now formed in the former stagnant fluid gap region and the shear layers reattach onto the cylinder (Sumner, 2010). At larger pile spacings of about  $G/D > 5$  (co-shedding regime) the downstream positioned cylinder is sufficiently far away from the upstream cylinder that vortex shedding from the upstream cylinder is developing. The downstream cylinder is now charged with the periodic collision of shed vortices from the upstream cylinder (Sumner, 2010). The flow field around the rear pile is influenced due to the obstruction of the flow, as described above. The given ranges of pile spacings can vary, e.g. due to a change in the Reynolds number, roughness, shape or other experimental conditions.

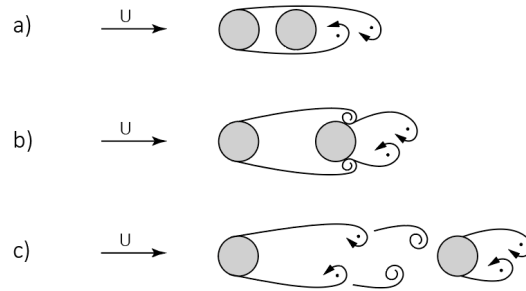


Figure 2.4.3. Simplified sketch of the flow pattern for two cylinders in tandem arrangement. a) extended-body regime,  $G \approx 1-2D$ ; b) reattachment regime,  $G \approx 2-5D$ ; c) co-shedding regime,  $G \geq 5D$  (redrawn figure, similar to Sumner, 2010).

Beyond the aforementioned flow regimes, the flow can also be influenced due to a change in the flow pattern based on the eroded or deposited sediment in front of the pile. The reinforcing effect (see Fig. 2.4.4) describes the increase of sediment transport in the vicinity of the upstream pile (Beg, 2008; Hosseini and Amini, 2015). The scour holes including the side slope of each local scour hole are overlapping in an area with an increased flow velocity and turbulence, which results in an increased erosion of sediment in between the piles and a change in the exit path of the flow. A sheltering effect at the downstream located cylinder may result from the obstruction of the flow, described in the aforementioned paragraph as well as from a deposition of sediment in front of the downstream positioned cylinder (Fig. 2.4.4). The latter effect causes a direction change of the flow, leading to a reduction in the power of the horseshoe vortex and a decreased erosion of sediment (Hosseini and Amini, 2015).

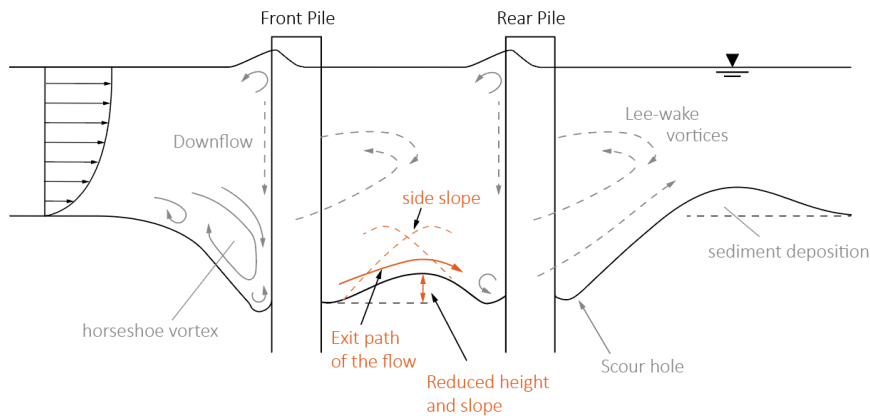


Figure 2.4.4. Sketch of the scour around two piles in tandem arrangement, highlighting the exit path of the flow, the reduced height and slope as well as the theoretical slope for one pile in orange to explain the reinforcing and sheltering effect.

Beg (2008) did a comprehensive study on the scour development under currents around two and three piles in various arrangements, including the tandem arrangement. The study of Beg (2008) is interesting for the present thesis as a large variety of pile spacings was investigated, unlike similar studies on this subject. Figure 2.4.5 was redrawn with data from Beg (2008). The figure shows the variation of the relative scour depth of two



piles in tandem arrangement with a varying pile spacing, starting with a ratio of  $G/D=0$  and incrementally increasing on up to  $G/D=90$ . The Figure reveals an increase of the scour depth at the front pile of up to 17% for  $G/D=1.5$  and a reduction of scour depth at the rear pile of up to 33% for  $G/D=12.5$ .

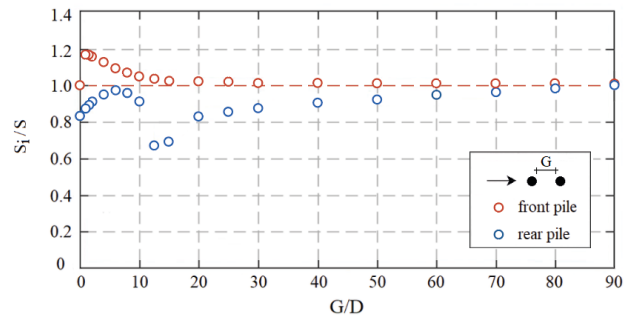


Figure 2.4.5. Variation of the relative scour depth  $S_i/S$  at two piles of the same size in tandem arrangement with varying pile spacing  $G/D$  for steady current clear-water conditions (where  $S_i$  = scour depth at the front or rear pile and  $S$  = scour depth at an isolated single pile), redrawn figure from Beg (2008).

Furthermore, Fig. 2.4.5 shows a considerable influence of the upstream positioned pile on the downstream located rear pile for distances of up to 80 times the pile diameter. Ataie-Ashtiani and Beheshti (2006) observed scouring similar to a single body for pile group spacings of  $G/D \leq 0.15D$  and observed a reduction of the interference effect between the piles for  $G/D > 2-4$ .

### Scouring mechanisms and interference effects in side-by-side arrangement

In case of a side-by-side arrangement of two cylindrical piles Sumner (2010) distinguishes the flow and vortex patterns into the “single bluff body” regime, the “biased” flow pattern and the flow regime with “parallel vortex streets” (see Fig. 2.4.6). The “single bluff body” regime is characterised by pile spacings of about  $0 < G/D < 0.1-0.2$ , where the two cylinders behave similar a single body, with one horseshoe vortex for both piles, as the gap between the piles is too small to generate a horseshoe vortex for each pile. The “biased” flow pattern in case of intermediate pile spacings of about  $0.1-0.2 < G/D < 1-1.2$ , in which the two piles have an asymmetrical or “biased” vortex pattern. In this condition, one of the piles has a smaller wake with a higher vortex frequency and an increased drag coefficient, combined with a deflection of the biased flow between the gap of the piles and a compression of the horseshoe vortex in between the piles. The flow regime with “parallel vortex streets” for about  $G/D > 1-1.5$ , in which both piles start to behave as independent piles with vortex shedding at the same frequency. With a growing pile spacing, the flow and vortex pattern, including the horseshoe vortex becomes increasingly independent and less compressed for each pile. However, if both piles are still in close proximity, shed vortices can still influence each other, which can lead to different anti-phase or in-phase vortex formations (Sumner, 2010). It is noted that the given ranges of the pile spacings might vary depending on the Reynolds number and each specific experimental condition.



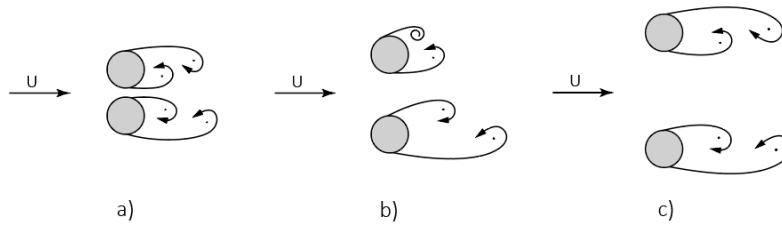


Figure 2.4.6. Simplified sketch of the flow pattern for two cylinders in a side-by-side arrangement. a) single bluff body regime,  $G \approx 0-0.2D$ ; b) biased flow pattern,  $G \approx 0.2-1.2D$ ; c) parallel vortex streets,  $G \geq 1.2D$ , (redrawn figure, similar to Sumner, 2010).

Sumer and Fredsøe (2002) showed experimental results of two piles in a side-by-side arrangement which reveal an increase of 5% of the flow velocity in the gap between the two piles in respect to the case of a single pile (with  $G/D = 4$ ). Beg (2008) also studied two piles in a side-by-side arrangement and found that for  $G/D=0$ , the scour depth compared to an isolated single pile is  $S_i/S \approx 2$ .

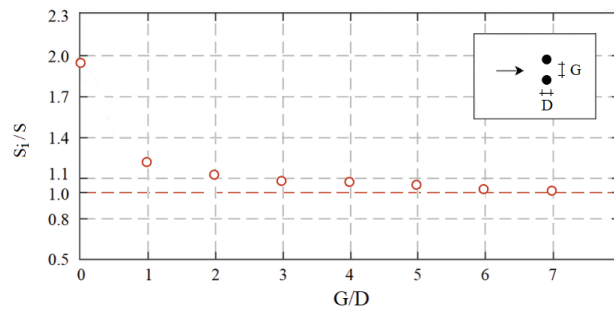


Figure 2.4.7. Variation of the relative scour depth  $S_i/S$  at two piles of the same size in side-by-side arrangement with varying pile spacing  $G/D$  for steady current clear-water conditions (where  $S_i$  = scour depth at one of both piles and  $S$  = scour depth at an isolated single pile), redrawn figure from Beg (2008).

For slightly larger pile spacings of  $G/D=1$  the scour depth decreased significantly on about 121%, while even larger pile spacings of  $G/D=6$  led to a scour depth smaller than 105% (see Fig. 2.4.7). These findings generally correspond to the information given by Sumner (2010), described above, which stated that a direct interaction of flow patterns is given in the “single bluff body” and “biased” flow regime for about  $G/D < 1-1.5$  and also corresponds to findings given for example in Hirai and Kuruta (1982) or Breusers (1972), which state that hydrodynamic interactions are relatively small for distances larger than  $6D$ .

However, these findings should not be transferred directly as a border of influence for global scour for more complex foundation structures as done in Bolle et al. (2012). In fact, these findings showcase that additional erosion and global scour in between the piles of more complex foundation structures (as jacket-type foundations) comes from the additional structural elements as diagonal or horizontal braces.

### Scour around two piles in combined waves and currents

Qi et al. (2019) investigated the influence of combined waves and current on the local scour at groups of two piles and compared these tests with experiments under current only conditions and PIV measurements. The authors conducted laboratory experiments, varying the pile spacing  $G/D$  at different angles from  $0^\circ$  (tandem arrangement) to  $90^\circ$  (side-by-side arrangement). They concluded that maximum scour depths under currents alone and combined waves and current conditions are generally in agreement for angles of  $0^\circ$  and  $30^\circ$ . In contrast an arrangement with an angle of  $60^\circ$  and  $90^\circ$  led to scour depth increase of up to 30% in case of combined waves and currents. Qi et al. (2019) found that the maximum swirling strength (which is a measure of the vorticity) of the horseshoe vortex (HSV) at two piles in a side-by-side arrangement with  $G/D=0$  (no gap) was about 45% larger than the single pile case HSV. While the maximum swirling strength of the HSV of two piles in a tandem arrangement was observed to be significantly lower than at a single pile, which they argued to be responsible for the reduced scour depth in tandem arrangements.

#### 2.4.3 Scour around jacket and tripod foundations

The estimation of scour depths around complex offshore foundations as tripods or jacket-type foundations often follows a classical scour depth formulation (see chapter 2.3), derived for single piles (Bolle et al., 2012). Due to the complexity of the prevalent processes, these approaches are affected by large uncertainties if they are applied to complex foundation structures. This obvious inconsistency can lead to an uncertain prediction (Rudolph et al., 2004) and thus to over- or underestimated local scour depths around the main piles. As for example shown by studies of Rudolph et al. (2004) or Baelus et al. (2019), complex foundation structures can also impose a superposition of global scouring processes, contributing to subsidence of the surrounding seabed as well as to increased local scour depths. In comparison to the knowledge about single pile or pile group foundations, only a limited understanding exists regarding the scour development at jacket-type and tripod foundations.

**Scour around jacket foundations** Rudolph et al. (2004) investigated field measurements of a jacket-type production platform and a jacket-type wellhead structure. The foundation structures were installed in water depths of 25m in the southern North Sea in front of the Dutch coast (at the so-called block L9). The production platform is based on six legs with  $D_1=1.5\text{m}$  with spacings of 16m and 20m between the legs. The jacket-type wellhead platform has four legs with a diameter of  $D_2=1.1\text{m}$  and spacings of 20m and 17m respectively, see Fig. 2.4.8 for the seabed structure connection. Both jacket structures were founded with additional post piles ( $D_{1,post}=1.5\text{m}$  and  $D_{2,post}=1.2\text{m}$ ), diagonal braces (approx. 0.55m) as well as horizontal braces close to the seabed (approx. 0.65m). Measurements of the seabed topography revealed local scouring up to 5m deep, exceeding the predicted scour depth with an empirical approach for single piles by a factor of 3–4 times.

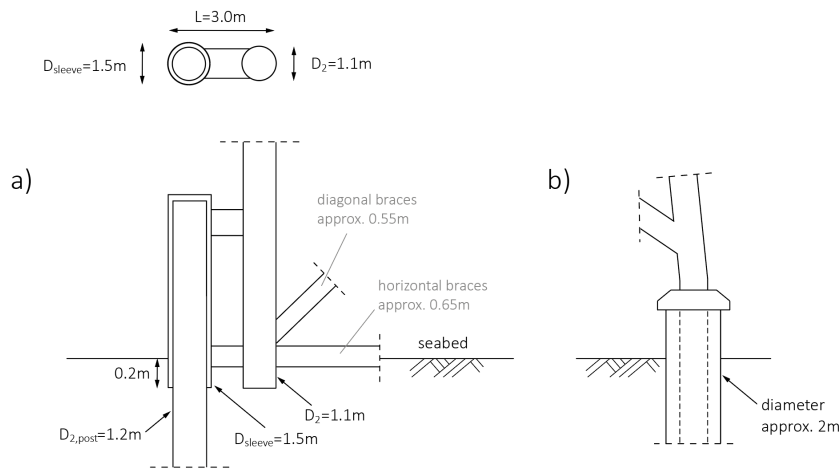


Figure 2.4.8. Schematic sketch (not to scale) of a jacket platform and the seabed a) of connection between the wellhead jacket platform and skirt piles at the seabed, in the text referred as post piles (redrawn figure, similar to Rudolph et al., 2004) b) of a seabed pile and the Jacket pin pile, in the text referred as pre-piled foundation (redrawn figure, similar to Baelus et al., 2019).

According to Rudolph et al. (2004), the bathymetric surveys also revealed global scour holes around the whole structure with an extent of about 50 m (40 times the pile diameter). The authors explained the increased scour depths with the flow disturbance of near-bed structural elements (see Fig. 2.4.8, a). The authors also clarified that comparable scour depths with a factor of up to 3-4 times the single pile scour depth prediction have been observed at different jacket structures in the North Sea. This indicates the measurements shown in Rudolph et al. (2004) are no exception.

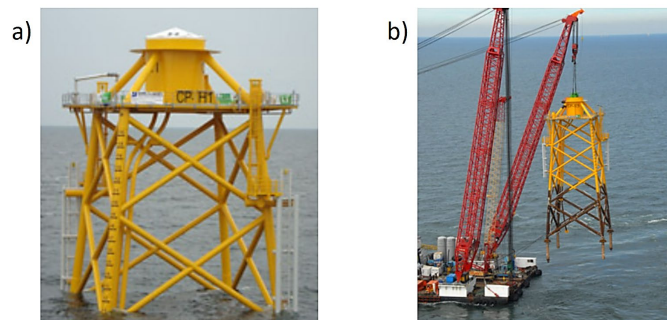


Figure 2.4.9. Photos of the jacket foundation of the C-Power wind farm, located about 30 km off the Belgian coast on the Thornton Bank, North Sea. This type of jacket foundation was investigated in Bolle et al. (2012) and Baelus et al. (2019) (see also Fig. 2.4.8, b for a sketch of the seabed structure connection). a) installed jacket structure; b) offshore installation of the jacket structure. Reproduced figures with permission, Copyright © C-Power NV.

Bolle et al. (2012) analysed the seabed topography around a jacket structure of the C-Power wind farm on the Thornton bank in the southern North Sea (see Fig. 2.4.9) with field measurements of multi-beam echo sounders. The investigated jacket structures were installed via a pre-piled foundation into the seabed. The seabed pile of the structure had a diameter

of approx.  $D=2\text{m}$  (see Fig. 2.4.8, b), a spacing between the pile centers of 18m and a distance between the lowest nodes of the jacket and the bed topography of 2.5-5.0m. Bolle et al. (2012) found an average scour depth of  $S/D=0.7-0.95$  as well as a maximum scour depth of about  $S/D=1.35$  only six months after the installation of the jacket structure. The authors also conducted an estimation of scour depths based on studies and existing prediction approaches for monopiles and pile groups (Breuers, 1972; Hirai and Kuruta, 1982; Sumer and Fredsøe, 2002). These studies also report only small hydrodynamic interactions between pile groups in a side-by-side arrangement if the distance between them exceeds about six times the pile diameter (see also chapter 2.4.2). However, as further outlined in chapter 4.1, these statements should not be transferred directly to more complex foundation structures. Chen et al. (2014) conducted laboratory experiments under tidal currents and perpendicular approaching waves with a jacket-type model of a foundation structure for conditions at the coast of Taiwan. The authors simulated shallow water conditions of 12-16m water depths, wave heights of 2.5-6.8m with wave periods of about 11.7s. The jacket structure model was scaled in 1:36, with a pile spacing of approx. 14m in real scale, a comparable large diameter of the main piles of  $D=2.08\text{m}$  and comparable thin near-bed diagonal braces of approx. 0.5m. In consequence, the influence due to the obstruction of the flow, stream line contraction and additional near-bed turbulence is expected to be less pronounced for the model investigated in Chen et al. (2014) as for example for structures with larger diameters or additional post piles (see e.g. Rudolph et al., 2004). Due to these effects, lower scour depths of  $S/D=0.2-1.3$  were measured under the combined load of waves and tidal currents.

Baelus et al. (2019) presented field data of the same jacket structure (see Fig. 2.4.9) of the C-Power wind farm on the Thornton Bank as studied by Bolle et al. (2012). Bolle et al. (2012) focused more on the short-term evolution of the developing scour (on up to six months after the installation), while Baelus et al. (2019) studied the long-term evolution as well as the continuous scour development and the associated hydrodynamic conditions. The authors studied multiple measurements of the bed topography at different points in time over a period of three years. A bathymetric survey two years after the installation of the structure revealed global scouring in a comparable extent and depth as shown in Rudolph et al. (2004). Baelus et al. (2019) also studied the different hydrodynamic parameters and found a large influence of the current velocity, the orbital velocity, and the wave direction on the continuous scour development. Depending on the wave direction, different changes of the scour depth were observed, while the influence of storm conditions was limited. Ahmad et al. (2020) used REEF3D, a three-dimensional open source software, solving the RANS equations with  $k-\omega$  turbulence closure and a morphological model to simulate scouring around a jacket structure. Good simulation results have been achieved, in comparison to the complexity of the simulated multiphase problem. The numerical model was validated on local scour measurements around a vertical pile in a steady currents and waves and afterwards applied on steady current and wave induced simulations of the scour development around a vertical jacket-type structure.

**Scour around tripod foundations** Stahlmann and Schlurmann (2010) and Stahlmann (2013) conducted 1:40 laboratory experiments in intermediate scale, 1:12 physical model tests in large scale and compared the model tests with measurements in the field. These field measurements have been conducted with fixed single beam echo sounders and ship-based multi-beam echo sounders. The maximum equilibrium scour depth at a tripod in 30m water depths were measured to  $S/D=1.1$  and 1.6 at the piles and  $S/D=3.0$  below the main column. The diameter of all three piles in the field is  $D=2,3\text{m}$ . The physical model tests in the large wave flume GWK have been conducted with a maximum amount of 3500 waves with regular waves and spectra. However, the large-scale experiments and field measurements are overall in good agreement, as local and global scour holes are matched in an adequate quality. Also, areas with deposited sediment are similar between the experiments and in the field. Nevertheless, scour depths in the physical model are in general smaller as measurements in the field. Stahlmann (2013) argues, that a main reason for the smaller scour depths are the simplified hydrodynamic conditions in the laboratory tests, as experiments have been conducted without the influence of a current. Stahlmann (2013) additionally presented a three-dimensional fluid flow model, which solves the RANS equations with a  $k-\omega SST$  turbulence closure incorporating a sediment transport module simulating bed load and suspended load transport, in the framework of OpenFOAM – a three-dimensional open source software for CFD. Good simulation results of the scour development could be achieved around a circular cylinder under steady current conditions and a complex tripod foundation under regular waves. A good agreement between the physical model tests and the numerical simulations could be achieved.

Yuan et al. (2017) conducted laboratory experiments under steady flow conditions in a scale of 1:60 with a diameter of the piles of 5.4cm. The experiments were conducted in a 2.4m wide, 0.3m deep and 16.5m long flume under clear-water conditions for two current velocities, four flow depths and three angles of attack. Scour depths were measured at several positions manually with a ruler and scale marks which have been painted on the model surface. Yuan et al. (2017) found that the maximum scour depth increased with a rising flow depth and an increasing current velocity. A maximum equilibrium scour depth of  $S/D=3.2$  was reached for the highest water depths of 0.25 m and the highest current velocities. The maximum scour depths in all tripod tests of Yuan et al. (2017) have been measured at one of the tripod legs and not below the large main pile as observed in the field (see Stahlmann, 2013). Furthermore, Yuan et al. (2017) presented empirical equations to estimate the clear-water scour depth at offshore wind tripod foundations.

## 2.5 Scour protection design of granular scour protections

### 2.5.1 *Principles and Failure mechanisms*

The following chapter introduces the principles and possible failure mechanisms of granular scour protections for offshore conditions. A reliable scour prediction (see chapter 2.3 and 2.4) is important as a prerequisite for the design process of an offshore foundation structure. The scour prediction process also determines the requirement of an additional scour protection system. If the estimated scour depths exceed certain threshold values, a scour protection system normally becomes the most economical option over the lifetime of an offshore foundation structure. According to May et al. (2002) and Schendel (2018) a scour protection concept can consist of scour reduction measures to optimise the flow path, structural measures which improve the structural design, a scour monitoring management program or scour protection measures. A scour monitoring management program helps to observe the actual in situ scour depths in the field, deciding if reconditioning of the scour hole has to be done (for example backfilling). The overall objective of a scour protection system is to significantly reduce the erosion of sediment around the offshore foundation structure. This reduction effect can be achieved with different measures, as for example sand or rock filled geotextile bags or container (e.g. Wilms et al., 2012), concrete mattresses or artificial plants. The classical granular scour protection system (also known as rock armour, riprap or rubble) consists of multiple layers of granular material in different sizes, including a protective armour layer (with larger stone sizes) on top and filter layers (smaller stone sizes) beneath. Due to the flexible, simple and cost-efficient installation, granular scour protection systems are the most applied protection systems for offshore foundations (Whitehouse et al., 2011). Due to the probabilistic nature of the erosion process itself, the calculation and design of scour protection systems still includes a remarkable empirical nature, typically leading to uncertainties. The requirement to reduce uncertainties combined with an improved estimate of the expected failure, led to recent studies on the topic of reliability based design of scour protections (e.g. Fazeres-Ferradosa et al., 2018b, 2019a and 2019b). Schendel (2018), Chiew and Lim (2000) as well as Sumer (2014) give a comprehensive description of failure mechanisms associated with granular scour protection systems. The main failures can be categorised as follows:

- **Shear failure** The armour layer stones are not large or heavy enough to withstand the hydraulic force acting on the grain.
- **Winnowing failure** The finer bed material is washed out through the voids of the coarser stones, potentially leading to sinking of the scour protection. According to Nielsen et al. (2011) the horseshoe vortex is the primary driver of winnowing erosion at cylindrical piles. Thus, the winnowing erosion can be controlled with the thickness of the scour protection layers.



- **Edge scour / failure** Scour development at the edges of the scour protection layer, due to changes in the roughness and elevation. Comprehensive laboratory tests on edge scour development have been conducted by Petersen et al. (2015). Despite the thickness and width of the scour protection, the pile diameter is also an important factor which controls the magnitude of the edge scour.
- **Bed-form induced failure** Bed destabilization of scour protection due to fluctuations of large bed-forms under live bed conditions (Chiew and Lim, 2000). Lauchlan and Melville (2001) found that the bed-form induced failure can be reduced if the scour protection layer is positioned below the seabed level.
- **Sinking due to liquefaction** Sinking of the scour protection due to reduced soil bearing capacity. Liquefaction is mainly generated by the buildup and overload of pore pressure (residual liquefaction) as well as by the upward vertical pressure gradient in the soil, which results from the passage of a wave through (momentary liquefaction) (Sumer, 2014).

### 2.5.2 *Damage analysis of dynamic scour protections*

A granular scour protection system prevents the seabed against erosion by hydrodynamic loads of waves and currents. The scour protection design has to consider different failure mechanisms (see chapter 2.5.1). The majority of granular scour protections are typically designed to be statically stable, thus no stone movement is allowed under all circumstances leading to conservative, large stone sizes (Soulsby 1997; Whitehouse 1998; Den Boon et al. 2004; De Vos et al. 2011). A comprehensive overview of design guidelines and statically stable design approaches is given in Schendel (2018). Damage analysis and damage characterisation in marine offshore structures finds its genesis in the studies performed e.g. on breakwaters, offshore foundations or similar coastal protection structures. Different studies have been carried out, introducing and utilizing different approaches, e.g. the eroded volume, the related area of moved armour units (Thompson and Shuttler, 1975; Broderick, 1984 or Van der Meer, 1988) or the erosion depth of the armour layer (Hofland et al., 2014 or De Almeida et al., 2019).

New design approaches allow a limited movement of armour layer stones, reducing the size and weight of the stones, and ultimately lead to significantly lowered costs over the life time of the foundation structure. The following paragraph focusses on the damage analysis and assessment of dynamically stable design approaches, which are subject of recent research and development. Den Boon et al. (2004) conducted physical model tests with statically and dynamically stable scour protections. They introduced a new design paradigm for scour protections around offshore foundations, initially introduced by Van der Meer (1988) which studied the damage at breakwaters, using small stone sizes and allowing a limited movement of the stones. Based on these concepts De Vos et al. (2012) conducted extensive physical model tests under combined wave and current conditions with irregular waves and derived a design approach to clearly define damage and formulate a damage criterion for dynamically stable

scour protections. The threshold criteria, applied in De Vos et al. (2012) defines the failure of the scour protection adopted from Den Boon et al. (2004). This failure criterion states that an ultimate failure of the scour protection is reached, if the filter layer below the armour layer is exposed over an area larger than  $4d_{50}^2$  ( $d_{50}$  being the average diameter of the stone). This failure criterion was also applied in subsequent studies (e.g. De Schoesitter et al., 2014; Whitehouse et al., 2014; Fazeres-Ferradosa et al., 2018a Schendel et al., 2018). According to De Vos et al. (2012), the protective armour layer of a scour protection can be designed for a reasonable and still acceptable damage at the scour protection, with the three-dimensional damage number  $S_{3D,sub}$  and guidelines presented in De Vos et al. (2012), based on the concept of Van der Meer (1988) in breakwater design and damage assessment:

$$S_{3D,sub} = \frac{V_e}{d_{n,50} A_{sub}} = \frac{V_e}{d_{n,50} \frac{\pi D^2}{4}} \quad (2.5.1)$$

The damage number  $S_{3D,sub}$  relates the eroded volume  $V_e$  to the surface area of a sub-area  $A_{sub}$  times the nominal median stone diameter, with  $D$  as the pile diameter. For a damage number of  $S_{3D,sub} = 1.0$ , the scour protection layer decreases over the considered sub-area by a depth of  $d_{n,50}$ . According to De Vos et al. (2012) the damage of a scour protection is calculated for each sub-area with Eq.(2.5.1) and the damage number  $S_{3D}$  is defined as the highest damage considering all sub-areas.

$$S_{3D} = \max_{i=1}^{\#sub-areas} (S_{3D,sub,i}) \quad (2.5.2)$$

De Vos et al. (2012) also introduced an empirical expression to estimate the damage number at scour protections as a function of the actual wave and current condition. Eq. (2.5.3) was derived from a parameter regression.

$$\frac{S_{3D}}{N^{0.243}} = 0.00076 \frac{U_w^3 T_{m-1.0}^2}{\sqrt{gh}(\rho_s/\rho - 1)^{3/2} d_{n,50}^2} + a_1 \left( -0.022 + 0.0079 \frac{(\bar{U}/w_s)^2 (\bar{U} + a_4 U_w)^2 \sqrt{h}}{g d_{n,50}^{3/2}} \right) \quad (2.5.3)$$

With  $N$  as the number of waves,  $T_{m-1.0}$  as the spectral wave period ( $T_{m-1.0} = T_p/1.107$ ),  $w_s$  as the fall velocity of the stone. Parameter  $a_1$  and  $a_4$  are related to the flow velocity, stone size and flow direction. A more detailed description of the derivation of Eq. (2.5.3) as well as an explanation of parameter  $a_1$  and  $a_4$  are given in De Vos (2008) and De Vos et al. (2012). Eq. (2.5.3) can be adopted to estimate the stone size for a given damage number.



## 2.6 Spatial analysis of sediment displacement processes

A main part of the present thesis, including several peer reviewed journal papers addresses the development of methods to analyse and predict spatial scour depth and deposition changes of the seabed topography around offshore foundations. Therefore, the following chapter 2.6.1 gives background information on spatial laboratory measurement techniques to capture bed elevation changes. Chapter 2.6.2 gives an overview on spatial analysing methodologies in the field of coastal, ocean and river engineering.

### 2.6.1 *Spatial measurement techniques*

The most basic measurement techniques to quantify the spatial change of a bed topography around an offshore foundation are rulers and scale marks (see also Porter et al., 2014) or sediment gauges, which are nowadays rarely used as a measurement technique to quantify scouring processes. An exception could be, if no other devices can be considered, for reasons of costs or difficult laboratory conditions. Yuan et al. (2017) used a ruler and scale marks and Stahlmann (2013) utilised sediment gauges to measure the scour depth below the near-bed braces of a tripod foundation.

A laser probe bottom profiler or laser distance sensor (LDS) is a more advanced and accurate measurement technique with an accuracy  $<1\text{mm}$  (Stahlmann, 2013). An LDS can be moved with a positioning system in x and y direction, allowing it to measure a specific topography. An LDS measures point to point non-intrusively with high vertical accuracy and can work under water if the device is waterproof. A disadvantage is that every measuring point has to be measured individually one after another. This significantly limits the spatial accuracy in x and y axis (see e.g. Hartvig et al., 2010; 1,5 cm grid spacing,  $\sim 5000$  data points). If the LDS is installed vertically on a positioning system, the LDS is not able to measure below the model (see Stahlmann and Schlurmann, 2010). Link et al. (2008) used an LDS to measure the scour hole radius around the pile. Therefore, the authors positioned the LDS inside a transparent cylinder, aligned in horizontal and radial direction.

Overcoming the rudimentary approach of rulers and singular measurements of LDS, 3D Laser scanning is a key technique providing a sub-millimeter accuracy in the vertical dimension (here z axis) combined with a very high horizontal accuracy in the x and y plane. Nowadays, terrestrial laser scanners can easily reach more than 100 million data points per scan (e.g. Focus 3D, FARO, Lake Mary, FL, USA). This enables quantifying spatial erosion processes in very high accuracy and allows various applications for different research topics (e.g. Hodge et al., 2009; Schendel et al., 2015; Yagci et al., 2017). Furthermore, it is possible to merge scans from different angles into one single scan, reducing the opacity. This also enables to successfully scan surfaces below or around more complex objects. Smith et al. (2012) even measured and processed terrestrial laser scans through the water surface, which requires an additional correction of the measured point cloud data, taking the systematic error from refraction into account. A different possibility is an underwater laser scanner, as for example the Seatronic 2G Robotics

ULS-200 as used by HR Wallingford. Underwater laser scanners have the benefit that no water has to be drained in between the tests. Under certain conditions (e.g. fast drainage of the water), the drainage of the water of a laboratory flume or tank can represent an additional uncertainty, as the test could be influenced (additional erosion during the drainage, additional deposition of the suspended load in the water). A disadvantage of an underwater laser scanner is a comparable low data density, leading to a coarser resolution compared to terrestrial laser scanner and a considerably smaller scanning area which makes the use of an automatic positioning system mandatory for larger scanning areas.

Photogrammetry is a suitable and less expensive alternative to generate high resolution digital elevation models (DEMs) (e.g. Umeda et al., 2008; Porter, 2016; Bouratsis et al., 2017). A high resolution of about ~3-5 mm grid size is achievable for laboratory conditions. Although the resolution might be below a 3D laser scanner, photogrammetry has various other advantages besides lower costs. With photogrammetry it is considerably easier as with a 3D laser scanner to correctly capture also very complex or very large surfaces. Bouratsis et al. (2017) used submerged cameras, which enabled spatiotemporal photogrammetric measurements of the bed topography around a cylinder.

An alternative measurement technique are single or multi beam echo sounders, measuring underwater (e.g. utilised in Stahlmann, 2013 or Porter et al., 2014). Although measurements can be affected by suspended sediment (Porter et al., 2014), echo sounders generally work much better than other instruments under actual test conditions - including tests with suspended sediment.

### 2.6.2 *Spatial analysing methods of bed topographies*

Studies and analyses on scouring processes around offshore foundations are still conducted more frequently via a pointwise or maximum scour depth analysis (see chapter 2.3, 2.4). In recent years, spatial measurement techniques (see chapter 2.6.1) are more commonly used to quantify and assess scour around offshore foundations. Even though these measurement techniques are increasingly applied, very few articles focus on the analyses of spatial erosion or deposition processes of sediment, via a systematic utilization of digital elevation models (DEM). Bearing this in mind, the following chapter reviews different interdisciplinary studies related to spatial analysing methods of bed topography DEMs, which go beyond the observation of bathymetric patterns.

Spatial analysing methods using DEMs have been applied in various studies in the field of hydraulic engineering and river morphology. In search of alternatives of the traditional grain size approach, various studies have been conducted in the last twenty years to characterise bed roughness (Powell, 2014). Powell (2014) made a comprehensive review on the scientific progress on flow resistance in gravel-bed rivers. Marion et al. (2003) adopted geostatistical methods to analyse the three-dimensional river bed surface during the armouring process and introduced new measures of bed surface characterisation. The measurements have been conducted with an LDS and an automated positioning system, which

measured a matrix of 384 x 384 point elevations, a degree of detail superior to comparable studies at this time period. The grain scale properties of the bed have been investigated in depth by Marion et al. (2003) with the probability density function and structure functions of the bed elevations. Structure functions are used to study the spatial structure of a surface, to reveal spatial correlations for different distances in 1D or 2D over the roughness height. Structure functions are used to find and characterise spatial scales and local concentrations in the patterns. Hodge et al. (2009) studied and introduced different methods to analyse DEMs, using terrestrial laser scanning data to collect the in-situ grain scale topography in a river. The introduced methodologies are: (a) the distribution of surface elevations; (b) the semivariance of the surface elevation (a structure function); (c) the surface inclination and aspect which identified smaller scale structures and grain-scale structures as the DEM has been detrended, and finally (d) the grain orientation. The introduced articles (Marion et al., 2003; Hodge et al., 2009; Powell, 2014) are representative examples on the field of geostatistical and morphometric studies on gravel bed river surfaces.

An ongoing multidisciplinary topic is also bed topography identification and the characterisation of dune migration. This topic is of interest, since more than a century (Cornish, 1901) and is still actively under research in the field of oceanography, geology, river morphology or coastal engineering. With the availability of high-resolution bathymetries, new spatial analysing methods evolved to analyse three dimensional dunes (Parsons et al., 2005). A good overview of the state of the art on this topic, is given by Best (2005) as well as some of the latest findings presented by Lefebvre and Winter (2021). A motivation of bathymetric studies addressing dune migration can include the general understanding of prevailing morphodynamic bedforms and topographic trends, e.g. in engineering to secure shipping in navigational waterways (Scheiber et al., 2021). Lisimenka and Kubicki (2017) derived bedform characteristics as the length and height of dunes, from spectral analyses of the spatial bed topography. The method describes the primary and secondary spectral component of an undulating seabed topography without the utilisation of band-pass filters. Another example of bedform related topographic analyses is given by Scheiber et al. (2021), which developed a method to analyse topographic bedforms of compound dunes with a repetitive evaluation of unfiltered bed elevation information in relation to five predefined length classes. Within this analysis, the height, length, crest and trough depths or bed slope asymmetries and bed sediment changes can be calculated. The introduced articles (Lisimenka and Kubicki, 2017; Scheiber et al., 2021) are recent examples, which are interesting in this context to get an overview of the variety of spatial analysing methodologies.

Spatial analysing methodologies utilising DEMs have also been applied in the field of coastal and ocean engineering for damage analysis in rubble mound scour protections. These approaches have been introduced in chapter 2.5.2.

Despite the studies, introduced in chapter 2.5.2, only few research articles concentrate on a systematic spatial analysis of erosion processes around offshore foundations. Margheritini et al. (2006) introduced a structural reference volume, a cube with an edge length of one diameter

of the pile, to normalise the eroded volume of scour holes, which enabled the comparison between different scales and models. The authors conducted tests under unidirectional and tidal currents and applied this dimensionless scour volume parameter to quantify the shape and the eroded volume of the scour hole. Margheritini et al. (2006) found for comparable flow velocities differences in the shape as well as larger eroded volumes for the tidal test case. Hartvig et al. (2010) introduced an equation predicting the dimensionless erosion volume of a scour hole around a pile in steady currents and combined waves and currents. The authors also used the normalised erosion volume, but also complemented the study of Margheritini et al. (2006) by proposing an additional “shape factor” with which they quantified and predicted the rough scour shape (differentiation between a flat or steep scour slope angle). Bouratsis et al. (2017) studied a developing gravel bed in close proximity of a cylinder exposed to steady current clear-water conditions. The usage of submerged cameras enabled spatiotemporal measurements of the dynamic changes of the seabed topography around the cylinder, which opened up new possibilities to quantify and describe the different temporal phases of the scour development around the pile.

## 2.7 Conclusions and knowledge gaps

The literature review presented in the previous chapters provides fundamental knowledge and recent advances on the topic of scour and erosion around offshore foundation structures. Several knowledge gaps, relating to the objectives of this thesis, are summarised and described in the following paragraph. Although the literature review of chapter 2.3 and 2.4 reveals that scour around monopiles and pile groups has been studied extensively, complex hydrodynamic conditions are seldomly taken into account. Available approaches to predict the degrading effects of scour often rely on simplified hydraulic conditions. Apparently, there is a lack of knowledge regarding the general understanding of realistic hydraulic conditions on the scouring process, as for example the simulation of tidal flow conditions in a laboratory or the investigation of the influence of multidirectional waves. Evidently, there is an even larger knowledge gap regarding scouring processes around more complex offshore foundations as for example jacket-type structures. As a result of the lack of knowledge, monopile related methodologies are often applied to complex structures in practical cases. The presented literature review (chapter 2.4.3) highlights that there is a considerable knowledge gap and requirement for a better understanding, since unexpected global scour or local scour depths of 3-4 times a common monopile scour depth are no exception for complex structures e.g., as jackets. Fundamental knowledge gaps are also revealed regarding the general understanding of the scour development process, the time scale of the scouring process and the equilibrium scour depth at jacket-type structures.

Most studies which can be found regarding scouring processes around offshore wind foundations deal with the analysis of a single pointwise or maximum scour depth. Seabed changes around offshore structures can be complex in their spatial extent. Despite the important contribution of spatial data, many studies neglect this additional information or concentrate

on the illustration of the bed topography. Only very few studies focus on a systematic spatial analysis of the seabed changes around offshore foundations (chapter 2.6.2). However, several aspects regarding spatial scour depth changes as well as the analysis of erosion and deposition patterns around offshore structures remain disregarded. For jacket-type offshore foundations, those aspects include, local and global scour depths, the global scour extent, the interaction of local and global scour and the influence of differences in the structural design on spatial scour depth changes. The general lack of appropriate analysing methods hinders the assessment and prediction of spatial seabed changes around offshore structures.

The prediction of spatial and temporal scour depths is also conducted as a precondition to calculate if a scour protection is necessary. The calculation of the scour protection stability is an important aspect of the design process. Dynamically stable design approaches allow a specific level of damage on the armour layer of the scour protection. In comparison, statically stable design approaches allow no movement of armour layer stones under all design conditions. Despite the comprehensive work of De Vos et al. (2012), only few studies focus on improvements regarding stability assessment and damage characterisation. However, several aspects regarding the stability assessment itself, scale effects related to the application of results of small-scale physical model tests on prototype conditions or the use of widely graded stone material are disregarded, which demand a further investigation.



### 3.1 Wave-current-induced scouring around monopiles

An important part of the reliable design and life-time management of offshore wind foundation structures is the emergence of scour, which needs to be taken into account. However unresolved questions remain for example regarding scouring processes induced by more natural hydrodynamic conditions as for example tidal current induced scour as well as scour induced by multidirectional waves combined with a current. Findings of experiments regarding the effect of hydrograph shape on tidal current-induced scour around a monopile are presented in a peer reviewed manuscript Schendel et al. (2019), summarised in the following.

**Paper 1:** *Schendel, A., Welzel, M., Hildebrandt, A., Schlurmann, T., Hsu, T.-W. (2019). Role and Impact of Hydrograph Shape on Tidal Current-Induced Scour in Physical-Modelling Environments. Water 11, 2636.*

This article presents results of an experimental study, regarding the influence of the hydrograph's shape on tidal current-induced scour around monopile offshore foundations. The influence of different generalizations of the hydrograph's shape on the scour development has not yet been investigated in a systematic manner. Therefore, hydraulic model tests were conducted, using different hydrographical shapes, including constant unidirectional velocities, stepped and square-tide velocity signals as well as continuously changing time series. The scour development in tidal currents is unsteady and characterised by stagnating and decreasing scour depths, controlled by sediment backfilling and displacement processes which can only be reproduced by hydrographs with a varying flow direction. For an accurate representation of the final scour depth, omitting a correct scour development over time, a constant unidirectional current with a suitable flow velocity was found representative. To determine the appropriate flow velocity and thus the correct hydraulic load, the effective flow work approach has been proven to be capable to identify such hydraulic loads.

Systematic laboratory tests were also carried out to further improve the understanding, regarding the influence of multidirectional (short-crested) waves combined with an oblique current on the scouring process around a pile. Findings of a peer reviewed manuscript, Schendel et al. (2020) are summarised in the following.

**Paper 2:** *Schendel, A., Welzel, M., Hildebrandt, A., Schlurmann, T., Hsu, T.-W. (2020). Scour around a monopile induced by directionally spread irregular waves in combination with oblique currents. Coastal Engineering 161, 103751.*

Laboratory experiments were carried out to further improve the understanding and prediction related to the effect of directionally spread (3D) irregular waves on the scouring process around a monopile in combination with oblique currents. The physical model tests were conducted in the 3D wave-current basin of the Ludwig-Franzius-Institute, Hannover, Germany. Even though multidirectional and unidirectional wave spectra were produced with an identical total wave energy, clear differences could be observed in the scour depth and scouring rate. This can only be associated to the influence of wave spreading on the scouring process at the pile. Wave only hydrodynamic conditions induced by multidirectional waves led on average to a 33% reduced final scour depth compared to unidirectional waves. The final scour depth decreased with a growing wave spreading. Combined multidirectional waves and current conditions yielded slightly larger scour depths and scouring rates as conditions of unidirectional waves combined with a current. An empirical prediction approach was proposed to estimate the maximum scour depth distinguished by either multi- or unidirectional random waves and a superimposed current.

### 3.2 Wave-current-induced scouring at jacket structures

Several aspects regarding the scouring processes around complex offshore foundations are still disregarded. To the authors knowledge, only few systematic studies have been conducted, regarding the scour development at jacket-type structures in waves and current conditions. Findings of experiments on the scour development due to combined waves and current conditions around a jacket structure are introduced in a summarised paragraph of a peer reviewed article Welzel et al. (2019a).

**Paper 3:** *Welzel, M., Schendel, A., Hildebrandt, A., Schlurmann, T. (2019a). Scour development around a jacket structure in combined waves and current conditions compared to monopile foundations. Coastal Engineering 152, 103515.*

Despite of the common use of jacket structures as a favourite foundation type for different marine conditions, only few systematic studies have been conducted regarding the scour development in waves and current. Therefore, systematic hydraulic model tests were conducted on a geometric length scale of 1:30 in a wave-current basin. Irregular waves propagating perpendicular to the current were simulated. Measurements of



the scour development over time could be achieved with echo sounding devices positioned at different locations on the upstream and downstream side of the jacket structure. A systematic experimental study has been conducted with respect to a wide range of Keulegan-Carpenter numbers between 6.7 and 23.4, combined with a relative wave-current velocity ratio, ranging from wave dominated up to current dominated conditions. Insights on the scour development and time scale were given with respect of the jacket leg position, upstream or downstream located, and compared to the scour development for monopile foundations. The experiments showed generally larger scour depths at the upstream side and a lower scour depth on the downstream side for each leg / pile of the jacket structure. In addition, a global scour was observed and measured, which intensified with an increasing wave-current velocity ratio. An empirical expression is proposed as a result of the measured scour depths, to reliably predict the local scour depth around a jacket foundation in combined waves and current conditions. Observed and predicted scour depths as well as time scales are finally compared and discussed with values related to monopile foundations.

### 3.3 Influence of structural elements on scour at Jacket Structures

Furthermore, additional laboratory tests (Welzel et al., 2020) were conducted to advance the knowledge of jacket-type structure induced scour. A systematic variation of certain relevant structural elements might be a key aspect to gain a deeper understanding on scouring around complex structures, as jacket-structures. In the following paragraph this is achieved by investigating the influence of the lowest structural nodes and lowest diagonal braces of the jacket structure on the scouring process.

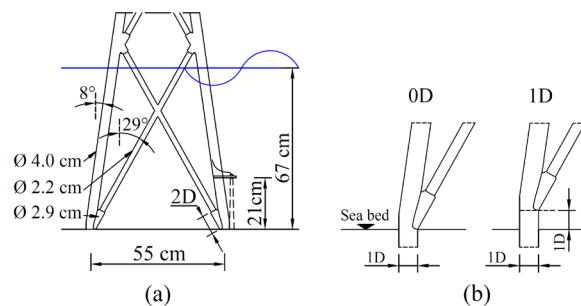


Figure 3.3.1. Schematic sketch of the investigated jacket model: a) side view, with dimensions, angles and water level,  $D = 4$  cm; b) side view on the lowest node positioned directly on seabed 0D, in comparison with a distance of 1D.

In the study presented (Paper 4), the model was installed with the lowest node ending directly on the seabed surface (within this study defined as 0D, see Fig. 3.3.1) to compare measurements of the present study with data measured under the same conditions, in a distance of 1D to the lowest node (see chapter 3.2).

**Paper 4:** *Welzel, M., Schendel, A., Goseberg, N., Hildebrandt, A., Schlurmann, T. (2020). Influence of structural elements on the spatial sediment displacement around a jacket-type offshore foundation. Water 12, 1651.*

This study advances the knowledge of jacket-type structure induced scour by revealing the influence of the lowest node and diagonal braces to the seabed on the scouring process. A laboratory study was conducted to compare the scour depths at different positions of two structural designs, distinguished in different distances of the foundation's lowest node to the seabed. Measurements of local scour depths over time have been conducted with eight echo sounding transducers located on the upstream and downstream side of the jacket. As a result, an improved empirical approach is proposed to predict the final scour depths at jacket structures, differentiating between the upstream and downstream side and additionally considering the distance of the lowest node to the seabed. The second part of this research article is pertaining to spatial analysing methods, discussed in chapter 4 and introduced accordingly in paragraph 4.2.

## SPATIAL ANALYSIS OF SCOUR DEPTH CHANGES AROUND OWF FOUNDATIONS

---

The understanding of the influence of offshore foundations on the sediment seabed environment is important as a precondition for a structurally stable and economically optimised foundation design as well as for the evaluation of impacts on the flora and fauna of the previously unaffected marine environment. Despite the large number of studies for offshore structures regarding a pointwise or maximum scour depth analysis (see chapter 2.3 and 2.4), only a limited understanding of spatial scour depth changes and deposition processes is given for offshore structures in general. However, spatial measurement techniques are nowadays more commonly used to measure seabed changes around offshore foundations (chapter 2.6.1). Although these measurement techniques are increasingly applied, very few studies concentrate on a systematic, volume-based assessment of spatial erosion or deposition patterns (chapter 2.6.2). A reason for this might also be the general lack of appropriate analysing methods, to assess, predict and compare highly complex morphological patterns.

### 4.1 Analysis and prediction of spatial scour depth changes

Systematic laboratory tests were conducted regarding the influence of combined waves and currents on the spatial erosion of sediment around a hydrodynamic transparent offshore foundation. A new approach was developed to quantify, assess and predict highly complex seabed changes around marine structures, summarised in the following paragraph of a peer reviewed article (Welzel et al., 2019b).

**Paper 5:** *Welzel, M., Schendel, A., Schlurmann, T., Hildebrandt, A. (2019b). Volume-based assessment of erosion patterns around a hydrodynamic transparent offshore structure. Energies 12, 3089.*

The present article presents results of a laboratory study on the assessment of erosion patterns around a hydrodynamic transparent offshore foundation exposed to combined waves and currents. The model tests were conducted under irregular, long-crested waves on a geometric scale of 1:30 in a wave-current basin. A terrestrial 3D laser scanner was used to acquire data of the sediment surface around the foundation structure. Tests have been conducted systematically varying from wave- to current-dominated conditions. Different volume analysing methods are introduced, which can be related to any offshore or coastal structure to disclose physical processes in complex erosion patterns. Empirical formulations are proposed for the quantification of spatially eroded sediment volumes and scour depths in the near-field and vicinity of the structure. Findings from the present study agree well with in-situ data (Rudolph et al., 2004; Bolle et al. (2012); Baelus et al., 2019) stemming from the field. Contrasting spatial erosion development between experimental and in-situ data determines a stable maximum of erosion intensity at a distance of  $1.25A$ , 1.25 times the structure's footprint  $A$ , as well as a global scour extent of  $2.1-2.7A$  within

the present study and about 2.7–2.8A from the field. By this means, a structure-induced environmental footprint as a measure for erosion of sediment affecting marine habitat is quantified.

#### 4.2 Effects of structural elements on spatial displacement patterns

Findings of experiments regarding the influence of structural elements of a jacket-type offshore foundation on the spatial sediment displacement are presented in a summarised paragraph of a peer reviewed manuscript (Welzel et al., 2020), revealing the morphological footprint of OWF foundations.

**Paper 4:** *Welzel, M., Schendel, A., Goseberg, N., Hildebrandt, A., Schlurmann, T. (2020). Influence of structural elements on the spatial sediment displacement around a jacket-type offshore foundation. Water 12, 1651.*

This research advances the understanding of jacket-type platform induced erosion and deposition processes for combined wave-current conditions. To this end, a laboratory study was carried out comparing the equilibrium scour depth for two structural designs that are differentiated in the geometrical distance of the structure's lowest node to the seabed. Terrestrial laser scans have been performed to obtain the digital elevation model of the surrounding sediment bed of the foundation structure. Novel methodologies were developed to describe and easily compare the relative volume change of the sediment bed per surface area due to structure-seabed interaction, enabling spatial analyses of highly complex erosion and deposition patterns. The application of this approach facilitates the assessment of the morphological footprint of offshore wind foundation structures, quantifying the effect on the sediment mobility and thus their impact on the surrounding benthic flora and fauna. The seabed sediment mobility around the structure is found to be highly sensitive to a change in the structural node distance (see Fig. 3.3.1). The decrease of 1D in the node distance results in enhanced values of eroded and deposited sediment volume around the structure. However, current-dominated conditions lead to significantly increased erosion volumes underneath the structure of up to 26%, combined with an increase of deposited sediment volume downstream of the structure over a distance of up to 6.5 times the footprint length. The results of this study highlight the requirement to consider the interaction of the structure with the surrounding seabed within the design process of offshore structures. Potential impacts on the local and global scour development as well as on the former unaffected marine environment stemming from the extensive sediment displacement and increased sediment mobility could be mitigated in the structural design process.

### 4.3 Statistical analysis of spatial scour depth changes

Additional research is presented in the following chapter, to develop geostatistical analysing methods based on the previously introduced findings, which provide additional means to quantify statistical values such as the standard deviation, quantiles or the cumulative distribution function of nondimensional spatial parameters representing the relative volume change per surface area of the seabed, which can be converted in spatial changes of the bed topography, e.g. scour depth changes.

While the equilibrium depths of the locally confined scour around cylindrical foundations has been investigated in detail in the past (e.g. Hjorth, 1975; Melville and Coleman, 2000; Sumer and Fredsøe, 1998, 2001, 2002), a systematic representation of the scour development around offshore wind foundations in terms of a spatial analysis of displaced sediment volumes has only been addressed by a small number of studies (Porter, 2016; Hartvig et al., 2010; Bouratsis et al., 2017) so far (see chapter 2.3 and 2.6). On the other hand, the introduced methods and results shown in Welzel et al. (2019b, 2020) reveal new possibilities to quantify, assess and predict the morphological footprint of marine devices in general. Thus, building upon the approaches introduced in Welzel et al. (2019b, 2020), the present study aims to propose a contribution regarding geostatistical and morphometric analysing methods of the sediment seabed around OWF foundations. The presented analysing techniques are demonstrated using 3D laser scan bed topographies introduced in Welzel et al. (2019b). The objectives of the study include:

- A discretization of interrogation areas into a grid of sub-areas, which allows to quantify and analyse each sub-area separately.
- To propose geostatistical analysing methods providing means to quantify statistical values such as quantiles, standard deviations, the cumulative distribution function or confidence bands of quantile values in a spatial reference.

#### 4.3.1 *Experimental setup and test conditions*

The present study is demonstrated using terrestrial laser scans presented and analysed in Welzel et al. (2019b). Thus, information on the experimental setup and test procedure can be found in Welzel et al. (2019b). JONSWAP wave spectra with a maximum number of 6500 waves were generated in each test to ensure that erosion and deposition around the structure reached an equilibrium stage (see Welzel et al. 2019a and 2019b). Overall, five tests have been conducted, starting with a wave only test, three tests in which the wave current velocity ratio ( $U_{cw} = U_c / (U_c + U_w)$ ) was stepwise increased and one test conducted under current only conditions, with  $U_c =$  undisturbed current and  $U_w =$  undisturbed orbital velocity. All tests have been conducted under live bed conditions (see Table 1, calculated after Soulsby, 1997), considering a critical Shields parameter of  $\theta_{cr} = 0.049$  using sand with a median diameter of  $d_{50}$ .

Table 4.3.1. Measured test conditions (waves are 90° to the current)

Test	$H_s$ [m]	$T_p$ [s]	$U_w$ [cm/s]	$U_c$ [cm/s]	$KC$ [-]	$U_{cw}$ [-]	Shields Parameter
							$\theta$ [-]
1	0.165	4.5	20.8	-	23.4	0.00	0.080
2	0.165	4.5	20.8	10.1	23.4	0.33	0.085
3	0.158	3.5	17.5	22.5	14.9	0.56	0.087
4	0.147	3.4	13.3	38.8	6.7	0.75	0.123
5	-	-	-	38.8	-	1.00	0.084

★ Test 1 - 5 are conducted within Welzel et al. (2019b)

#### 4.3.2 Calculation of spatial parameters

The parameters introduced in Welzel et al. (2019b, 2020) to describe the spatial distribution of erosion are briefly summarised in the following. Only eroded volumes  $V_i(a_i)$  without the additional influence of deposited sediment of a considered interrogation area  $a_i$  were calculated by subtracting the post scan from the reference level at the start of a test. The dimensionless volume  $V_{D,i}$  is defined as the eroded sediment volume  $V_i$  within the considered sub-area  $a_i$  and normalised by a structural reference volume. For the considered jacket structure, a structural reference volume was used that corresponds to  $n = 4$  times a cube with the side length  $D$ .

$$V_{D,i} = \frac{V_i(a_i)}{n D^3} \quad (4.3.1)$$

The following two parameters are based on the dimensionless volume  $V_{D,i}$ . The cumulative volume  $V_{A,i}$  uses increasing total areas  $a_i/a_1$ , while the incremental volume parameter  $V_{I,i}$  utilises increasing incremental areas  $a_i/a_1 - a_{i-1}/a_1$  (see Fig. 4.3.1). Both are dimensionless ratios of displaced erosion volume in relation to a specific interrogation area, using the structure footprint area  $a_1$  of the jacket structure as an additional reference.

$$V_{A,i} = \frac{V_{D,i}}{a_i/a_1} \quad (4.3.2)$$

$$V_{I,i} = \frac{V_{D,i} - V_{D,i-1}}{a_i/a_1 - a_{i-1}/a_1} \quad (4.3.3)$$

In addition, two parameters complementary to  $V_{A,i}$  and  $V_{I,i}$  are introduced calculating the erosion depth in reference to the pile diameter, enabling a direct comparison between scour depths and bathymetric data.

$$D_{A,i} = \left( \frac{V_i}{a_i} \right) / D \quad (4.3.4)$$

$$D_{I,i} = \left( \frac{V_i - V_{i-1}}{a_i - a_{i-1}} \right) / D \quad (4.3.5)$$

In the present study, each total area  $a_i$  or incremental area  $a_i - a_{i-1}$  is divided into an underlying grid of sub-areas (see Fig. 4.3.1) to provide additional information on the directionality, spatial distribution and variability of eroded sediment volume. To this end, in addition to the volume of eroded sediment, the individual position in  $x$  and  $y$  directions

is obtained for each sub-grid area (see sub-grid, Fig. 4.3.1). Additionally,  $x$  and  $y$  axis distances are expressed as multiples of the value  $A$ , which is defined as the structure's footprint reference distance ( $A = x$  or  $y$  distance / structure footprint distance; e.g.,  $0.5A = 0.275\text{m}/0.55\text{m}$ ). In accordance with the pile diameters of the investigated jacket structure, the sub-grid resolution in this study was set to  $4 \times 4$  cm. However, the sub-grid resolution might also be chosen in adaption to the analysed erosion pattern or, in case the damage to a granular scour or bed protection is considered, in reference to the stone diameter. The latter would allow to directly link the distribution of damage to the failure of the scour or bed protection as described in Schendel et al. (2018) or Fazeres-Ferradosa et al. (2020).

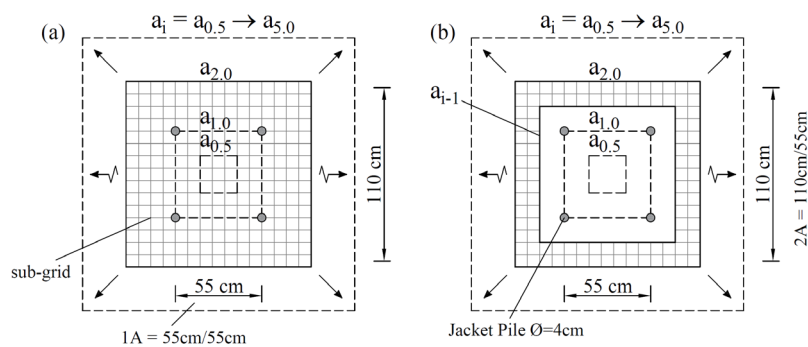


Figure 4.3.1. Schematic sketch of increasing rectangular interrogation areas around the model, (a) sketch of an area  $a_i = a_2$ , related to Eq. (4.3.2) and (4.3.4); (b) increasing incremental areas  $a_i - a_{i-1}$  in relation to Eq. (4.3.3) and (4.3.5). In the present study each area  $a_i$  or  $a_i - a_{i-1}$  has an additional underlying sub-grid

So far, failure of a scour protection has been identified mostly by visual observation as in Den Boon et al. (2004), De Vos et al. (2012) or Whitehouse et al. (2014), in which a scour protection layer is considered to have failed when the exposure of the filter layer exceeds four times the area of the size of an armour unit stone (i.e.,  $4d_{50}^2$ ). With the method introduced in this study, this visual failure criterion could be assessed automatically.

### 4.3.3 Results

The bed topography of the 3D laser scans (see Fig. 4.3.2) reveals a complex spatial structure which is strongly dependent on the hydraulic condition. Wave dominated conditions of irregular waves coming from  $90^\circ$  lead to backfilling of eroded areas as well as to significantly lower local (around the piles) and global scour depths (see Fig. 4.3.2, T1-T3), whose erosion patterns appear to align with the direction of the waves (see Fig. 4.3.2, T2-T3). In contrast current dominated conditions are clearly leading to a deeper local and global scour elongated in current direction (see Fig. 4.3.2, T4-T5). These bed topographies are used in the present study as an example for complex erosion patterns.



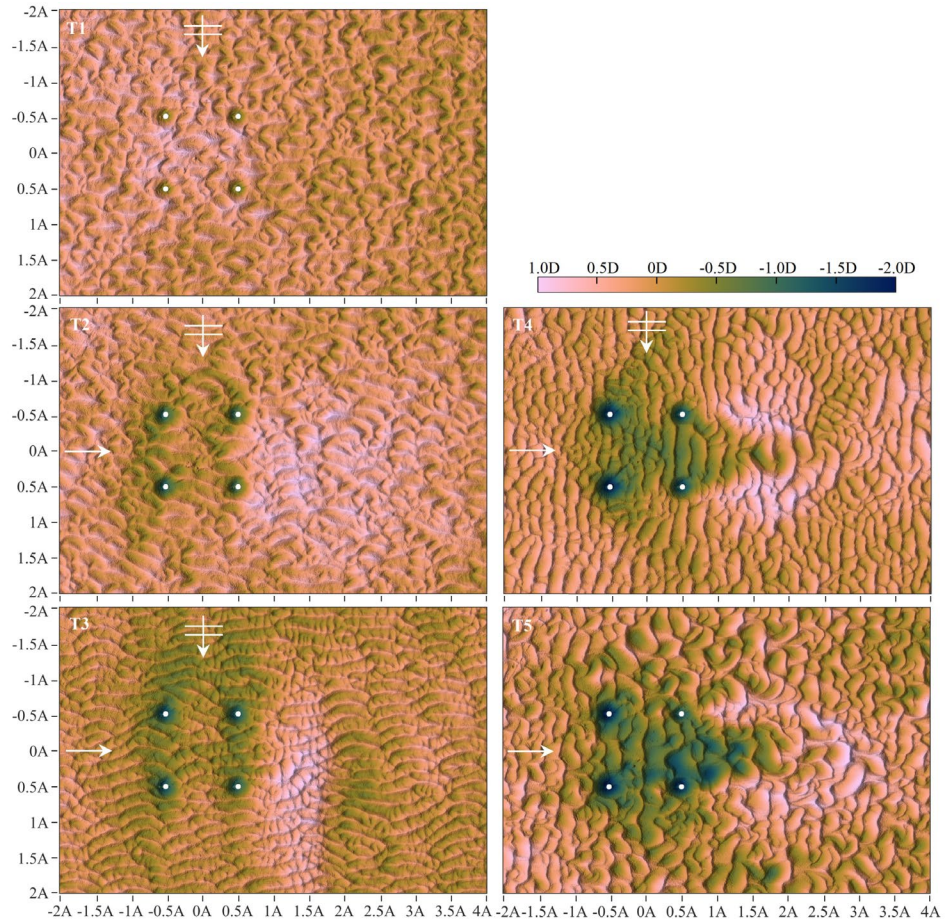


Figure 4.3.2. Bed topography of test 1-5, top view around the jacket for current only conditions, the current is coming from left side ( $0^\circ$ ), x and y distances are given as multiples of the structure's footprint length (adapted figure from Welzel et al., 2019b).

Figure 4.3.3 (a) shows the incremental volume  $V_{I,i}$  over the structure footprint length  $A$ . In test 1-3 wave spectra with a higher orbital velocity and a lower current velocity have been studied ( $U_{cw} = 0 \rightarrow 0.56$ ). Figure 4.3.3 (a) illustrates a reduced intensity of erosion within distances of  $0.5A - 1A$  and an increased erosion intensity for  $1A - 1.4A$  for test 1-3. In this regard, erosion volumes calculated for test 1-3 reveal a more locally pronounced erosion (around the main piles) and a less pronounced erosion in between the structure footprint. In comparison, test 4-5 (current dominated,  $U_{cw} = 0.75 - 1$ ) show higher erosion volumes in general, combined with a more globally pronounced erosion pattern (relatively increased values of  $V_{I,i}$  between  $0.5A - 1A$ ). Figure 4.3.3 (a) additionally reveals a stable peak at  $1.2-1.25A$  for all test cases. At this distance, the local scour around each pile is superimposed with the global scour around the foundation. Beyond  $1.25A$ , the erosion intensity decreases equally. Furthermore, the measured erosion volumes of test 1-5 are compared with values that are calculated by the empirical expression proposed in Welzel et al. (2019b), which highlights the possibility to predict and calculate physical processes in such complex erosion patterns.

In addition, Fig. 4.3.3 (b) reveals the standard deviation of each data point previously calculated as the total amount of eroded sediment



referring to an incremental area  $a_i - a_{i-1}$  (see Fig. 4.3.1, b). In the present approach, each area  $a_i - a_{i-1}$  consists of numerous sub-areas, enabling additional statistical and spatial analyses. Generally, it is shown that the standard deviation of eroded sediment volume increases with an increasing wave current velocity ratio  $U_{cw}$ , which correlates to the progression of  $V_{I,i}$  shown in Fig. 4.3.3 (a). Furthermore, a peak of the standard deviation at the same distance as in Fig. 4.3.3 (a) is observed which might be expected as a high erosion intensity is allocated primary around the main piles. In contrast to the progression of  $V_{I,i}$  shown in Fig. 4.3.3 (a), the standard deviation of test 5 reveals several smaller peaks at  $2A$ ,  $2.5A$  and  $3.5A$ . In comparison to test 1–4, these peaks imply an increased variation of erosion, which can be located in downstream direction of the jacket structure of the elongated erosion pattern (see Fig. 4.3.2, T5).

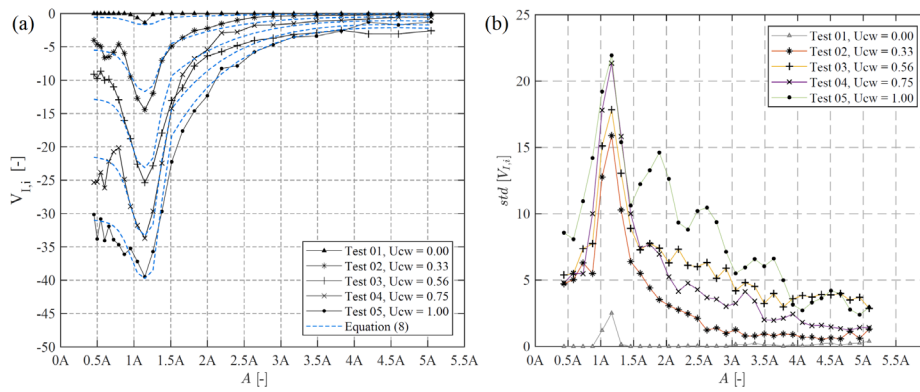


Figure 4.3.3. (a) Incremental volume  $V_{I,i}$  illustrated over the structure footprint length  $A$ , (blue dotted line) in comparison with the empirical equation derived for these tests (Figure from Welzel et al. 2019b); (b) standard deviation for each data point shown in (a), derived with data of the introduced sub-grid.

The use of small sub-grid areas, related to each total interrogation area (see Fig. 4.3.1), gives a large sample of the related parameter describing the erosion intensity (eroded volume per surface area), which in turn allows the analysis of the overall range of the spatially dependent scour depth. Figure 4.3.4 exemplarily illustrates the empirical cumulative distribution function (ECDF) of the erosion intensity  $D_{A,i}$  for test 3 and 5. Figure 4.3.4 shows a general increase of the probability of occurrence of higher erosion intensities from test 3 to test 5, highlighting the impact from more wave to current dominated hydrodynamic conditions ( $U_{cw} = 0.56 \rightarrow 1.0$ ). The comparison also highlights a relatively increased erosion depth for quantiles below 0.2 for test 3, while test 5 reveals more equally distributed quantiles of the erosion depth  $D_{A,i}$ . As an example, a critical scour depth value of  $-1 D_{A,i}$  (comparable to a scour depth of 1 diameter) is illustrated in Fig. 4.3.4. By this means, the ECDF of bathymetric surveys around offshore foundations also helps to verify and quantify the quantile of eroded sediment which exceeds a certain critical value. While the sub-grid areas provide a tool for additional statistical analysis as the ECDF, this information can also be connected with the related x and y position of each sub-grid area. In this regard, Fig. 4.3.4 additionally links the absolute value

of the mean x and y position to the related quantile of sub areas. For example, Fig. 4.3.4 shows that sub areas with quantiles of 5% and lower (for test 3 below  $1D_{A,i}$  and for test 5 above  $1D_{A,i}$ ) are located in a distance of  $0.95 - 1.0A$  in x and y direction. Additionally, the spatial distribution of sub areas in x direction (current direction) shows that the main share (quantile of 68%) of eroded sediment of test 3 is distributed in a distance  $> 0.9A$ . This is contrary to the spatial distribution of test 5 which is distributed more even in x and y direction.

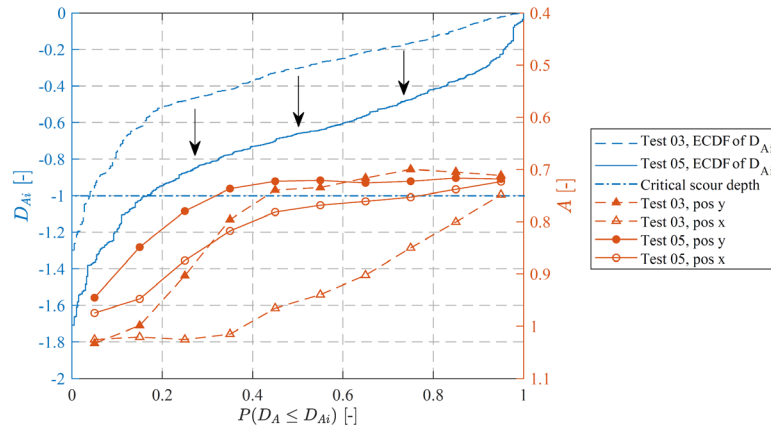


Figure 4.3.4. Empirical cumulative distribution function (ECDF) of the erosion depth value  $D_{A,i}$  of test 3 and 5, the spatial distribution in x and y axis related to the cumulative distribution of  $D_{A,i}$ , an example of a critical scour depth value.

Figure 4.3.5 depicts the total value of each interrogation area (Fig. 4.3.5, a)  $a_i - a_{i-1}$ , here shown in black (cp. with Fig. 4.3.1 & 4.3.3, a) in comparison to the value related to a quantile of 15%, (see Fig. 4.3.5, b) of sub areas related to each interrogation area. By this means, sub areas related to a quantile of 15% ( $q_{15}$ ) represent an example with a lower probability of exceedance and thus a course of a more critical and larger scour depth represented by the parameter  $D_{I,i}$ . The  $q_{15}$  quantile of sub areas related to Fig. 4.3.5 (b) reveals a larger erosion depth of  $D_{I,i}$  as the total mean value of each interrogation area depicted in Fig. 4.3.5 (a). Similar to the total value of each interrogation area, Fig. 4.3.5 (b) shows in general an increase of the erosion depth with a rising wave current velocity ratio, relatively increased for  $q_{15}$  values in comparison to total values measured and analysed within Welzel et al. (2019a). Similar to the findings of the standard deviation of test 5 (see Fig. 4.3.3, b), a relatively increased erosion depth is observed for distances above  $1.5A$  for test 5. This corresponds to the elongated global scour under current only conditions (see Fig. 4.3.2, T5). Additionally, Fig. 4.3.5 (b) provides a confidence band with  $\pm 5\%$  above and below the depicted  $D_{I,i}$   $q_{15}$  value in a spatial reference.

This example shows the possibility to spatially investigate interrogation areas in further detail, with critical statistical values with a lower probability of exceedance, including lower and upper confidence bounds.

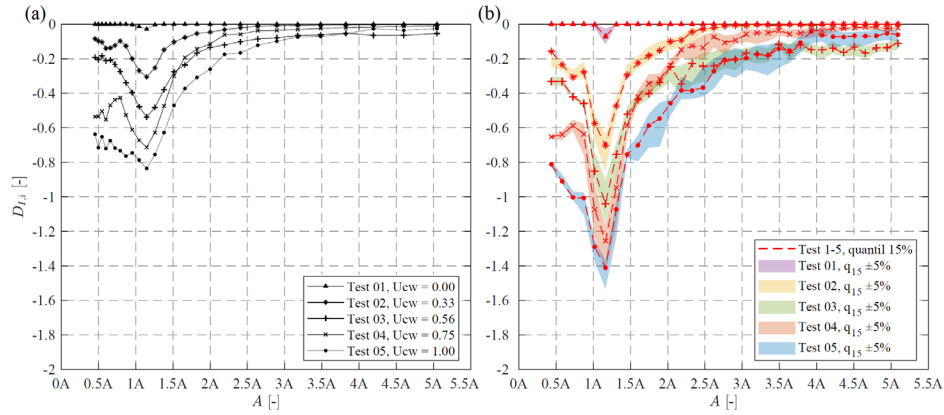


Figure 4.3.5. (a) Incremental erosion depth  $D_{I,i}$  around the jacket structure, plotted over the structure footprint length  $A$ , total value of each interrogation area, see Fig. 4.3.1, (Figure adapted from Welzel et al., 2019b) (b) Confidence bands of a quantile of 15% for test 1-5 of the incremental erosion depth  $D_{I,i}$  over the structure footprint length.

#### 4.3.4 Conclusions

Assessment or prediction approaches describing erosion processes around offshore structures are commonly developed to give information on the maximum value, usually of a single pointwise or a locally limited measurement of the scour depth or damage level of a scour protection layer. 3D laser scans of hydraulic model tests presented in Welzel et al. (2019b) were utilised in the present study to demonstrate new possibilities to statistically analyse changes in digital elevation models around offshore wind foundations. Building upon the approach introduced in Welzel et al. (2019b), the present study provides means to further analyse complex erosion patterns with help of an additional grid of sub areas to quantify different statistical parameters. The following conclusions were derived from the present study:

- The analysis of tests 1-5 allowed the identification of the standard deviation of erosion depth values. It is shown that the standard deviation of eroded sediment volume increases with an increasing wave current velocity ratio, which correlates to the progression of  $V_{I,i}$ . In contrast to the course of  $V_{I,i}$  of each total interrogation area (cp. Welzel et al. 2019b) the standard deviation of test 5 revealed several peaks at 2-3.5A, which indicates an increased variation in comparison to test 1-4, indicating peaks of the erosion intensity, which can be located in downstream direction of the foundation structure.
- It is shown that the cumulative distribution function of a bathymetric survey of erosion depths can be linked to the spatial distribution of sub areas, rendering additional characteristics accessible, such as critical quantile values exceeding a certain scour depth or damage level connected to the related distribution in the x or y axis.

- Additionally, the present study introduces a novel method to analyse erosion patterns around a jacket structure with confidence bands of a chosen quantile value of 15%, representing an example of a critical statistical value with a lower probability of exceedance in a spatial reference.

Similar as presented in Welzel et al. (2019b), the approach introduced in the present study can be used to improve the assessment and prediction of spatial erosion or deposition patterns describing the statistical distribution of erosion depths or damage of scour protection systems.

## DAMAGE CHARACTERISATION AND SCOUR PROTECTION DESIGN

---

Depending on the depth of the developing scour hole, the structural stability can be affected. In consequence, the emerging scour has to be considered thoroughly in the design process of offshore foundations. As maintenance costs over the lifetime can increase to an unpredictable value for scour depth which exceed a certain threshold, the installation of a scour protection system often becomes the most economical solution. Due to a cost-efficient production and installation, single-layer widely graded stone material could be an appropriate alternative solution of classical multi-layer protection systems. However few studies have been conducted on this topic and no general design criteria have been developed for wide-graded scour protection material around offshore foundations. Unresolved research questions and potential for further improvements remain also regarding scale effects (as most studies are conducted in small scale) and the characterisation and assessment of the stability of scour protection systems.

### 5.1 Large-scale experiments to improve scour protection design

Large-scale experiments around a monopile foundation regarding different gradings of the scour protection material have been conducted in a joint group under combined waves and currents, summarised in the following paragraph (Chavez et al., 2019) of a peer reviewed article.

**Paper 6:** *Chavez, C.E.A., Stratigaki, V., Wu, M., Troch, P., Schendel, A., Welzel, M., Villanueva, R., Schlurmann, T., De Vos, L., Kisacik, D., Pinto, F.T., Fazeres-Ferradosa, T., Santos, P.R., Baelus, L., Szengel, V., Bolle, A., Whitehouse, R., Todd, D. (2019). Large-scale experiments to improve monopile scour protection design adapted to climate change—the PROTEUS project. Energies 12.9, 1709.*

The present study aims to improve the design of scour protection around offshore wind turbine monopiles, as well as future-proofing them against the impacts of climate change. A series of large-scale experiments have been performed in the context of the European HYDRALAB-PLUS PROTEUS project (Protection of offshore wind turbine monopiles against scouring) in the Fast Flow Facility in HR Wallingford, United Kingdom. Statically and dynamically stable scour protections were investigated in large scale under the combined load of waves and currents around a monopile in two different scales 1:16 and 1:8 to circumvent the clear lack of large-scale experimental datasets. Five tests were conducted for statically stable design conditions, allowing no movement of the armor layer stones. The onset of motion of armor layer stones were observed during regular wave trains of 12 waves together with a superimposed current. Each Test was divided in to sub tests, in which the wave height and wave period was adjusted until the onset of motion could be observed. Eight tests have been conducted in total for dynamically stable design conditions, allowing a certain defined motion of the scour protection material, including tests

under different scales, different mean  $d_{50}$  stone diameter as well as three different gradations of the Material ( $d_{85}/d_{15}=2.48$ ; 6; 12). These experiments make use of state of the art optical and acoustic measurement techniques. For each test an under water laser scan was conducted prior of each test, after 1000 and after 3000 waves. The experimental program also focusses on the investigation of the grading of scour protection materials as a stabilising parameter, which has never been done under the combined action of waves and currents at a large scale. Scale effects are reduced and, thus, design risks are minimised. Moreover, the generated data support the development of future scour protection designs and the validation of numerical models used by researchers worldwide. The testing program objectives were: (i) to compare the performance of single-layer wide-graded material used against scouring with current design practices; (ii) to verify the stability of the scour protection designs under extreme flow conditions; (iii) to provide a benchmark dataset for scour protection stability at large scale; and (iv) to investigate the scale effects on scour protection stability.

## 5.2 Characterisation of damage patterns in scour protections

Findings of a study (Fazeres-Ferradosa et al., 2020) regarding a new approach to define the sub-area size and to determine and characterise damage in a statistical distribution are introduced in a summarised paragraph of a peer reviewed manuscript in the following.

**Paper 7:** *Fazeres-Ferradosa, T., Welzel, M., Schendel, A., Baelus, L., Santos, P.R., Pinto, F.T. (2020). Extended characterisation of damage in rubble mound scour protections. Coastal Engineering 158, 103671.*

The analysis of damage in rubble mound scour protections is crucial for the armour stability assessment. Former methodologies focused on the analysis of the maximum damage number. State-of-the-art methodologies for damage and armour stability assessment of dynamically stable scour protections are discussed and compared in detail. Therefore, a detailed comparison and discussion of the sub-area size and arrangement was conducted to define points for further improvements and define additional research questions. It was shown and discussed that these sub-area arrangements do not account adequately for damage occurring in the intersection between sub-areas, a varying armour layer thickness or varying angles of waves or currents, also only applied on monopiles.

The present work introduces a complementary methodology to determine and characterise damage statistical distribution based on a flexible arrangement of sub-areas. Overlapping ring sections and overlapping circle sub-areas are utilised. To capture the variation of damage with changing sub-area layout, the methodology is coupled with a statistical evaluation of damage numbers, which is enabled by the definition of a grid ratio between armour stone size and sub-area size,  $D_{n,50}^2/A_{sub}$ . The methodology is applied to high resolution bathymetric surveys from two stability tests as a demonstration of the approach of large-scale rip-rap scour protection around a monopile foundation and combined wave and

current loading. A study regarding the influence of the ratio between stone and sub-area size on the calculated damage revealed a significant influence of the sub-area on the damage description. Characteristic measures as the maximum damage number and standard deviation become stable at a grid ratio  $D_{n,50}^2/A_{sub}$  equal to 1/4. Results show that the methodology provides a complementary understanding of damage distribution to the maximum damage acquired from previous methodologies. Furthermore, it was concluded for the first time that the visual failure criteria proposed by Den Boon et al. (2004) was an accurate criterion from the mathematical and physical point of view, demonstrated with the grid ratio.





## SUMMARY & OUTLOOK

---

This thesis concerns recent advantages regarding the degrading effect of scour and erosion around offshore foundation structures. This work mainly aims to reduce uncertainties regarding the assessment and prediction of complex erosion processes around offshore structures previously not addressed. In search of available space and higher wind energy load factors in the contested coastal areas, offshore wind parks are more often planned and installed further away from the shore and in deeper waters. As a result, complex offshore foundation structures such as jacket-type foundations are favoured, as they are more stable in deeper waters. A series of novel hydraulic model tests were carried out to systematically investigate (I) the scouring processes induced by more natural hydrodynamic conditions around monopiles and jacket-type structures; (II) the spatial scour depth changes and deposition patterns around offshore foundation structures; (III) the damage and stability of scour protections.

### 6.1 Wave-current induced scouring

Important elements for the representation of realistic hydrodynamic conditions are tidal currents and multidirectional waves. Thus, different generalizations of hydrographical shapes were investigated in hydraulic model tests to deepen the knowledge regarding the effect on tidal current induced scouring processes around monopiles. It was found that the characteristic scour development in tidal currents can only be reproduced by hydrographs with a varying flow direction. The effective flow work approach has been found to be able to identify the appropriate flow velocity for an accurate representation of tidal current induced final scour depths.

Systematic laboratory tests were also conducted to improve the understanding of the influence of multidirectional irregular waves combined with an oblique current on the scour development around monopiles. The scour development under unidirectional and multidirectional wave spectra were compared with an identical total wave energy, revealing clear differences in the scour depth and scouring rate, which can only be associated to the influence of wave spreading on the scouring process. It was found that multidirectional waves without a current led on average to a reduction of the final scour depth by 33% compared to unidirectional wave conditions. Additionally, it was revealed that the final scour depth decreased with a growing wave spreading. However, a combination of multidirectional waves with a superposed current led to slightly larger scour depths and scouring rates as for unidirectional wave conditions. An empirical approach was derived to estimate the maximum scour depth for either uni- or multidirectional random waves combined with a superimposing current.

Despite the common use of jacket structures as a suitable foundation type, only few systematic studies have been conducted on the scour development around them. Several aspects regarding local and global erosion processes around complex offshore foundations are still disregarded. Thus, novel laboratory experiments on the scour development around a jacket structure under irregular waves and combined currents were carried out. Continuous scour depth measurements over time were achieved with small echo sounding devices, positioned at eight locations on the upstream and downstream side of the jacket structure. A systematic laboratory study was conducted with relative wave-current velocities ranging from wave to current dominated conditions, KC numbers between 6.7 and 23.4 as well as an additional differentiation in two structural designs, distinguished in the distance of the foundation's lowest node to the seabed. The main conclusions are:

- An infilling of sediment from the edges of the scour hole combined with displacement of sediment within the scour hole of each jacket leg pile resulted in a significant variation of the scour development over the time. With respect to the current flow direction, a larger scour depth was observed at the upstream side of the jacket pile, than at the downstream side. This imbalance was more pronounced at the upstream located pile, than at the downstream located pile, indicating a more current dominated scour development at the upstream side of the jacket. In addition, an increased scour depth was observed underneath the diagonal braces, indicating an increased contraction and bed shear stress.
- An increasing global scour depth was observed around the jacket with an increasing wave current velocity ratio  $U_{cw}$ , revealing scour depths of around 17% for  $U_{cw}=0.55$ , around 20% for  $U_{cw}=0.75$  and up to 30% for  $U_{cw}=1$  in comparison of those measured directly at the jacket piles.
- The laboratory experiments revealed a scour development and time scale for jacket piles which proved to be clearly different as the pile was either directly exposed to the combined wave-current load (upstream pile) or affected by the upstream positioned piles and the neighbouring structural elements (downstream pile). A comparison of dimensionless time scales revealed a slower scouring rate at the jacket structure than at a monopile. Furthermore, a faster scour development was observed at the jacket structure for combined wave current conditions than under steady current conditions.
- While in general larger scour depths were observed on the upstream than on the downstream side positioned pile, a faster scouring rate for  $U_{cw}<0.52$  combined with a slower for  $U_{cw}>0.52$  was observed on the downstream positioned pile in comparison to the upstream positioned pile.
- Furthermore, an empirical approach was proposed to predict the equilibrium scour depth at jacket structures in combined wave current conditions, with a differentiation between the scour depth on the upstream and downstream side of the pile and an additional distinction between the distance of the lowest node to the seabed.

## 6.2 Spatial analysis of sediment redistribution patterns

Volumetric measurements of the sediment seabed were conducted with a terrestrial 3D laser scanner. A series of hydraulic experiments from wave-to current-dominated conditions were conducted in a wave-current basin regarding the influence of combined waves and currents on the spatial erosion around a jacket-type offshore foundation. Furthermore, an additional series of model tests were conducted regarding the influence of two different distances of the lowest node to the seabed on the spatial sediment displacement around the jacket model. A novel approach was developed to quantify, predict, and easily compare the relative volume change of the sediment bed per surface area due to structure-seabed interaction. This approach enables spatial analyses of highly complex erosion and deposition patterns, revealing physical processes in erosion or deposition patterns around any offshore or coastal structure. The main conclusions are as follows:

- Jacket structures are often considered as hydrodynamic transparent structures. However, the flow vortex system and as a result also the morphodynamics around the structure are clearly affected by the structure's elements. In dependence to the hydrodynamic conditions, the scour pattern can be distinguished in local scour at the piles and global scour underneath and around the structure, as shown and compared with field data.
- An empirical expression is proposed which allows to quantify the erosion intensity (eroded volume per surface area) in reference to the spatial extent around the foundation structure. The approach also enables to estimate spatial scour depths or volumes of eroded or deposited sediment in relation to the hydraulic condition. Furthermore, the results calculated by the approach agree well with in-situ data in the field.
- A structure-induced global footprint was found as a measure of erosion affecting the surrounding marine environment around jacket structures. A maximum of eroded volume per surface area was found at a distance of 1.25 times the structure's footprint, as well as a global scour extent of 2.1-2.8 times the footprint for different jacket structures in the field and the experimental study. The global scour extent and depth varies in respect to the hydrodynamic conditions (wave or current dominated) as well as the temporal condition (whether an equilibrium condition is reached or not). This could be shown on laboratory and field data.
- This also enables a realistic assessment of the portion of soil that is displaced and eroded, enabling an improved assessment and calculation of the natural frequency and structural stability of OWF's (see Prendergast et al., 2015 and Mayall 2019 for monopiles). These Information might be also of practical use for the prediction of spatial scour depth changes and the design of scour protection systems in a graduated intensity over the structure-induced global footprint.

- The seabed sediment mobility around the jacket structure is found to be highly sensitive to a change in node distance. A decrease of the lowest node by 1D results in an increased erosion depth below the foundation structure of about 26%. The increased erosion leads to a growing deposition of sediment on the downstream side over a distance of up to 6.5 times the structural footprint length.
- Furthermore, the analysing method was improved by an additional grid of sub areas to optionally quantify statistical parameters to improve the assessment and prediction of spatial erosion or deposition patterns even further. Additional statistical means as the standard deviation, a cumulative / spatial distribution function or confidence bands of specific quantile values enable to assess additional characteristics as for example critical spatial scour depths which exceed a certain threshold or damage level.

### 6.3 Damage characterisation and scour protection design

Large-scale laboratory experiments have been conducted in a joint group in the Fast Flow Facility in HR Wallingford. Different stone gradings were investigated regarding the impact of combined waves and currents on the stability of granular scour protections around a monopile foundation. High resolution measurements of the bed topography have been conducted with an underwater 3D laser scanner.

State-of-the-art methodologies for damage and armour stability assessment of dynamically stable scour protections are discussed and compared in detail. Therefore, a comparison and discussion of the sub-area size and arrangement was conducted to define points for further improvements and additional research. It was shown and discussed that these sub-area arrangements do not account adequately for damage occurring in the intersection between sub-areas, a varying armour layer thickness, varying angles of waves or currents or scour protections with a similar maximum damage number but different magnitudes of damage in other sub-areas. Furthermore, it is noted that available approaches mainly calculate just a single maximum damage number that is also based on different sub-area grids, which can lead to varying damage numbers for the same erosion pattern. These damage numbers have to be assessed separately for the specific arrangement and the approaches may not be directly comparable. The main conclusions are:

- A flexible approach with a new definition of overlapping sub-areas to assess and characterise damage was developed. Overlapping ring sections and overlapping circle sub-areas are utilised.
- In contrast to former studies which concentrated on a maximum damage number, a complementary methodology was introduced which can additionally determine damage by a statistical distribution. The methodology enables statistical analyses such as the cumulative distribution function of the damage, which allows an improved perception of the erosion patterns and enables to circumvent former described disadvantages of state-of-the-art approaches.

- A study regarding the influence of the ratio between stone and sub-area size on the calculated damage revealed a significant influence of the sub-area on the damage description. It was found that characteristic measures as the maximum damage number or the standard deviation of the damage number of all sub-areas become stable at a ratio between stone size and sub-area size  $D_{n,50}^2/A_{sub}$  equal to 1/4.
- Furthermore, it was concluded for the first time that the visual failure criteria proposed by Den Boon et al. (2004) is an accurate criterion from the mathematical and physical point of view, demonstrated with the grid ratio

#### 6.4 Future work

A reliable estimate of scour depths is an essential part of the design process of an offshore foundation structure. As a result of the decreased embedment depth, the structural stability can be affected, e.g. by an increased bending moment, or accelerated fatigue damage due to a change in the natural frequency and cyclic loading of the rotor. Simultaneously, the prediction and quantification of the influence of offshore wind farms on the near- and far-field sediment mobility is an important prerequisite to assess and better understand OWF induced impact on the natural marine environment, including benthic habitats.

In order to minimise uncertainties regarding scouring processes around offshore foundations, realistic hydraulic conditions should be considered more often in future studies. This includes remaining knowledge gaps regarding scour development aspects of rotary currents, the influence of the tidal range or aspects regarding the effect of multiple storms or a wider range of wave spreading for different offshore foundation types.

Also, very few numerical studies exist on the topic of scouring around complex offshore wind foundations. Numerical studies regarding a three-dimensional simulation of the flow, free surface and sediment transport due to fluid-structure interaction are quite complex and commonly concentrate on the simulation of less complex hydraulic conditions for monopiles. The numerical prediction of scouring processes, also around complex foundation structures or due to complex hydrodynamic conditions (e.g. as combined waves and currents) stands out as an important engineering challenge, with potential for improvements and open research questions for future studies.

The present thesis highlights a considerable lack of knowledge regarding an empirical prediction of scouring processes around complex foundation structures. An example is the equilibrium scour depth at jacket structures. In this context, the time scale and in particular the influence of the global scour (generated over long time periods) on the local scour development seems to be an aspect, which was studied and discussed in the present thesis, but should be considered more detailed to gain a better understanding of equilibrium scour conditions at jacket-type structures. As the scour development can differ significantly, it also seems to be necessary to further study the influence of different structural designs on the scour development. Future studies should strive towards a systematic

investigation by an incremental change of near-bed structural features such as the number and diameter of pin piles / pile sleeves or the angle, vertical offset and diameter of diagonal or horizontal braces.

A limited understanding of spatial erosion and deposition processes is given for offshore foundations in general. Even less is known on the intrinsic drivers, the spatial extent and spatial erosion depth around more complex foundation structures. A better spatial understanding of the morphological processes around offshore foundations is not only important for an improvement of the prediction of scour depths and an improved design of scour protection systems. An improved understanding of spatial scouring or deposition processes is also an important aspect to evaluate and predict the man-made impact of offshore foundations on the previously unaffected marine environment. The studies introduced in the present thesis should represent a first step towards addressing a variety of open research questions and builds the potential for further improvements in this research area. As demonstrated by an empirical expression for the erosion pattern around a jacket-type structure, such empirical approaches enable to disclose physical processes in complex erosion patterns, allowing the spatial calculation and assessment. However, there are many examples of an application and potential for further improvements, e.g. the adaptation, utilisation and further development for different foundation types as well as potential for further improvements regarding geostatistical and morphometric analysis, as presented in chapter 4.3.

A main aspect of future work might also be the calculation and prediction of the structure-induced sediment redistribution footprint (erosion and deposition) for actual field data of offshore wind parks, considering the additional complexity of the natural bed topography. New research questions and required improvements might also result of the arising challenges of a required integrated modelling approach of the multiple stressor impacts on the marine ecosystems.

In order to further develop existing methodologies and minimise uncertainties regarding the design of scour protection systems, the results of the present thesis show large potential for future studies. The results show that the introduced methodology to assess the damage and armour stability of a dynamically stable scour protection provides useful additional information on the damage pattern, in particular for those cases, in which an adequate consideration of damage is difficult. However, there are still aspects for further improvements and additional research, including the validation on a large test program, which implies that the presented method to assess damage at scour protections cannot be used as a standard design method on its own yet.

## BIBLIOGRAPHY

---

- Abhinav, K.A. and Saha, N. (2018). "Nonlinear dynamical behaviour of jacket supported offshore wind turbines in loose sand." In: *Marine Structures* 57, pp. 133-151. DOI: [10.1016/j.marstruc.2017.10.002](https://doi.org/10.1016/j.marstruc.2017.10.002).
- Achmus, M.; Kuo, Y.-S.; Abdel-Rahman, K. (2010). "Numerical investigation of scour effect on lateral resistance of windfarm monopiles." In: *Proc. 20th International Offshore and Polar Engineering Conference (ISOPE)*. Beijing, China.
- Ahmad, N.; Kamath, A. and Bihs, H. (2020). "3D numerical modelling of scour around a jacket structure with dynamic free surface capturing." In: *Ocean Engineering* 200, 107104. DOI: [10.1016/j.oceaneng.2020.107104](https://doi.org/10.1016/j.oceaneng.2020.107104).
- Amanatidis, G. (2019). "European policies on climate and energy towards 2020, 2030 and 2050." Policy Department for Economic, Scientific and Quality of Life Policies Directorate-General for Internal Policies, pp. 1-12.
- Amini, A.; Melville, B.W.; Ali, T.M.; Ghazali, A.H. (2012). "Clear-water local scour around pile groups in shallow-water flow." In: *Journal of Hydraulic Engineering* 138.2, pp. 177-185. DOI: [10.1061/\(ASCE\)HY.1943-7900.0000488](https://doi.org/10.1061/(ASCE)HY.1943-7900.0000488).
- Andersen, M.T. (2016). "Floating foundations for offshore wind turbines." Ph.D. thesis, Faculty of Engineering and Science, Aalborg University, Aalborg, Denmark. DOI: [10.5278/vbn.phd.engsci.00175](https://doi.org/10.5278/vbn.phd.engsci.00175).
- Ataie-Ashtiani, B. and Beheshti, A.A. (2006). "Experimental investigation of clear-water local scour at pile groups." In: *Journal of Hydraulic Engineering* 132.10, pp.1100-1104. DOI: [10.1061/\(ASCE\)0733-9429\(2006\)132:10\(1100\)](https://doi.org/10.1061/(ASCE)0733-9429(2006)132:10(1100)).
- Baelus, L.; Bolle, A.; Szengel, V. (2019). "Long term scour monitoring around offshore jacket foundations on a sandy seabed." In: *Proc. of Ninth International Conference on Scour and Erosion (ICSE)*, Taipei, Taiwan, November 5.-8., 2018.
- Baghbadorani, D.A.; Ali-Asghar, B.; and Behzad, A.-A. (2017). "Scour hole depth prediction around pile groups: review, comparison of existing methods, and proposition of a new approach." *Natural Hazards* 88.2, pp. 977-1001. DOI: [10.1007/s11069-017-2900-9](https://doi.org/10.1007/s11069-017-2900-9).
- Baker, C.J. (1979). "The laminar horseshoe vortex." In: *J. Fluid Mechanics* 95.2, pp. 347-367. DOI: [10.1017/S0022112079001506](https://doi.org/10.1017/S0022112079001506).
- Baker, C.J. (1985). "The position of points of maximum and minimum shear stress upstream of cylinders mounted normal to flat plates." In: *Journal of Wind Engineering and Industrial Aerodynamics* 18.3, pp. 263-274. DOI: [10.1016/0167-6105\(85\)90085-6](https://doi.org/10.1016/0167-6105(85)90085-6).
- Baker, R.E. (1986). "Local scour at bridge piers in non-uniform sediment." Tech. Rep. No. 402. Auckland, New Zealand: University of Auckland.
- Baykal, C.; Sumer, B.M.; Fuhrman, D.R.; Jacobsen, N.G.; Fredsøe, J. (2017). "Numerical simulation of scour and backfilling processes around a circular pile in waves." In: *Coastal Engineering* 122, pp. 87-107. DOI: [10.1016/j.coastaleng.2017.01.004](https://doi.org/10.1016/j.coastaleng.2017.01.004).
- Bayram, A. and Larson, M. (2000). "Analysis of scour around a group of vertical piles in the field." In: *J. of Waterw., Port, Coast., and Ocean Eng.* 126.4, pp. 215-220. DOI: [10.1061/\(ASCE\)0733-950X\(2000\)126:4\(215\)](https://doi.org/10.1061/(ASCE)0733-950X(2000)126:4(215)).
- Beg, M. (2008). "Effect of mutual interference of bridge piers on local scour." Ph.D. thesis, Department of Civil Engineering, Aligarh Muslim University, Aligarh, India.

- Best, J. (2005). “The fluid dynamics of river dunes: A review and some future research directions.” In: *Journal of Geophysical Research: Earth Surface*, 110, F04S02. DOI: [10.1029/2004JF000218](https://doi.org/10.1029/2004JF000218).
- Bolle, A.; De Winter, J.; Goossens, W.; Haerens, P.; Dewaele, G. (2012). “Scour monitoring around offshore jackets and gravity based foundations.” In: *Proc. of Sixth International Conference on Scour and Erosion (ICSE)*, 27.-31. August 2012 in Paris.
- Bouratsis, P.; Diplas, P.; Dancey, C.L.; Apsilidis, N. (2017). “Quantitative Spatio-Temporal Characterization of Scour at the Base of a Cylinder.” In: *Water* 9.3, 227. DOI: [10.3390/w9030227](https://doi.org/10.3390/w9030227).
- Breusers, H.N.C. (1972). “Local Scour Near Offshore Structures.” Publication. Delft Hydraulics Laboratory, Delft.
- Breusers, H.N.C.; Nicollet, G.; Shen, H.W. (1977). “Local Scour Around Cylindrical Piers.” In: *Journal of Hydraulic Research* 15.3, pp. 211–252. DOI: [10.1080/00221687709499645](https://doi.org/10.1080/00221687709499645).
- Broderick, L.L. (1984). “Riprap Stability versus Monochromatic and Irregular Waves.” Ph.D. thesis. Oregon State University. [Link](#).
- Carpenter, J.R.; Merckelbach, L.; Callies, U.; Clark, S.; Gaslikova, L.; Baschek, B. (2016). “Potential Impacts of Offshore Wind Farms on North Sea Stratification.” In: *PLOS ONE* 11.8, e0160830. DOI: [10.1371/journal.pone.0160830](https://doi.org/10.1371/journal.pone.0160830).
- Cebeci, T. and Chang, K.C. (1978). “Calculation of incompressible rough-wall boundary-layer flows.” In: *AIAA Journal* 16.7, pp. 730–735. DOI: [10.2514/3.7571](https://doi.org/10.2514/3.7571).
- Chan, D. and Wu, Q. (2015). “Significant anthropogenic-induced changes of climate classes since 1950.” In: *Scientific Reports* 5, Article number: 13487. DOI: [10.1038/srep13487](https://doi.org/10.1038/srep13487).
- Chavez, C.E.A.; Stratigaki, V.; Wu, M.; Troch, P.; Schendel, A.; Welzel, M.; Villanueva, R.; Schlurmann, T.; De Vos, L.; Kisacik, D.; Pinto, F.T.; Fazerer-Ferradosa, T.; Santos, P.R.; Baelus, L.; Szengel, V.; Bolle, A.; Whitehouse, R.; Todd, D.; (2019). “Large-scale experiments to improve monopile scour protection design adapted to climate change—the PROTEUS project.” In: *Energies* 12.9, 1709. DOI: [10.3390/en12091709](https://doi.org/10.3390/en12091709).
- Chen, I.-W.; Wong, B.-L.; Lin, Y.-H.; Chau S.-W.; Huang, H.-H. (2016): “Design and analysis of jacket substructures for offshore wind turbines.” In: *Energies* 9.4, 264. DOI: [10.3390/en9040264](https://doi.org/10.3390/en9040264).
- Chen, H.-H.; Yang, R.-Y.; Hwung, H.-H. (2014). “Study of hard and soft countermeasures for protection of the jacket-type offshore wind turbine foundation.” In: *Journal of Marine Science and Engineering* 2.3, pp. 551–567. DOI: [0.3390/jmse2030551](https://doi.org/10.3390/jmse2030551).
- Chiew, Y.-M. (1984). “Local scour at bridge piers.” Ph.D. thesis. Auckland University, New Zealand.
- Chiew, Y.-M. and Lim, F.-H. (2000). “Failure behaviour of riprap layer at bridge piers under live-bed conditions.” In: *Journal of Hydraulic Engineering* 126.1, pp. 43–55. DOI: [10.1061/\(ASCE\)0733-9429\(2000\)126:1\(43\)](https://doi.org/10.1061/(ASCE)0733-9429(2000)126:1(43)).
- Cornish V. 1901. “On sand-waves in tidal currents.” In: *The Geographical Journal* 18.2, pp. 170–200.
- De Almeida, E.; van Gent, M.; Hofland, B. (2019). “Damage characterization of rock slopes.” In: *Journal of Marine Science and Engineering* 7.1, 10, pp. 1–15. DOI: [10.3390/jmse7010010](https://doi.org/10.3390/jmse7010010).



- De Schoesitter, P.; Audenaert, S.; Baelus, L.; Bolle, A.; Brown, A.; Das Neves, L.; Ferradosa, T.; Haerens, P.; Pinto, F.T.; Troch, P.; Whitehouse, R. (2014). “Feasibility of a dynamically stable rock armour layer scour protection for offshore wind farms.” In: *International Conference on Ocean, Offshore and Arctic Engineering (OMAE)*. American Society of Mechanical Engineers, San Francisco, California, pp. 1–10. DOI: [10.1115/OMAE2014-24426](https://doi.org/10.1115/OMAE2014-24426).
- De Vos, L. (2008). “Optimisation of Scour Protection Design for Monopiles and Quantification of Wave Run-Up.” Engineering the Influence of an Offshore Wind Turbine on Local Flow Conditions, Ph.D. thesis, Ghent University, Ghent, p. 319.
- De Vos, L.; De Rouck, J.; Troch, P.; Frigaard, P. (2011). “Empirical design of scour protections around monopile foundations. Part 1: Static Approach.” In: *Coastal Engineering* 58.6, pp. 540–553. DOI: [0.1016/j.coastaleng.2011.02.001](https://doi.org/0.1016/j.coastaleng.2011.02.001).
- De Vos, L.; De Rouck, J.; Troch, P.; Frigaard, P. (2012). “Empirical design of scour protections around monopile foundations. Part 2: Dynamic Approach.” In: *Coastal Engineering* 60, pp. 286–298. DOI: [10.1016/j.coastaleng.2011.11.001](https://doi.org/10.1016/j.coastaleng.2011.11.001).
- Den Boon, J. H.; Sutherland, J.; Whitehouse, R.; Soulsby, R.; Stam, C.J.; Verhoeven, K.; Høgedal, M.; and Hald T. (2004). “Scour behaviour and scour protection for monopile foundations of offshore wind turbines.” In: *European Wind Energy Conference and Exhibition (EWEC)*, London.
- Dornhelm, E.; Seyr, H.; Muskulus, M. (2019). “Vindby – A Serious offshore wind farm design game.” In: *Energies* 12.8, 1499. DOI: [10.3390/en12081499](https://doi.org/10.3390/en12081499).
- Eadie, R.W. and Herbich, J.B. (1986). “Scour about a single cylindrical pile due to combined random waves and a current.” In: *Proc. of the 20th International Conference on Coastal Engineering*, November 9–14, 1986, Taipei, Taiwan, pp. 1858–1870. DOI: [10.1061/9780872626003.136](https://doi.org/10.1061/9780872626003.136).
- Elliott, M. (2002). “The role of the DPSIR approach and conceptual models in marine environmental management: An example for offshore wind power.” In: *Marine Pollution Bulletin* 44.6, pp. iii–vii. DOI: [10.1016/S0025-326X\(02\)00146-7](https://doi.org/10.1016/S0025-326X(02)00146-7).
- Ettema, R. (1976). “Influence of bed material gradation on local scour.” Tech. Rep., University of Auckland, New Zealand.
- Ettema, R. (1980). “Scour at bridge Piers.” University of Auckland, New Zealand.
- Fenton, J.D. and McKee, W.D. (1990). ”On calculating the lengths of water waves.” In: *Coastal Engineering* 14.6, pp. 499–513. DOI: [10.1016/0378-3839\(90\)90032-R](https://doi.org/10.1016/0378-3839(90)90032-R).
- Fazeres-Ferradosa, T.; Taveira-Pinto, F.; Reis, M.T.; Das Neves, L. (2018a). “Physical modelling of dynamic scour protections: analysis of the Damage Number.” In: *Proc. of the Inst. of Civil Engineering - Maritime Engineering* 171.1, pp. 11–24. DOI: [10.1680/jmaen.2017.26](https://doi.org/10.1680/jmaen.2017.26).
- Fazeres-Ferradosa T.; Taveira-Pinto, F.; Romão, X.; Vanem, E.; Reis, T. and das Neves, L. (2018b). “Probabilistic design and reliability analysis of scour protections for Offshore Windfarms.” In: *Engineering Failure Analysis* 91, pp. 291–305. DOI: [10.1016/j.engfailanal.2018.04.035](https://doi.org/10.1016/j.engfailanal.2018.04.035).
- Fazeres-Ferradosa T.; Taveira-Pinto, F.; Romão, X.; Reis, T.; das Neves, L. (2019a). “Reliability Assessment of Offshore Dynamic Scour Protections using Copulas.” In: *Wind Engineering* 43.5, pp. 506–538. DOI: [10.1177/0309524X18807033](https://doi.org/10.1177/0309524X18807033).

- Fazeres-Ferradosa T.; Welzel, M.; Taveira-Pinto, F.; Rosa-Santos, P. and Chambel, J. (2019b). “Brief review on the limit state function of dynamic scour protections.” In: IOP Conf. Series: Materials Science Engineering 700, 012027. DOI: [10.1088/1757-899x/700/1/012027](https://doi.org/10.1088/1757-899x/700/1/012027).
- Fazeres-Ferradosa, T.; Welzel, M.; Schendel, A.; Baelus, L.; Rosa Santos, P.; Taveira Pinto, F. (2020). “Extended characterization of damage in rubble mound scour protections.” In: *Coastal Engineering*, Volume 158, June 2020, 103671. DOI: [10.1016/j.coastaleng.2020.103671](https://doi.org/10.1016/j.coastaleng.2020.103671).
- Fredsøe, J.; Sumer, B.M.; Arnskov, M.M. (1992). “Time scale for wave/current scour below pipelines.” In: *International Journal of Offshore and Polar Engineering* 2.2, pp. 13–17.
- Fuhrman, D.R.; Baykal, C.; Sumer, B.M.; Jacobsen, N.G.; Fredsøe, J. (2014). “Numerical simulation of wave-induced scour and backfilling processes beneath submarine pipelines.” In: *Coastal Engineering* 94, pp. 10–22. DOI: [10.1016/j.coastaleng.2014.08.009](https://doi.org/10.1016/j.coastaleng.2014.08.009).
- Gao, D.G.; Posada, L.G.; Nordin, C.F. (1993). “Pier scour equations used in the people's Republic of China: Review and Summary.” Tech. Rep., Department of Civil Engineering, Colorado State University, Fort Collins, Colorado.
- Golightly, C. (2014). “Tilting of monopiles long, heavy and stiff; pushed beyond their limits.” In: *Ground Engineering*, January 2014.
- Grabemann, I.; Groll, N.; Möller, J.; Weisse, R. (2015). “Climate change impact on North Sea wave conditions: A consistent analysis of ten projections.” In: *Ocean Dynamics* 65, pp. 255–267. DOI: [10.1007/s10236-014-0800-z](https://doi.org/10.1007/s10236-014-0800-z).
- Grashorn, S. and Stanev, E.V. (2016). “Kármán vortex and turbulent wake generation by wind park piles.” In: *Ocean Dynamics*, 66, 1543–1557. DOI: [10.1007/s10236-016-0995-2](https://doi.org/10.1007/s10236-016-0995-2).
- Grass, A. J. (1970). “Initial instability of fine bed sand.” In: *Journal of the Hydraulics Division* 96.3, pp. 619–632.
- Guan, D.; Chiew, Y.-M.; Wei, M.; Hsieh, S.-C. (2019). “Characterization of horseshoe vortex in a developing scour hole at a cylindrical bridge pier.” In: *International Journal of Sediment Research* 34.2, pp. 118–124. DOI: [10.1016/j.ijsrc.2018.07.001](https://doi.org/10.1016/j.ijsrc.2018.07.001).
- Lee, J. and Zhao, F. (2019). “Global Wind Report 2019.” Global Wind Energy Council, Brussels.
- Lefebvre, A. and Winter, C. (2021). “Marine and river bedforms dynamics, MARID VI.” In: *Earth Surface Processes and Landforms* 46, pp. 1646–1651. DOI: [10.1002/esp.5091](https://doi.org/10.1002/esp.5091).
- Lisimenka, A. and Kubicki, A. (2017). “Estimation of dimensions and orientation of multiple riverine dune generations using spectral moments.” In: *Geo-Marine Letters*, 37.1, pp. 59–74. DOI: [10.1007/s00367-016-0475-1](https://doi.org/10.1007/s00367-016-0475-1).
- Hartvig, P.A.; Thomsen, J.M.; Frigaard, P.; Andersen, T.L. (2010). “Experimental Study of the development of scour and backfilling.” In: *Coastal Engineering Journal* 52.2, pp. 157–194. DOI: [10.1142/S0578563410002154](https://doi.org/10.1142/S0578563410002154).
- Heery, E.C.; Bishop, M.J.; Critchley, L.P.; Bugnot, A.B.; Airoidi, L.; Mayer-Pinto, M.; Sheehan, E.V.; Coleman, R.A.; Loke, L.H.L.; Johnston, E.L.; Komyakova, V.; Morris, R.L.; Strain, E.M.A.; Naylor, L.A.; Dafforn, K.A. (2017). “Identifying the consequences of ocean sprawl for sedimentary habitats.” In: *Journal of Experimental Marine Biology and Ecology* 492, pp. 31–48. DOI: [10.1016/j.jembe.2017.01.020](https://doi.org/10.1016/j.jembe.2017.01.020).

- Hirai, S. and Kuruta, K. (1982). "Scour Around Multiple- and Submerged Circular Cylinders." *Memoirs of the Faculty of Engineering* 23, Osaka City University, pp. 183–190.
- Hjorth, P. (1975). "Studies on the Nature of Local Scour." In: *Bull. Series A*, No. 46, Department of Water Resources Engineering, Lund Inst. of Technol., University of Lund, Lund, Sweden.
- Hodge, R.; Brasington, J.; Richards, K. (2009). "Analysing laser-scanned digital terrain models of gravel bed surfaces: linking morphology to sediment transport processes and hydraulics." In: *Sedimentology* 56.7, pp. 2024–2043. DOI: [10.1111/j.1365-3091.2009.01068.x](https://doi.org/10.1111/j.1365-3091.2009.01068.x).
- Hofland, B.; Disco, M.; van Gent, M. (2014). "Damage characterization of rubble mound roundheads." In: *Proc. of the 5th International Conference on the Application of Physical Modelling to Port and Coastal Protection (CoastLab14)*, Varna, Bulgaria, 29.09 – 02.10.2014.
- Hosseini, R. and Amini, A. (2015). "Scour depth estimation methods around pile groups." In: *KSCE Journal of Civil Engineering* 19, pp. 2144–2156. DOI: [10.1007/s12205-015-0594-7](https://doi.org/10.1007/s12205-015-0594-7).
- IPCC (2014). "Climate Change 2014: Synthesis Report." Contribution of Working Groups I, II and III to the Fifth Assessment Report of the Intergovernmental Panel on Climate Change. [Core Writing Team, R.K. Pachauri and L.A. Meyer (eds.)]. IPCC, Geneva, Switzerland, p. 151.
- IRENA (2018). "Renewable Energy Statistics 2018.", The International Renewable Energy Agency, Abu Dhabi.
- IRENA (2019). "Future of Wind: Deployment, investment, technology, grid integration and socio-economic aspects.", The International Renewable Energy Agency, Abu Dhabi.
- Keulegan, G.H. and Carpenter, L. H. (1958). "Forces on cylinders and plates in an oscillating fluid." *Journal of research of the National Bureau of Standards* 60.5: 423–440. DOI: [10.6028/jres.060.043](https://doi.org/10.6028/jres.060.043).
- Kobayashi, T. and Oda, K. (1994). "Experimental study on developing process of local scour around a vertical cylinder." In: *Proc. 24th International Conference on Coastal Engineering*, Kobe, Japan. DOI: [10.1061/9780784400890.094](https://doi.org/10.1061/9780784400890.094).
- Lauchlan, C.S. and Melville, B.W. (2001). "Riprap protection at bridge piers." In: *Journal of Hydraulic Engineering* 127.5, pp. 412–418. DOI: [10.1061/\(ASCE\)0733-9429\(2001\)127:5\(412\)](https://doi.org/10.1061/(ASCE)0733-9429(2001)127:5(412)).
- Liang, D.; Gotoh, H.; Scott, N.; Tang, H. (2013). "Experimental study of local scour around twin piles in oscillatory flows." In: *J. Waterw. Port, Coast., and Ocean Eng.* 139.5. DOI: [10.1061/\(ASCE\)WW.1943-5460.0000192](https://doi.org/10.1061/(ASCE)WW.1943-5460.0000192).
- Link, O.; Pflieger, F.; Zanke, U. (2008). "Characteristics of developing scour-holes at a sand-embedded cylinder." In: *Int. J. Sediment Research* 23.3, pp. 258–266. DOI: [10.1016/S1001-6279\(08\)60023-2](https://doi.org/10.1016/S1001-6279(08)60023-2).
- Marion, A.; Tait, S.J.; McEwan, I.K. (2003). "Analysis of small-scale gravel bed topography during armoring." In: *Water Resources Research*, 39.12, 1334, DOI: [10.1029/2003WR002367](https://doi.org/10.1029/2003WR002367).
- Margheritini, L.; Frigaard, P.; Martinelli, L.; Lamberti, A. (2006). "Scour around monopile foundations for off-shore wind turbines." In: *Proc. of the First International Conference on the Application of Physical Modelling to Port and Coastal Protection (CoastLab06)*, Porto, Portugal, 8–10 May 2006. Faculty of Engineering, University of Porto.
- May, R.W.P.; Ackers, J.C.; Kirby, A.M. (2002). "Manual on scour at bridges and other hydraulic structures." Vol. 551, London: Ciria.
- Mayall, R. (2019). "Monopile Response to Scour and Scour Protection." Ph.D. Thesis, University of Oxford, Oxford, UK.

- Mayall, R.; McAdam, R.A.; Whitehouse, R.J.S.; Burd, H.J.; Byrne, B.W.; Heald, S.G.; Sheil, B.B.; Slater, P.L. (2020). “Flume Tank Testing of Offshore Wind Turbine Dynamics with Foundation Scour and Scour Protection.” In: *J. of Waterw., Port, Coast., and Ocean Eng.* 146.5: 04020033. DOI:[10.1061/\(ASCE\)WW.1943-5460.0000587](https://doi.org/10.1061/(ASCE)WW.1943-5460.0000587).
- Melville, B. W. and Chiew, Y.-M. (1999). “Time scale for local scour at bridge piers.” In: *Journal of Hydraulic Engineering* 125.1, pp. 59–65. DOI: [10.1061/\(ASCE\)0733-9429\(1999\)125:1\(59\)](https://doi.org/10.1061/(ASCE)0733-9429(1999)125:1(59)).
- Melville, B.W. and Coleman, S.E. (2000). “Bridge Scour.” Water Resources Publication, CO.
- Melville, B.W. and Sutherland, A.J. (1988). “Design method for local scour at bridge piers.” In: *Journal of Hydraulic Engineering* 114.10, pp. 1210–1226. DOI: [10.1061/\(ASCE\)0733-9429\(1988\)114:10\(1210\)](https://doi.org/10.1061/(ASCE)0733-9429(1988)114:10(1210)).
- Miller, R.G.; Hutchison, Z.L.; Macleod, A.K.; Burrows, M.T.; Cook, E.J.; Last, K.S.; Wilson, B. (2013). “Marine renewable energy development: Assessing the Benthic Footprint at multiple scales.” In: *Frontiers in Ecology and the Environment* 11.8, pp. 433–440. DOI: [10.1890/120089](https://doi.org/10.1890/120089).
- Mory, M.; Larrourdé, P.; Carreiras, J.; Seabra Santos, F.; (2000). “Scour around pile groups.” In: *Proc. Coastal Structures 99*, Santander, Spain, 7–9 June 1999.
- Myrhaug, D. and Rue, H. (2005). “Scour around group of slender vertical piles in random waves.” In: *Applied Ocean Research* 27.1, pp. 56–63. DOI: [10.1016/j.apor.2005.06.001](https://doi.org/10.1016/j.apor.2005.06.001).
- Nagel, T.; Chauchat, J.; Bonamy, C.; Liu, X.; Cheng, Z. (2020). “Three-dimensional scour simulations with a two-phase flow model.” In: *Advances in Water Resources* 138, 103544. DOI: [10.1016/j.advwatres.2020.103544](https://doi.org/10.1016/j.advwatres.2020.103544).
- Nielsen, A.W.; Sumer, B.M.; Fredsøe, J.; Christensen, E.D. (2011). “Sinking of armour layer around a cylinder exposed to a current.” In: *Proc. ICE, Maritime Engineering* 164.4, pp. 159–172. DOI: [10.1680/maen.2011.164.4.159](https://doi.org/10.1680/maen.2011.164.4.159).
- Nazariha, M. (1996). “Design relationships for maximum local scour depth for bridge pier groups.” Ph.D. thesis, University of Ottawa.
- Nikuradse, J. (1933). “Strömungsgesetze in rauhen Röhren.“ (In German), VDI-Verlag, Forschungsheft 361.
- Paintal, A. S. (1971). “Concept of critical shear stress in loose boundary open channels.” In: *Journal of Hydraulic Research* 9.1, pp. 91–113. DOI: [10.1080/00221687109500339](https://doi.org/10.1080/00221687109500339).
- Parsons, D.R.; Best, J.L.; Orfeo, O.; Hardy, R.J.; Kostaschuk, R.; Lane, S.N. (2005). “Morphology and flow fields of three-dimensional dunes, Rio Paraná, Argentina: Results from simultaneous multibeam echo sounding and acoustic Doppler current profiling.” In: *Journal of Geophysical Research: Earth Surface* 110, F04S03.
- Petersen, T.U.; Sumer, B.M.; Fredsøe, J. (2012). “Time scale of scour around a pile in combined waves and currents.” In: *Proc. of 6th International Conference on Scour and Erosion (ICSE)*, Paris, France.
- Petersen, T.U.; Sumer, B.M.; Fredsøe, J.; Raaijmakers, T.C.; Schouten, J.-J. (2015). “Edge scour at scour protections around piles in the marine environment: Laboratory and field investigation.” In: *Coastal Engineering* 106, pp. 42–72. DOI: [10.1016/j.coastaleng.2015.08.007](https://doi.org/10.1016/j.coastaleng.2015.08.007).
- Pizarro, A.; Manfreda, S.; Tubaldi, E. (2020). „The science behind scour at bridge foundations: a review.” In: *Water* 12.2, 374. DOI: [10.3390/w12020374](https://doi.org/10.3390/w12020374).

- Platis, A.; Siedersleben, S.K.; Bange, J.; Lampert, A.; Bärfuss, K.; Hankers, R.; Cañadillas, B.; Foreman, R.; Schulz-Stellenfleth, J.; Djath, B.; Neumann, T.; Emeis, S. (2018). “First in situ evidence of wakes in the far field behind offshore wind farms.” In: *Scientific Reports* 8, 2163. DOI: [10.1038/s41598-018-20389-y](https://doi.org/10.1038/s41598-018-20389-y).
- Porter, K.E. (2016). “Seabed Scour Around Marine Structures in Mixed and Layered Sediments.” Ph.D. Thesis, University College London (UCL), London, UK.
- Porter, K.; Simons, R.; Harris, J. (2014). “Comparison of three techniques for scour depth measurement: Photogrammetry, Echosounder profiling and a calibrated pile.” In: *Proc. of the International Conference on Coastal Engineering* 34, Seoul, Korea, 15–20 June 2014. DOI: [10.9753/icce.v34.sediment.64](https://doi.org/10.9753/icce.v34.sediment.64).
- Powell, D.M. (2014). “Flow resistance in gravel-bed rivers: Progress in research.” In: *Earth-Science Reviews* 136, pp. 301–338. DOI: [10.1016/j.earscirev.2014.06.001](https://doi.org/10.1016/j.earscirev.2014.06.001).
- Prendergast, L.J.; Gavin, K.; Doherty, P. (2015). “An investigation into the effect of scour on the natural frequency of an offshore wind turbine.” In: *Ocean Engineering* 101, 1–11. DOI: [10.1016/j.oceaneng.2015.04.017](https://doi.org/10.1016/j.oceaneng.2015.04.017).
- Qi, W.-G. and Gao, F.-P. (2014). “Physical modelling of local scour development around a large-diameter monopile in combined waves and current.” In: *Coastal Engineering* 83, pp. 72–81. DOI: [10.1016/j.coastaleng.2013.10.007](https://doi.org/10.1016/j.coastaleng.2013.10.007).
- Qi, W.-G.; Li, Y.-X.; Xu, K.; Gao, F.-P. (2019). “Physical modelling of local scour at twin piles under combined waves and current.” In: *Coastal Engineering* 143, pp. 63–75. DOI: [10.1016/j.coastaleng.2018.10.009](https://doi.org/10.1016/j.coastaleng.2018.10.009).
- Raudkivi, A.J. (1986). “Functional trends of scour at bridge piers.” In: *Journal of Hydraulic Engineering* 112.1, pp. 1–13. DOI: [10.1061/\(ASCE\)0733-9429\(1986\)112:1\(1\)](https://doi.org/10.1061/(ASCE)0733-9429(1986)112:1(1)).
- Raudkivi, A.J. (1990). “Loose boundary hydraulics.” 3rd edition. Pergamon Press, Oxford, U.K.
- Raudkivi, A.J. and Ettema, R. (1983). “Clear-water scour at cylindrical piers.” In: *Journal of Hydraulic Engineering* 109.3, pp. 338–350. DOI: [10.1061/\(ASCE\)0733-9429\(1983\)109:3\(338\)](https://doi.org/10.1061/(ASCE)0733-9429(1983)109:3(338)).
- Richardson, E.V. and Davis, S.R. (2001). “Evaluating scour at bridges.” In: *Hydraulic Engineering Circular* 18, Rep. No. FHWA NHI 01-001, Federal Highway Administration, Washington, D.C.
- Roulund, A.; Sumer, B.M.; Fredsøe, J.; Michelsen, J. (2005). “Numerical and experimental investigation of flow and scour around a circular pile.” In: *Journal of Fluid Mechanics* 534, pp. 351–401. DOI: [10.1017/S0022112005004507](https://doi.org/10.1017/S0022112005004507).
- Rudolph, D. and Bos, J.K. (2006). “Scour around a monopile under combined wave-current conditions and low KC-numbers.” In: *Proc. of 3rd International Conference on Scour and Erosion (ISCE)*. November 1–3, 2006, Amsterdam, The Netherlands.
- Rudolph, D.; Bos, K.J.; Luijendijk, A.P.; Rietema, K.; Out, J.M.M. (2004). “Scour around offshore structures - analysis of field measurements.” In: *Proc. of Second International Conference on Scour and Erosion (ICSE)*. November 14.–17., 2004, Singapore.
- Salim, M. and Jones, J.S. (1996). “Scour around exposed pile foundations.” North American Water and Environment Congress & Destructive Water, pp. 2202–2211, ASCE.



- Sánchez, S.; López-Gutiérrez, J.-S.; Negro, V.; Esteban, M.D. (2019). “Foundations in Offshore Wind Farms: Evolution, Characteristics and Range of Use. Analysis of Main Dimensional Parameters in Monopile Foundations.” In: *Journal of Marine Science and Engineering* 7.12, 441. DOI: [10.3390/jmse7120441](https://doi.org/10.3390/jmse7120441).
- Schendel, A.; Goseberg, N.; Schlurmann, T. (2018). “Influence of reversing currents on the erosion stability and bed degradation of widely graded grain material.” In: *International Journal of Sediment Research*, 33.1, pp. 68–83. DOI: [10.1016/j.ijsrc.2017.07.002](https://doi.org/10.1016/j.ijsrc.2017.07.002).
- Schendel, A. (2018). “Wave-Current-Induced Scouring Processes and Protection by Widely Graded Material.” Ph.D. thesis, Gottfried Wilhelm Leibniz Universität: Hannover, Germany. DOI:[10.15488/4453](https://doi.org/10.15488/4453).
- Schendel, A.; Goseberg, N.; Schlurmann, T. (2015). “Experimental Study on the Erosion Stability of Coarse Grain Materials under Waves.” In: *Journal of Marine Science Technology* 23.6, pp. 937–942. DOI: [10.6119/JMST-015-0610-12](https://doi.org/10.6119/JMST-015-0610-12).
- Schendel, A.; Welzel, M.; Hildebrandt, A.; Schlurmann, T.; Hsu, T.-W. (2019). “Role and Impact of Hydrograph Shape on Tidal Current-Induced Scour in Physical-Modelling Environments.” In: *Water* 11.12, 2636. DOI: [10.3390/w11122636](https://doi.org/10.3390/w11122636).
- Schendel, A.; Welzel, M.; Schlurmann, T.; Hsu, T.-W. (2020). “Scour around a monopile induced by directionally spread irregular waves in combination with oblique currents”. In: *Coastal Engineering* 161, 103751. DOI: [10.1016/j.coastaleng.2020.103751](https://doi.org/10.1016/j.coastaleng.2020.103751).
- Schlichting, H. and Gersten, K. (2006). “Grenzschichttheorie.” (In German), Ed. by H. Schlichting and K. Gersten. Springer-Verlag.
- Scheiber, L.; Lojek, O.; Götschenberg, A.; Visscher, J.; Schlurmann, T. (2021). “Robust methods for the decomposition and interpretation of compound dunes applied to a complex hydromorphological setting.” In: *Earth Surface Processes and Landforms* 46.2, pp. 478–489. DOI: [10.1002/esp.5040](https://doi.org/10.1002/esp.5040).
- Sheppard, D.M.; Odeh, M.; Glasser, T. (2004). “Large scale clear-water local pier scour experiments.” In: *Journal of Hydraulic Engineering* 130.10, pp. 957–963. DOI: [10.1061/\(ASCE\)0733-9429\(2004\)130:10\(957\)](https://doi.org/10.1061/(ASCE)0733-9429(2004)130:10(957)).
- Sheppard, D.M.; Melville, B.; Demir, H. (2014). “Evaluation of existing equations for local scour at bridge piers.” In: *Journal of Hydraulic Engineering* 140.1: pp. 14–23. DOI: [10.1061/\(ASCE\)HY.1943-7900.0000800](https://doi.org/10.1061/(ASCE)HY.1943-7900.0000800).
- Sheppard, D.M. and Renna, R. (2005). “Bridge scour manual.” Florida Department of Transportation, Florida.
- Shields, A. (1936). “Anwendung der Ähnlichkeitsmechanik und der Turbulenzforschung auf die Geschiebebewegung.” (In German), In: *Mitteilungen der Preußischen Versuchsanstalt für Wasserbau und Schiffbau, Berlin*.
- Shields, M.A.; Woolf, D.K.; Grist, E.P.M.; Kerr, S.A.; Jackson, A.C.; Harris, R.E.; Bell, M.C.; Beharie, R.; Want, A.; Osalusi, E.; Gibb, S.W.; Side, J. (2011). “Marine renewable energy: The ecological implications of altering the hydrodynamics of the marine environment.” In: *Ocean & Coastal Management* 54.1, pp. 2–9. DOI: [10.1016/j.ocecoaman.2010.10.036](https://doi.org/10.1016/j.ocecoaman.2010.10.036).
- Smith, M.; Vericat, D.; Gibbins, C. (2012). “Through-water terrestrial laser scanning of gravel beds at the patch scale.” *Earth Surface Processes and Landforms* 37.4, pp. 411–421.
- Soulsby, R. (1995). “Bed shear-stresses due to combined waves and currents. Advances in Coastal Morphodynamics: An Overview of the G8-Coastal Morphodynamics project.” Tech. rep. Delft Hydraulics.

- Soulsby, R.; Hamm, L.; Klopman, G.; Myrhaug, D.; Simons, R.R.; Thomas, G.P. (1993). "Wave-current interaction within and outside the bottom boundary layer." In: *Coastal Engineering* 21.1-3, pp. 41-69. DOI: [10.1016/0378-3839\(93\)90045-A](https://doi.org/10.1016/0378-3839(93)90045-A).
- Soulsby, R. (1997). "Dynamics of marine sands: A manual for practical applications." Thomas Telford Publications, London.
- Soulsby, R. (2006). "Simplified calculation of wave orbital velocities." Tech. Report 155. HR Wallingford.
- Soulsby, R. and Whitehouse, R.J.S. (1997). "Threshold of sediment motion in coastal environments." In: *Proc. Pacific Coasts and Ports Conference 97*, Christchurch, University of Canterbury, New Zealand.
- Stahlmann, A. (2013). "Experimental and numerical modelling of scour at offshore wind turbines." Ph.D. thesis, Gottfried Wilhelm Leibniz Universität: Hannover, Germany. DOI: [10.15488/8173](https://doi.org/10.15488/8173).
- Stahlmann, A. and Schlurmann, T. (2010). "Physical Modeling of Scour around Tripod Foundation Structures for Offshore Wind Energy Converters." In: *Proc. of the International Conference on Coastal Engineering 32*, Shanghai, China, pp. 1-12. DOI: [10.15488/1841](https://doi.org/10.15488/1841).
- Stümpel, M.; Marx, S.; Schaumann, P.; Seidl, G.; Göhlmann, J. (2017). "An innovative hybrid substructure for offshore wind turbines." In: *Proc. 27th International Ocean and Polar Engineering Conference (ISOPE)*, San Francisco, USA.
- Sumer, B.M.; Bundgaard, K.; Fredsøe, J. (2005). "Global and local scour at pile groups." In: *Proc. 15th International Ocean and Polar Engineering Conference (ISOPE)*, Seoul, Korea.
- Sumer, B.M. and Fredsøe, J. (1997). "Hydrodynamics around cylindrical structures." Advanced Series on Ocean Engineering 26, World Scientific.
- Sumer, B.M. and Fredsøe, J. (1998). "Wave scour around group of vertical piles." In: *J. of Waterw., Port, Coast., and Ocean Eng.* 124.5, 248-256. DOI: [10.1061/\(ASCE\)0733-950X\(1998\)124:5\(248\)](https://doi.org/10.1061/(ASCE)0733-950X(1998)124:5(248)).
- Sumer, B.M. and Fredsøe, J. (2001). "Scour around pile in combined waves and current." In: *Journal of Hydraulic Engineering* 127.5, pp. 403-411. DOI: [10.1061/\(ASCE\)0733-9429\(2001\)127:5\(403\)](https://doi.org/10.1061/(ASCE)0733-9429(2001)127:5(403)).
- Sumer, B.M.; Whitehouse, R.J.S.; Tørum, A. (2001). "Scour around coastal structures: A summary of recent research." In: *Coastal Engineering* 44.2, pp.153-190. DOI: [10.1016/S0378-3839\(01\)00024-2](https://doi.org/10.1016/S0378-3839(01)00024-2).
- Sumer, B.M. and Fredsøe, J. (2002). "The Mechanics of Scour in the Marine Environment." World Scientific.
- Sumer, B.M.; Christiansen, N.; Fredsøe, J. (1992a). "Time scale of scour around a vertical pile." In: *Proc. 2nd International Offshore and Polar Engineering Conference (ISOPE)*, June 14.-19, San Francisco, USA.
- Sumer, B.M.; Fredsøe, J.; Christiansen, N. (1992b). "Scour around vertical pile in waves." In: *J. of Waterw., Port, Coast., and Ocean Eng.* 118.1, pp. 15-31. DOI: [10.1061/\(ASCE\)0733-950X\(1992\)118:1\(15\)](https://doi.org/10.1061/(ASCE)0733-950X(1992)118:1(15)).
- Sumer, B.M.; Christiansen, N.; Fredsøe, J. (1997). "The horseshoe vortex and vortex shedding around a vertical wall-mounted cylinder exposed to waves." In: *Journal of Fluid Mechanics* 332, pp. 41-70. DOI: [10.1017/S0022112096003898](https://doi.org/10.1017/S0022112096003898).
- Sumer, B.M. (2014). "Liquefaction around marine structures." World Scientific. DOI: [10.1142/9789814335102\\_0007](https://doi.org/10.1142/9789814335102_0007).
- Sumner, D. (2010). "Two circular cylinders in cross-flow: A review." In: *Journal of Fluids and Structures* 26.6, pp. 849-899. DOI: [10.1016/j.jfluidstructs.2010.07.001](https://doi.org/10.1016/j.jfluidstructs.2010.07.001).

- Thompson, D.M. and Shuttler, R.M. (1975). “Riprap Design for Wind-Wave Attack, a Laboratory Study in Random Waves.” [Wallingford report EX707 for CIRIA](#).
- Umeda, S.; Yamazaki, T.; Ishida, H. (2008). “Time Evolution of Scour and Deposition around a Cylindrical Pier in Steady Flow.” In: *Proc. 4th International Conference on Scour and Erosion*, November 5–7, 2008, Tokyo, Japan, pp. 140–146.
- Uzunoglu, E.; Karmakar, D.; Soares, C.G. (2016). „Floating Offshore Wind Platforms.” In: *Floating Offshore Wind Platforms* (pp.53–76). Green Energy and Technology. Springer, Cham. DOI: [10.1007/978-3-319-27972-5\\_4](#).
- Van der Meer, J.W. (1988). “Rock slopes and gravel beaches under wave attack.” Ph.D. thesis, Faculty of Civil Engineering and Geosciences, Delft Hydraulics, Delft, The Netherlands. [Link](#).
- Van Driest, E.R. (1956). “On turbulent flow near a wall.” In: *Journal of Aeronautic Sciences* 23.11, pp. 1007–1036. DOI: [10.2514/8.3713](#).
- Van Rijn, L.C. (1993). “Principles of sediment transport in rivers, estuaries and coastal seas.” Aqua Publications, Amsterdam.
- Vanhellemont, Q. and Ruddick, K. (2014). “Turbid wakes associated with offshore wind turbines observed with Landsat 8.” In: *Remote Sensing of Environment* 145, pp. 105–115. DOI: [10.1016/j.rse.2014.01.009](#).
- Wang, R.-K. and Herbich, J.B. (1983). “Combined current and wave-produced scour around a single pile.” Department of Civil Engineering, Texas Eng. Expt. Station.
- Welzel, M.; Kreklow, T.; Schlurmann, T.; Hildebrandt, A. (2016). „Excitation and dynamic responses of jacket structures in regular waves for offshore installation.” *Coastal Engineering Conference*, 35th ICCE. DOI: [10.9753/icce.v35.management.12](#).
- Welzel, M.; Schendel, A.; Hildebrandt, A.; Schlurmann, T. (2019a). “Scour development around a jacket structure in combined waves and current conditions compared to monopile foundations.” In: *Coastal Engineering* 152, 103515. DOI: [10.1016/j.coastaleng.2019.103515](#).
- Welzel, M.; Schendel, A.; Schlurmann, T.; Hildebrandt, A. (2019b). “Volume-based Assessment of Erosion Patterns around a Hydrodynamic Transparent Offshore Structure.” In: *Energies* 12.16, 3089. DOI: [10.3390/en12163089](#).
- Welzel, M.; Schendel, A.; Goseberg, N.; Hildebrandt, A.; Schlurmann, T. (2020). “Influence of Structural Elements on the Spatial Sediment Displacement around a Jacket-Type Offshore Foundation.” In: *Water* 12.16, 1651. DOI: [10.3390/w12061651](#).
- Whitehouse, R.J.S. (1998). “Scour at marine structures: A manual for practical applications.” Thomas Telford Publications, London.
- Whitehouse, R.J.S. ; Brown, A.; Audenaert, S.; Bolle, A.; de Schoesitter, P.; Haerens, P.; Baelus, L.; Troch, P.; das Neves, L.; Ferradosa, T.; Pinto, F. (2014). “Optimising scour protection stability at offshore foundations.” In: *Proc. 7th International Conference on Scour and Erosion*, CRC Press, Perth, Australia, pp. 593–600.
- Whitehouse, R.J.S.; Harris, J.M.; Sutherland, J. (2011). “Evaluating scour at marine gravity foundations.” In: *Proc. ICE, Maritime Engineering* 164.4, pp. 143–157. DOI: [10.1680/maen.2011.164.4.143](#).
- Williamson, C.H.K. (1989). “Oblique and parallel modes of vortex shedding in the wake of a circular cylinder at low Reynolds numbers.” In: *Journal of Fluid Mechanics* 206, pp. 579–627.



- Wilms, M.; Stahlmann, A.; Schlurmann, T. (2012). "Investigations on scour development around a gravity foundation for offshore wind turbines." In: *Coastal Engineering Proceedings*, December 2012. DOI: [10.9753/icce.v33.structures.35](https://doi.org/10.9753/icce.v33.structures.35).
- Wilson, J. and Elliott, M. (2009). "The Habitat-creation Potential of Offshore Wind Farms." In: *Wind Energy* 12.2, pp. 203–212. DOI: [10.1002/we.324](https://doi.org/10.1002/we.324).
- WindEurope (2019). "Offshore Wind in Europe: Key trends and statistics 2018." Tech. Rep. WindEurope 2019.
- Yagci, O.; Yildirim, I.; Celik, M.F.; Kitsikoudis, V.; Duran, Z.; Kirca, V.S.O. (2017). "Clear water scour around a finite array of cylinders." In: *Applied Ocean Research* 68, pp. 114–129. DOI: [10.1016/j.apor.2017.08.014](https://doi.org/10.1016/j.apor.2017.08.014).
- Yalin, M.S. and Karahan, E. (1979). "Inception of sediment transport." In: *Journal of the Hydraulics Division* 105.11, pp. 1433–1443.
- Yang, Y.; Qi, M.; Li, J.; Ma, X. (2018). "Evolution of hydrodynamic characteristics with scour hole developing around a pile group." In: *Water* 10.11, 1632. DOI: [10.3390/w10111632](https://doi.org/10.3390/w10111632).
- Yuan, C.; Melville, B.W.; Adams, K.N. (2017). "Scour at wind turbine tripod foundation under steady flow." In: *Ocean Engineering* 141, pp. 277–282. DOI: [10.1016/j.oceaneng.2017.06.038](https://doi.org/10.1016/j.oceaneng.2017.06.038).
- Zanke, U. (1982). "Grundlagen der Sedimentbewegung." (In German), Springer-Verlag.
- Zanke, U. (1990). "Der Beginn der Sedimentbewegung als Wahrscheinlichkeitsproblem." (In German), In: *Wasser und Boden* 1, pp. 40–43.
- Zhao, G. and Sheppard, D.M. (1998). "The effect of flow skew angle on sediment scour near pile groups." Stream Stability and Scour at Highway Bridges, compendium of papers presented at conferences sponsored by Water Resources Engineering ASCE.

## LIST OF FIGURES

---

Figure 2.1.1	Modified Shields diagram for the initiation of motion including compiled data by Yalin and Krahan (1979), reproduced figure from Sumer and Fredsøe (2002) with permission, Copyright © 2002 by World Scientific. . . . .	11
Figure 2.2.1	Common offshore wind foundation types used in Europe. From left to right: monopile, suction bucket, jacket, tripod, spar, semi-submersible and tension-leg platform. Adapted figure, from Dornhelm et al. (2019). . . . .	12
Figure 2.3.1	Sketch of the flow around a circular cylinder, with $\delta$ as the boundary layer thickness. . . . .	14
Figure 2.3.2	Sketch of vortex shedding as the dominant scouring mechanism under wave conditions. The left and right sketch depict each half cycle of the wave. . . . .	15
Figure 2.3.3	Sketch of the maximum scour depth, scour shape and main mechanisms, including the horseshoe vortex in a scour hole under equilibrium conditions. . . . .	16
Figure 2.3.4	Sketch of the temporal development of the scour depth under clear-water conditions, including the time scale $T$ and the time $t_e$ to reach the equilibrium scour depth $S_e$ at which the increase of the scour depth is not exceeded by a value of 5% of the pile diameter length in one day. . . . .	18
Figure 2.4.1	Global and total scour depth for an $N \times N$ pile group in a steady current for live bed conditions, (a) maximum global equilibrium scour depth to pile diameter ratio ( $S_G$ as the global scour depth and $S_T$ the total scour depth); (b) the maximum of the total equilibrium scour depth to single pile $S_0$ scour depth ratio (pile spacing $G/D=4$ ), reproduced figure from Sumer et al. (2001) with permission, Copyright © 2001 Elsevier. . . . .	23
Figure 2.4.2	Definition sketch. Two circular cylinders with an equal pile diameter in a tandem and side-by-side arrangement. . . . .	23
Figure 2.4.3	Simplified sketch of the flow pattern for two cylinders in tandem arrangement. a) extended-body regime, $G \approx 1-2D$ ; b) reattach-ment regime, $G \approx 2-5D$ ; c) co-shedding regime, $G \gtrsim 5D$ (redrawn figure, similar to Sumner, 2010). . . . .	24

Figure 2.4.4	Sketch of the scour around two piles in tandem arrangement, highlighting the exit path of the flow, the reduced height and slope as well as the theoretical slope for one pile in orange to explain the reinforcing and sheltering effect. . . . .	25
Figure 2.4.5	Variation of the relative scour depth $S_i/S$ at two piles of the same size in tandem arrangement with varying pile spacing $G/D$ for steady current clear-water conditions (where $S_i$ = scour depth at the front or rear pile and $S$ = scour depth at an isolated single pile), redrawn figure from Beg (2008), p.119. . . . .	26
Figure 2.4.6	Simplified sketch of the flow pattern for two cylinders in a side-by-side arrangement. a) single bluff body regime, $G \approx 0-0.2D$ ; b) biased flow pattern, $G \approx 0.2-1.2D$ ; c) parallel vortex streets, $G \gtrsim 1.2D$ , (redrawn figure, similar to Sumner, 2010). . . . .	27
Figure 2.4.7	Variation of the relative scour depth $S_i/S$ at two piles of the same size in side-by-side arrangement with varying pile spacing $G/D$ for steady current clear-water conditions (where $S_i$ = scour depth at one of both piles and $S$ = scour depth at an isolated single pile), redrawn figure from Beg (2008), p.183. . . . .	27
Figure 2.4.8	Schematic sketch (not to scale) of a jacket platform and the seabed a) of connection between the wellhead jacket platform and skirt piles at the seabed, in the text referred as post piles (redrawn figure, similar to Rudolph et al., 2004) b) of a seabed pile and the Jacket pin pile, in the text referred as pre-piled foundation (redrawn figure, similar to Baelus et al., 2019). . . . .	29
Figure 2.4.9	Photos of the jacket foundation of the C-Power wind farm, located about 30 km off the Belgian coast on the Thronton Bank, North Sea. This type of jacket foundation was investigated in Bolle et al. (2012) and Baelus et al. (2019) (see also Fig. 2.4.8, b for a sketch of the seabed structure connection). a) installed jacket structure; b) offshore installation of the jacket structure. Reproduced figures with permission, Copyright © C-Power NV. . . . .	29
Figure 3.3.1	Schematic sketch of the investigated jacket model: a) side view, with dimensions, angles and water level, $D = 4$ cm; b) side view on the lowest node positioned directly on seabed $0D$ , in comparison with a distance of $1D$ . . . .	43
Figure 4.3.1	Schematic sketch of increasing rectangular interrogation areas around the model, (a) sketch of an area $a_i = a_2$ , related to Eq. (4.3.2) and (4.3.4); (b) increasing incremental areas $a_i - a_{i-1}$ in relation to Eq. (4.3.3) and (4.3.5). In the present study each area $a_i$ or $a_i - a_{i-1}$ has an additional underlying sub-grid. . . . .	49

Figure 4.3.2	Bed topography of test 1-5, top view around the jacket for current only conditions, the current is coming from left side ( $0^\circ$ ), x and y distances are given as multiples of the structure's footprint length (adapted figure from Welzel et al., 2019b). . . . .	50
Figure 4.3.3	(a) Incremental volume $V_{I,i}$ illustrated over the structure footprint length $A$ , (blue dotted line) in comparison with the empirical equation derived for these tests (Figure from Welzel et al. 2019b); (b) standard deviation for each data point shown in (a), derived with data of the introduced sub-grid. . . . .	51
Figure 4.3.4	Empirical cumulative distribution function (ECDF) of the erosion depth value $D_{A,i}$ of test 3 and 5, the spatial distribution in x and y axis related to the cumulative distribution of $D_{A,i}$ , an example of a critical scour depth value. . . . .	52
Figure 4.3.5	(a) Incremental erosion depth $D_{I,i}$ around the jacket structure, plotted over the structure footprint length $A$ , total value of each interrogation area, see Fig. 4.3.1, (Figure adapted from Welzel et al., 2019b) (b) Confidence bands of a quantile of 15% for test 1-5 of the incremental erosion depth $D_{I,i}$ over the structure footprint length. . . . .	53

## LIST OF TABLES

---

Table 4.3.1	Measured test conditions (waves are $90^\circ$ to the current)	48
-------------	--	----

## APPENDIX

---

### A.1 CURRICULUM VITAE

#### Personal Data

---

Name	Mario Welzel
Date of Birth	November 26th, 1983
Place of Birth	Berlin, Germany
Nationality	German
Marital status	married, 2 kids
Email	<a href="mailto:welzel@lufi.uni-hannover.de">welzel@lufi.uni-hannover.de</a>



#### Education

---

2007-2013	Master of Engineering, Urban Infrastructure Planning, Beuth University of Applied Sciences Berlin  Master Thesis: „Investigation of the energy conservation and reinforcement of riverbeds behind a overflow weir“
2014-2020	Research Associate and PhD student Work on different research projects as well as on the dissertation / the doctoral thesis Ludwig-Franzius-Institute for Hydraulic, Estuarine and Coastal Engineering Leibniz Universität Hannover

#### Professional experience

---

2011 - 2014	BDC DORSCH Consult Engineering Company, Department of Hydraulic Engineering, Project Engineer
2014 - 2019	Leibniz University Hannover, Ludwig-Franzius-Institute, Research Associate
2019 - 2021	TU Braunschweig, Leichtweiß-Institute for Hydraulic Engineering and Water Resources, Dept. of Hydromechanics, Coastal and Ocean Engineering, Research Associate

## Research Projects

---

2014 - 2018	<p>Project “HyConCast”</p> <p>Development of an innovative hybrid jacket foundation structure for offshore wind turbines. Analysis of the offshore installation process, the local and global scouring /erosion and deposition around the offshore wind foundation structure.</p>
2016 - 2018	<p>Project “TEXbase”</p> <p>Development of an innovative, complex heavy weight foundation structure for offshore wind turbines. Physical and numeric simulation of sediment transport processes around the foundation structure.</p>
2017 - 2019	<p>Project “NFR”</p> <p>High Resolution Numerical Modeling of Flexible Fish Cage Structures. Conduction of model tests with different floating bodies for validation of the numerical model.</p>
2018 - 2020	<p>Project “PROTEUS”</p> <p>Large scale experiments (Fast Flow Facility, HR Wallingford, United Kingdom) to improve offshore monopile scour protection design adapted to climate change under combined action of waves and current.</p>
2019 - 2021	<p>Project “EnviSim4mare”</p> <p>Experimental investigations of hydrodynamic loads by marine growth on foundation structures of offshore wind foundation structures.</p>
2019 - 2021	<p>Project “marTech”</p> <p>Development of Renewable Maritime Technologies for Reliable and Sustainable Energy Supply, scientific support of the subproject marTech-B. Investigations and model tests regarding a natural flow in the extended GWK+ including three pilot studies on renewable energies (regarding offshore wind foundation structures and wave energy converters).</p>

## Selected Projects, Engineering Company

---

2012	Fish ladder „Clausdorf“; Preliminary planning, design engineering and approval planning.
2012	Renaturation of the waterway „Kirschkanaal Spreewald“; Preliminary planning

- 2012 Replacement construction of the weir „Großes Fließ Spreewald“; Investigation of the state of construction, production of a preliminary planning.
- 2013 Rehabilitation of the flood channel „Umfluter Doberlug-Kirchhain“; Preliminary planning, design engineering and approval planning.
- 2013 Replacement construction of the weir „Hartmannsdorf, Nördlicher Spreewald“; Preliminary planning, design engineering and approval planning.
- 2014 Replacement construction of the weir „Neue Mühle, Berlin“; Investigation of the state of construction, preliminary planning.

## Individual contribution on the publications

---

The main results of this thesis are published in peer reviewed international journal papers. These publications are:

1. Schendel, A., **Welzel, M.**, Hildebrandt, A., Schlurmann, T., Hsu, T.-W. (2019). Role and Impact of Hydrograph Shape on Tidal Current-Induced Scour in Physical-Modelling Environments. *Water* 2019, 11, 2636. DOI: 10.3390/w11122636.
2. Schendel, A., **Welzel, M.**, Hildebrandt, A., Schlurmann, T., Hsu, T.-W. (2020). Scour around a monopile induced by short-crested waves combined with oblique currents. *Coastal Engineering*, Vol. 161, 2020 103751. DOI: 10.1016/j.coastaleng.2020.103751.
3. **Welzel, M.**, Schendel, A., Hildebrandt, A., Schlurmann, T. (2019). Scour development around a jacket structure in combined waves and current conditions compared to monopile foundations. *Coastal Engineering*, Vol. 152, 103515. DOI: 10.1016/j.coastaleng.2019. 103515.
4. **Welzel, M.**, Schendel, A., Goseberg, N., Hildebrandt, A., Schlurmann, T. (2020). Influence of structural elements on the spatial sediment displacement around a jacket-type offshore foundation. *Water* 2020, 12, 1651. DOI: 10.3390/w12061651.
5. **Welzel, M.**, Schendel, A., Schlurmann, T., Hildebrandt, A. (2019). Volume-based assessment of erosion patterns around a hydrodynamic transparent offshore structure. *Energies* 2019, 12, 3089. DOI: 10.3390/en12163089.
6. Chavez, C.E.A., Stratigaki, V., Wu, M., Troch, P., Schendel, A., **Welzel, M.**, Villanueva, R., Schlurmann, T., De Vos, L., Kisacik, D., Pinto, F.T., Fazeres-Ferradosa, T., Santos, P.R., Baelus, L., Szengel, V., Bolle, A., Whitehouse, R., Todd, D., 2019. Large-scale experiments to improve monopile scour protection design adapted to climate change—the PROTEUS project. *Energies* 12 (9), 1709. DOI: 10.3390/en12091709.
7. Fazeres-Ferradosa, T.; **Welzel, M.**; Schendel, A.; Baelus, L.; Santos, P.R.; Pinto, F.T. Extended characterization of damage in rubble mound scour protections. *Coast. Eng.* 2020, 103671. DOI: 10.1016/j.coastaleng.2020.103671.

As the main author of publication 1 and 2, Alexander Schendel was primarily responsible for the planning, conduction, analysis and description of the tests of these publications. As the second author, I supported with content related discussions, critical revisions and editing of the publications.

As the main author of publication 3 to 5, I was primarily responsible for the planning, conduction, analysis and description of the tests of these publications. As the second author, Alexander Schendel supported with content related discussions, critical revisions and editing of the publications. Nils Goseberg and Arndt Hildebrandt supported as additional co-authors with a critical revision of the manuscript. Arndt Hildebrandt also



contributed with helpful ideas during the planning of the physical model tests. Torsten Schlurmann was the leader of the corresponding research projects, within which these publications were produced. Torsten Schlurmann supported in particular also with a critical discussion and revision of the publications.

Publication 6 includes the description and first analyses of large-scale physical model tests, which were conducted in an international group as part of the HYDRALAB-PLUS research project PROTEUS. The planning and conduction of the physical model tests were done in the whole group of the project partners (see co-authors) in the Fast Flow Facility in HR Wallingford, United Kingdom. As the main author of publication 6, Carlos Emilio Arboleda (Ghent University) was primarily responsible for the analysis and description of the tests of the publication. As a co-author, I supported publication 6 with the planning and conduction of the physical model tests as well as with revision of the manuscript.

As the second author of publication 7, I supported with planning and writing of the original draft of the paper and content related discussions. Furthermore, I was primarily responsible for the development of the method, related analyses and figures. As the main author, Tiago Fazerese-Ferradosa was primarily responsible for the idea and planning of the manuscript as well as primarily for the writing and description of the analyses. Alexander Schendel supported as a co-author and helped in particular with content related discussions, critical revisions, editing and creation of figures.

Hannover, 15. November 2020

Mario Welzel